Scuola Normale Superiore

DOCTORAL THESIS

Study of cortical and hippocampal specification using embryonic stem cell-derived neurons

Author:

Marco Terrigno

Supervisor:

Federico Cremisi

January 2019

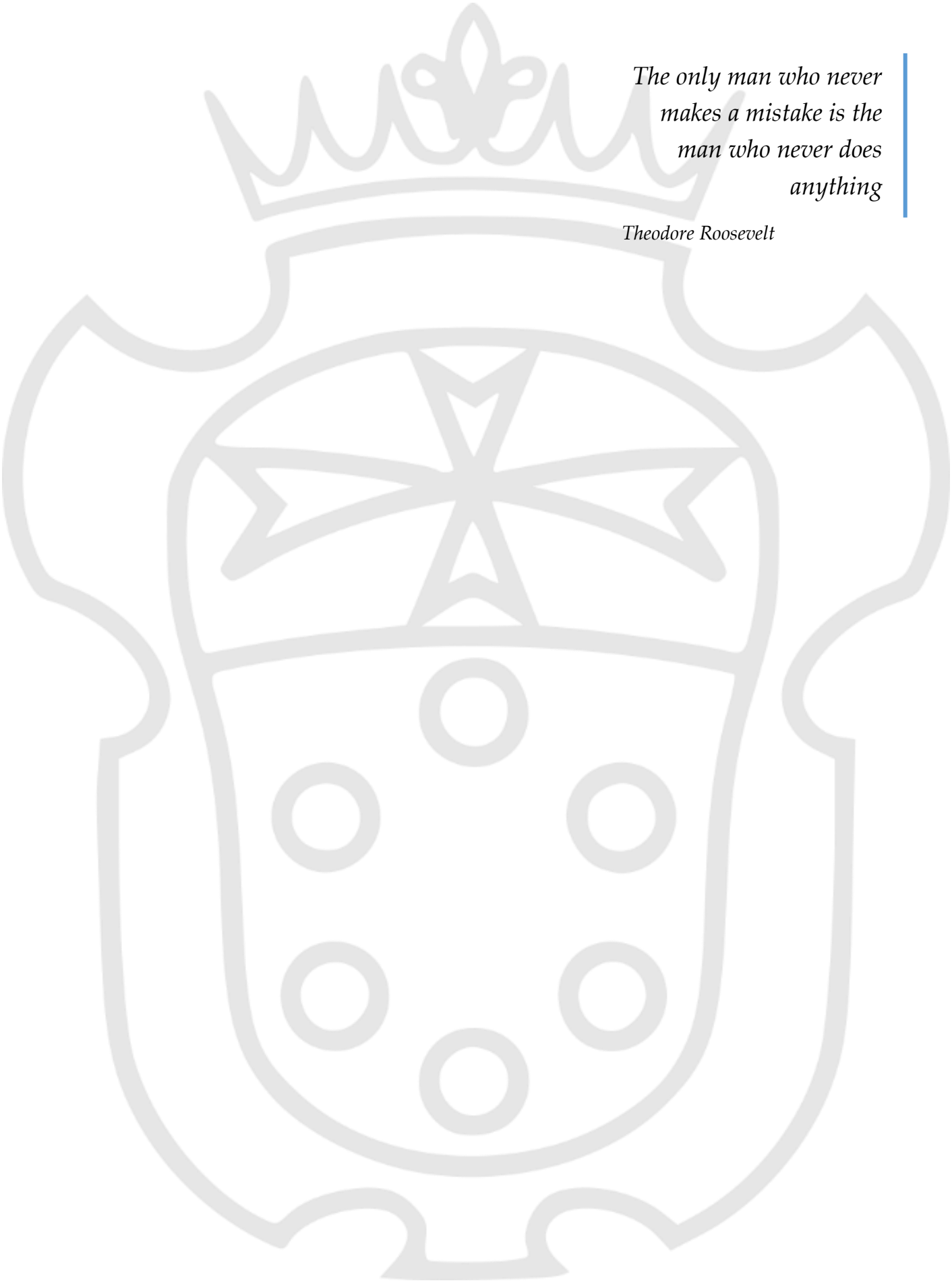

The only man who never makes a mistake is the man who never does anything

Theodore Roosevelt

TABLE OF CONTENTS

TABLE OF FIGURES

INTRODUCTION

Early embryonic development

All vertebrates, although different in shape and size, develop similarly. In mammalian embryos, starting from the fertilized egg, rapid complete cell divisions give rise to a solid symmetric sphere called morula. At the morula stage, all the cells are totipotent, thus they can give rise to any tissue of the future embryo *(Wilton and Trounson, 1989)*. Subsequently, 3.5 days post fertilization in mice, further cell divisions generate an asymmetric hollow sphere called blastula. The cells inside the blastula are called inner cell mass and give rise to the embryonic tissues, whereas the cells on the external surface form the trophectoderm and give rise to the extra-embryonic tissues, such as the placenta *(Winkel and Pedersen, 1988; Snow, 1976)*.

After the implantation of the blastocyst in the uterine walls, the cells of the inner cells mass, facing the internal cavity of the blastocoel, form the epiblast, while the cells below originate the hypoblast *(Solnica-Krezel L and Sepich D.S., 2012; Tam P.P.L and Behringer R.R., 1997)*. At this point, the relatively simple blastocyst goes through a series of morphogenetic movements and differentiation events, the

gastrulation, which defines the antero-posterior axis of the embryo and generate a more complex three-layered structure. During mammalian gastrulation, epiblast cells migrate through a small invagination called primitive streak toward the hypoblast underneath. Most of the involuting cells give rise to mesodermally derived tissues, such as muscles and bones. While the embryo begins to elongate in the antero-posterior axis, the cells that migrate first and further through the primitive streak originate the most anterior part of the embryos. At the end of the gastrulation, the superficial epiblast form the ectoderm, the migrated cells originate the mesoderm and the hypoblast give rise to the endoderm *(Bellairs, 1986; Hashimoto and Nakatsuji, 1989; reviewed by Tam et al., 1997)*.

Development of the nervous system

Neural induction

In the early twentieth century, classic embryological experiments showed that the nervous system of the vertebrates arise from the dorsal ectoderm. In those pioneering experiments, scientists assayed the specification of the embryonic tissues dissecting and culturing *in vitro* small fragments of embryo and analysing the composition of the resulting tissues. During gastrulation, as the three embryonic layers are formed, cells are committed toward specific identities. In particular, when isolated before the gastrulation, fragments of dorsal ectoderm

mainly originates epidermidis, whereas if isolated in gastrulating embryo, they generate neural tissues, such as brain and eyes. These observations led Hans Spemann to theorize that the default fate of the ectoderm was epidermidis, and that the tissues rearrangements occurring at the gastrulation specified the dorsal ectoderm to a neural fate *(Hamburger et al., 1969)*. The quest for understanding the nature of such neural induction would take half a century. At the time, investigators identify as possible inducer of neural identity the involuting mesoderm. According to this model, the epiblast cells migrating through the blastopore, the equivalent of the primitive streak in the amphibian, would induce the epiblast above to acquire neural identity.

Indeed, heterotopic transplantation of the dorsal lip of the blastopore inside the cavity of another embryo induced the formation of a second body axis, complete with brain, eyes and spinal cord. Moreover, successive experiments showed that these structures arose from the host embryo and not from the tissues of the donor. Subsequently, Richard Harland *(Lamb et al., 1993; Smith et al., 1993)* and De Robertis *(Piccolo S. et al., 1996)* isolated the first two neural inducers Noggin and Chordin, respectively. These factors are secreted protein expressed by the dorsal lip of the blastopore when neural induction occurs. Both factors were able to induce neural identity in isolated fragments of dorsal ectoderm and were able to induce the formation of complete secondary axis when overexpressed in the ventral part of a developing embryo. Notably, a similar mechanism for neural induction

is conserved also in invertebrates. In fact, in Drosophila the *short gastrulation* (*sog*) gene, homolog of the vertebrate Chordin, is important for the dorso-ventral patterning of the embryo and for the induction of the neural tissue *(François V and Bier E., 1995)*. Moreover, studies in Drosophila showed that *sog* gene interacts with *deacapentaplegic*, or *dpp*, a TGF-beta-like protein related to the vertebrate BMPs *(Biehs B. et al., 1996)*. Since these two factors actively inhibits each other, their mutation has opposite phenotypes. Indeed, *sog* mutant showed an expansion of the epidermidis at the expenses of the neurogenic region of the ectoderm, while *dpp* mutant had an expanded neurogenic region. Moreover, ectopic overexpression of *sog* was able to induce neural identity in non-neurogenic region of the ectoderm. These studies in Drosophila shed light on the mechanism of neural induction in vertebrates as well, leading scientists to the conclusion that the various neural inducers shared the same mechanism of inhibition of TGF-beta signalling.

In the same years, Melton *(Hemmati-Brivanlou et al., 1994)* discovered a third candidate neural inducer, Follistatin, a known inhibitor of a factor member of the TGF-beta family, activin. In addition, TGF-beta signalling loss-of-function, via overexpression of a dominant-negative form of activin receptor, induced dorsal ectoderm cells to acquire neural identity. These observations suggested that neural induction was realized antagonising the epidermal default fate of the ectoderm promoted by the endogenous expression of neural inhibitors belonging to the TGF-beta family. Indeed, BMP4 is expressed in the

developing gastrula of the vertebrate and amphibian embryos and its expression is repressed in the neurogenic regions and near the organizer. Moreover, further biochemical studies showed that both neural inducers Noggin and Chordin bind to extracellular BMP4, inhibiting its function, while Follistatin has a greater affinity for secreted Activin and BMP7. The thesis that self-produced factors committed ectoderm toward an epidermal fate was further corroborated by ex-vivo culture experiments. In fact, as previously mentioned, a dorsal ectoderm fragment, dissected and cultured intact ex-*vivo*, differentiates into epidermidis, whereas dorsal ectodermal cells dissociated and cultured at low density, thus greatly diluting the secreted factors, differentiate into neurons. Moreover, BMP4 was shown to be able to antagonize the neuralizing effect of Noggin, Chordin or Follistatin on isolated dorsal ectodermal fragments and to inhibit the spontaneous differentiation of dissociated ectodermal cells into neurons *(Piccolo S. et al., 1996; Thomsen G. H., 1997)*. In addiction, experiments in mouse showed that Chordin and Noggin loss-of-function during gastrulation resulted in severe defects in head development. It was therefore proposed a 'default model' for neural induction, where the three neural inducers acted by shielding the prospective neural ectoderm from the endogenous BMP signalling *(Weinstein DC and Hemmati-Brivanlou A, 1997; Hemmati-Brivanlou A and Melton D, 1997; Stern CD, 2006)*.

Furthermore, evidence in ascidians and chick embryo suggests that BMP inhibition alone is not sufficient for neural induction and support the important role of FGF signalling as neural inducer. In

fact, in both ascidians and chick FGF inhibition prevents the early phase of neural induction *(Streit et al., 2000; Bertrand et al., 2003)*, while FGF signalling is required for the expression of Chordin and Noggin in *Xenopus (Branney et al., 2009; Delaune et al., 2005; Fletcher and Harland, 2008)*. Indeed, evidence suggests that FGF and BMP signalling converge on the SMAD proteins, BMP-downstream signalling effectors, that can be inhibited by phosphorylation by FGF signalling *(Pera et al., 2003)*. Finally, FGF and BMP signalling regulate together the expression of two transcription factors essential for the neural commitment of the ectoderm, Zic1 and Zic3 *(Mizuseki et al., 1998; Marchal et al., 2009)*.

Morphogenesis and segmentation of the Neural Tube

Neural induction is followed by the rapid thickening of the prospective neural ectoderm, which originates a placode, the Neural Plate *(Schoenwolf, 1988)*. The formation of folds at the lateral extremes of the neural plates, where the neural tissue contacts the remaining ectoderm, precedes the bending of the neural plate and the formation of the neural tube. During the first phase of the bending, the furrowing, three hinge points forms: two at the level of the lateral folds and one medial. In particular, the medial hinge is specified by the underlying notochord, which secretes the morphogen SHH, and will become the most ventral part, or floor plate, of the future neural tube *(Jessell and Sanes, 2000)*. The second phase, the folding, involves the rotation of the neuralectoderm around the hinge points. Successively, the elevation of the lateral folds give rise to a trough-like structure, the Neural Groove, and requires both

changes in the cells in the neural plate and in the surrounding epidermal ectoderm *(Schoenwolf, 1988; Moury and Schoenwolf, 1995)*. Finally, the bending of the neural plate brings the paired neural folds in contact along the dorsal midline, the future roof plate, where they adhere and fuse to each other separating the neural tissue from the surrounding ectoderm and forming the Neural Tube.

The interaction between the neural and the epidermal ectoderm specifies a third cellular population, the neural crest cells. These cells contributes to several structures such as the peripheral nervous system (including Schwann cells, neurons and glia of the sensory and autonomic ganglia and the neurons of the gastric plexus), pigment cells and the cranial skeleton *(Anderson, 1999; Garcia-Castro and Bronner-Fraser, 1999; LaBonne C and Bronner-Fraser, 1999; Le Douarin and Kalcheim, 1999)*. As soon as the anterior part of the neural tube closes, it goes through a series of morphogenetic changes originating three primary vesicles that layout the basal organization of the brain: prosencephalon (forebrain), mesencephalon (midbrain) and rombencephalon (hindbrain). Subsequently, the forebrain is further subdivided in anterior secondary prosencephalon, including telencephalon and hypothalamus, and diencephalon. While the hindbrain give rise to the metenchepalon, which originates the cerebellum, and the myelencephalon, which form the medulla oblongata.

Dorsoventral patterning

The progressive regionalization of the neural tube is operated by multiple, different and overlapping patterning mechanisms generating a Cartesian map of distinct regions across the neuroepitelium, each with its own histogenetic competence. The patterning of the neural tube is realized through gradients of soluble molecules that diffuse across the neuroepithelium along its two main Cartesian axes: dorso-ventral (DV, starting as medio-lateral patterning in the two-dimensional neural plate) and antero-posterior (AP).

The ventral patterning of the neural plate is realized by the soluble morphogen Sonic Hedgehog (SHH) secreted by the underlying axial mesoderm of the notochord. At first, mesodermally derived SHH signalling activates in the most ventral region of the overlying neural epithelium a specific genetic program conferring it the identity of floor plate. Consequently, the floor plate acquires the ability to secrete SHH and acts as second organizer in the patterning of the neighbouring areas of the neural tube. *(Chiang et al., 1996; Echelard et al., 1993; Ericson et al., 1996; Hynes et al., 1995; Roelink et al., 1994, 1995; Shimamura and Rubenstein, 1997; Tanabe et al., 1995; for review see Tanabe and Jessel, 1996)*.

The dorso-ventral patterning of the neuroepithelium is determined by a second signalling center secreting TGF-beta (BMPs) and WNTs factors. The location of this second organizer is originally established in the neural plate at the interface between neuroectodem and epidermal ectoderm, which expresses WNTs and BMPs (BMP4 and

BMP7). Subsequently, the most dorsal part of the neural tube, the roof plate, acquires the identity of dorsalizing center and thus the ability to secrete dorsal morphogens. *(Basler et al., 1993; Dickinson et al., 1995; Liem et al., 1995; Shimamura and Rubenstein, 1997)*. These two signalling centers create a combined interactive molecular code along the dorso-ventral axis of the neural tube, identifying, from ventral to dorsal throughout the neuroepithelium, four longitudinal domains: the floor, the basal, the alar and the roof plates. *(Basler et al., 1993; Dickinson et al., 1995; Lee and Jessell, 1999; Liemet al., 1995; Shimamura and Rubenstein, 1997)*.

Rostrocaudal patterning

The antero-posterior patterning of the neuroepithelium begins at the early stage of Neural Plate as the results of signals coming from the organizer, the underlying axial mesoderm and the surrounding epidermal ectoderm. Cerberus is a soluble factor, inhibitor of WNT signalling, secreted by the endomesoderm underneath the prospective forebrain, the precordal plate, and mediates the acquisition of anterior neural identity: forebrain and midbrain. Indeed, Cerberus ectopic expression in *Xenopus* results in the induction of complete forebrain structures *(Bouwmeester et al., 1996)*. In addition, Lim1 is the transcription factor responsible for the production of Cerberus by the endomesoderm. In fact, Lim1 mutation results in the complete loss of anterior neural structures *(Shawlot and Behringer, 1995)*. Moreover, Otx2 mediates the anteriorizing effect of Cerberus in the neuroepithelium *(Acampora et al.,*

1995; Ang et al., 1996; Matsuo et al., 1995; Shawlot and Behringer, 1995). In the precordal plate, Cerberus expression colocalize with Lim1 and the neural inducer Chordin.

Indeed, several authors observed how the neural inducers secreted by the organizer Chordin, Noggin and Follistatin commit the prospective neural ectoderm toward a rostral rather than a posterior neural identity *(Hemmati-Brivanlou et al., 1994; Lamb and Harland, 1995; Liguori et al., 2003 and 2009; for review see Doniach, 1993)*. In addition, classical embryological experiments of heterotopic transplantation showed that ectodermal explants gave rise to both anterior and posterior neural structures only when grafted to the posterior neural plate of a host embryo *(Nieuwkoop et al., 1954)*. These observations have led to the formulation of the activator-transformer model for neural induction. According to this model, the neural inducing signals coming from the organizer ("activator") originate primarily anterior neural structures, while a second signal ("transformer") is necessary for the production of the posterior ones. Among the molecules that act as transformers of the neuroepithelium there are the Retinoic Acid *(Blumberg et al., 1997; Durston et al., 1989; Papalopulu et al., 1991; Ruiz I Altaba and Jessell, 1991a, 1991b)*, FGF2 *(Cox and Hemmati-Brivanlou, 1995; Hemmati-Brivanlou and Melton, 1997; Kelly and Melton, 1995; Lamb and Harland, 1995)* and WNT signalling *(Elkouby et al., 2010)*.

In addition to Cerberus, several other inhibitors of WNT signalling are expressed in the organizer region during neural induction, such as FrzB and Dickkopf *(Glinka et al., 1998)*, creating a caudo-rostral

gradient of WNT/beta-catenin signalling along the AP axis of the embryo *(Kiecker and Niehrs, 2001)*. Moreover, several studies showed that WNT inhibition synergize with the BMP inhibition in committing the prospective neural ectoderm toward an anterior neural fate. *(Elkouby et al., 2010; Mukhopadhyay et al., 2001)*. Indeed, Dickkopf mutant shows a headless phenotype, lacking all the neural structures anterior to the hindbrain, close to the Noggin/Chordin double mutant *(Mukhopadhyay et al., 2001)*. Similarly, mutation in the WNT-inhibitor signalling component Axin results in the complete lack of forebrain and posteriorization of the neural tube *(Heisenberg et al., 2001; Masai et al., 1997; van de Water et al., 2001)*

Several transforming factors regulate the expression of Hox genes, a family of closely related genes coding for homeodomain transcription factors *(Pearson et al., 2005)*. Hox genes show highly defined and overlapping expression domains creating, along the antero-posterior axis of the neural tube, position-specific Hox-code within the neuropithelial cells *(Hooiveld et al, 1999; Marín et al., 2008)*. The vertebrate hindbrain is a fine example of the control exert by Hox genes on the positional identity of neurepithalial cells. The hindbrain contains sets of motor neurons that control head movements through the cranial nerves. During development, the romboencephalon is segmented in several, defined compartments (rombomers) along the AP axis, each one giving rise to a specific set of motor neurons *(Lumsden and Keynes, 1989)*. For instance, rombomers 2 and 3 originate the motorneurons that innervates the trigeminal nerve, while motor neurons of cranial nerve VII form in

rombomers 4 and 5. The neat separation and compartmentalization of the rombomers is the result of a nested and partly overlapping expression of Hox genes, creating a Hox code that specifies the positional identity of each rombomer and, thus, its histogenetic competence. In particular, deletion of specific Hox genes greatly influences rombomers specification. For instance, deletion of Hoxa1, which is expressed in rombomer 4, results in the complete loss of rombomer 4 and the fusion of rombomers 4 and 5 in an single compartment. Moreover, the motor neurons of the facial nerve, originated in rombomers 4 and 5 are defective, while the abducent nerve, originated in rombomer 5, fails to develop *(Carpenter et al., 1993; Mark et al., 1993)*. Notably, deletion of *Pbx*, an important interactor of homeodomain transcription factors, causes the loss-of-function of all Hox genes, resulting in a single romboencephalic compartment, which is misspecified as rombomer 1. *(Waskiewisz et al., 2002)*.

One of the molecules involved in the regulation of the expression of Hox genes is the "transforming" morphogen Retionoic Acid. This factor diffuses through cell membrane and binds to an intracellular receptor (RAR), which in turns migrates into the nucleus exerting the transcriptional effect of RA signalling on the promoter of genes carrying Retinoic Acid Response Elements (RAREs). During vertebrate development, the production of RA by the posterior paraxial mesoderm, immediately adjacent to the neural tube, and its active degradation in most rostral part of the nervous system, creates a caudo-rostral gradient of RA along the AP axis of the neuroepithelium. RA

signalling is responsible for the expression pattern of Hox genes, such as Hoxa1 and Hoxb1. Indeed, *Xenopus* embryos treated with RA fail to develop the most anterior neural structures, while increasing concertation of RA activates posterior Hox genes at the expenses of the anterior ones *(Durston et al, 1989)*.

A third family of morphogen important in the AP patterning of the neuroepithelium is the FGF family. In particular, FGF signalling acts both as a neural inducer *(Streit et al., 2000; Bertrand et al., 2003; Branney et al., 2009; Delaune et al., 2005; Fletcher and Harland, 2008)* and as a "transformer" factor. In fact, FGF-treatment steer dorsal ectoderm committed toward neural fate by BMP inhibition to a posterior neural identity *(Slack and Tannahill, 1992)*. Moreover, similarly to RA, higher concertation of FGF activates more posterior neural and Hox genes both in amphibian and in chick *(Kengaku and Okamoto, 1995; Liu et al, 2001)*.

The regionalization of the neural tube creates several compartments of neuroepithelial cells along the AP axis with different histogenetic competence and response to specific inductive signals. *(Ericson et al., 1995; Hynes et al., 1995; Shimamura and Rubenstein, 1997; Simon et al.,1995)*. For instance, although SHH expression is ubiquitous in the ventral neural tube, it activates specific genetic networks at different axial levels. In fact, the expression of Nkx2.1 and Nkx2.6 is confined to the anterior and the posterior neural plate, respectively. As a result, SHH signalling specify a ventral column of oligodendroglial cells only in the more posterior regions of the neural tube, such as the spinal cord *(Garcia-Lopez and Martinez, 2010; Perez-Villegas et al., 1999)*.

Finally, FGF8 is yet another example of the different competence of the regionalized neuroepithelium toward an inductive signal. In fact, FGF signalling activates the expression of the anterior neural marker FoxG1 in isolated fragments of prospective forebrain, while it induces more posterior markers, such as En2, in the midbrain. *(Crossley et al., 1996; Shimamura and Rubenstein, 1997)*.

Local signalling centers: the Midbrain/Hindbrain boundary

In the rostral neuroepithelium other homeodomain transcription factors functionally replace the Hox genes, whose expression domains end at the anterior border of the metencephalon, as main regulators of positional identity. In fact, already in the early neural plate Gbx2 and Otx2, two homeodomain proteins, show defined and adjacent expression domains. Gbx2 is expressed from the posterior neural plate to the midbrain/hindbrain boundary, while Otx2 domain is complementary and localized in the anterior regions of the brain *(Joyner et al., 2000; Hidalgo-sanchez et al., 2005)*. As previously mentioned Otx2 is among the firsts anterior neural markers expressed in the neural plate and mediates the anteriorizing effect of the transforming factor Cerberus. Indeed, Otx2 deletion results in the loss of the forebrain, while gbx2-mutant shows an opposite phenotype and lacks the hindbrain *(Matsuo et al., 1995; Acampora et al., 1995; Millert et al., 1999; Wassarman et al., 1997)*.

Another important family of genes in the early pattering of the neural plate is the Iroquois family (Irx). Most vertebrates have six

Iroquois genes expressed in specific domains along the AP axis of the embryo *(de la Calle-Mustienes et al., 2005; Rodríguez-Seguel et al., 2009)*. The mutual interaction among these genes is responsible for their pattern of expression. For instance, Irx1 activates both Otx2 and Gbx2, which in turn repress each other creating the neat boundary at the border between mesencephalon and metencephalon (mes-met; *Glavic et al, 2002*).

During the early neural patterning specific regions of the neuroepithelium acquire special developmental functions; likewise roof and floor plates, these cells act as second organizers, secreting morphogens and influencing the patterning of the surrounding neuroepithelium. In particular, early heterotopic transplantation experiments showed that the midbrain/hindbrain boundary (MHB) greatly influences the development of the surrounding tissues *(Alvaro-Mallart; 1993)*. In fact, fragments of quail metencephalon grafted in to the chick prosencephalon generated both ectopic cerebellum and midbrain in the host tissue. Therefore, the hindbrain fragment respecified part of the of the chick forebrain to a more posterior identity. WNT1, FGF8 and En1 are key factors for the formation of the mes-met organizer and its activity. In particular, deletion of WNT1, which is expressed in the MHB and in the dorsal mesencephalon, results in the complete loss of midbrain and cerebellum *(McMahon and Bradley, 1990)*. Moreover, WNT1 signalling at the mes-met boundary activates the expression of transcription factor En1, which is also critical for the development of this region. Consistently, En1 mutant has a defective

phenotype close to the WNT1-deficent mouse *(Wurst et al., 1994)*. Finally, FGF8 is necessary for both the induction of the MHB and its instructive role on the surrounding neuroepithelium. In fact, similarly to the WNT1 and En1 mutants, FGF8-defiecient mice show defects in the specification of both hindbrain and midbrain *(Meyers et al., 1998; Meyers and Martin, 1999)*. Moreover, beads imbibed of FGF8 and grafted into the chick prosenchepalon induce an ectopic and MHB, cerebellum and midbrain *(Crossley et al., 1996)*. Therefore, FGF8 signalling is not only necessary for its formation and maintenance of the MHB, but it is also sufficient to induce the repatterning of the anterior regions into midbrain and hindbrain. Furthermore, all the factors important for the activity of the mes-met organizer interact with each other in a genetic network of cross-regulation and mutual repression.

According to the current model, irx1 activates the expression of Otx2 and Gbx2, whose mutual repression defines the position of the MHB boundary. In addition, the interaction between Gbx2 and Oxt2 maintains the expression of FGF8, which in turn activates En1 in the cells coexpressing Irx1 and Oxt2 *(Rhinn and Brand, 2001)*.

Local signalling centers: the Anterior Neural Ridge

Foxg1 is the key transcription factor for the specification of the telencephalon *(Hebert and McConnell, 2000; Shimamura and Rubenstein, 1997; Shimamura et al., 1995; Tao and Lai, 1992)*. Its expression requires inductive signals from a local patterning center, the anterior neural ridge (ANR), which forms early at the rostral end of the neural plate; possibly

through inductive BMP signalling from the surrounding non-neural ectoderm *(Barth et al., 1999; Houart et al., 2002)*. Indeed, the ablation of the ANR results in the loss of the telencephalon *(Shimamura and Rubenstein, 1997)* and telencephalic markers, such as Foxg1, Emx1, Emx2 and Dlx2 *(Houart et al., 1998)*. Conversely, ANR heterotopic transplantation in the posterior prosencephalon induces ectopic expression of telencephalic markers *(Houart et al., 1998, 2002)*. Therefore, the ANR acts as a second organiser and its function is both necessary and sufficient for the induction of telencephalic identity in the surrounding neural tissue.

Interestingly, FGF signalling plays a central role both at MHB and in the ANR. In fact, fragments of prospective anterior neural plate cocultured with FGF8-imbibed beads activates the expression of FoxG1 *(Shimamura and Rubenstein, 1997)*. Moreover, several FGFs are expressed at the ANR, such as FGF3, FGF8, FGF15, FGF17 and FGF18 *(Crossley and Martin, 1995; Maruoka et al., 1998; McWhirter et al., 1997; Shinya et al., 2001)*. Consequently, the effect of FGF8 deletion on telencephalic development is relatively small and limited to the ventral forebrain *(Storm et al., 2006; Theil et al., 2008; Gutin et al., 2006; Storm et al., 2006)*. However, when FGF signalling is tuned down, via ablation of the three main FGF receptors (FGFR1, FGFR2, FGFR3), FoxG1 expression disappears and most telecephalic cells undergo apoptosis, thus mimicking the ablation of the ANR *(Houart et al., 1998; Paek et al., 2009)*. Therefore, Foxg1 and FGF signalling mutually regulate each other and support cell survival and proliferation in the developing forebrain

(Martynoga et al., 2005; Paek et al., 2009; Shimamura and Rubenstein, 1997; Storm et al., 2003).

The double function of FGF signaling in specifying different regions anticipates a central concept about the mechanisms regulating neural patterning: the same molecular machinery of intracellular signaling, when activated in different times and/or in different regions exerts distinct effects. The outcome results form the interaction of different signalings acting in the cell and its previous developmental history. Indeed, the competence of the cell to respond to signaling and the type of modification depends on the current pattern of gene expression.

Finally, as previously mentioned, WNT signalling repression in necessary for the specification of the forebrain *(Heisenberg et al., 2001; Masai et al., 1997; van de Wateret al., 2001)*. Indeed, Spemann's organizer expresses several WNT signalling inhibitors, such as Cerberus, Dikkopf and FrzB, which act in synergy with the neural inducers in the commitment of the prospective neuroectoderm toward and anterior neural identity *(Glinka et al., 1998; Kiecker and Niehrs, 2001; Elkouby et al., 2010; Mukhopadhyay et al., 2001)*. In addition, the expression of Tlc, a WNT signalling inhibitor member of Frizzled-related protein (sFrp), in the anr of the zebrafish is necessary and sufficient for FGF8 expression and telencephalic induction *(Houart et al., 2002)*.

Early telencephalic patterning and development

Several patterning mechanisms establish, prior the closure of the neural tube, two main dorsal (pallial) and ventral (subpallial) domains in the telencaphalic neural plate. The dorsal pallium is subdivied along its dorso-ventral axis in three regions: the medial pallium, which originates the hippocampus and the hem, the dorsal pallium, containing the neocortical primordium, the lateral pallium, where the piriform cortex forms, and the ventral pallium, which contributes to the claustroamygdaloid complex. Moreover, three main regions compose the ventral domain of the telencephalon: the medial ganglionic eminescence (MGE) and the lateral and caudal ganglionic eminescences (LGE, CGE). Each region give rise to different type of interneurons that either form the basal ganglia of the forebrain, including amygdala and accumbens nucleus, or migrate and populate the entire cortex.

After the closure of the neural tube at E9, the anteromedial cerebral pole (ACP) replace the ANR as main organizer of the rostral forebrain. The ACP secretes several FGF factors, such as FGF8, FGF3, FGF15, FGF17 and FGF18, *(Cholfin and Rubenstein, 2008)* which, diffusing along the anteromedial to posterolateral axis of the telencephalon, pattern the surrounding pallial and subpallial tissue *(Cholfin and Rubenstein, 2007, 2008; Fukuchi-Shimogori and Grove, 2001; Garel et al., 2003; Toyoda et al., 2010)*. In particular, the expression of FGF15 and FGF3, excluded from the dorsal midline of the pallium, extends in the ventral telecephalon and is involved in the patterning of the subpallium *(Bachler and Neubuser, 2001; Walshe and Mason, 2003)*. Later in

development, the ACP contributes to the formation of the medial prefrontal cortex, the septum and the commissural plate, which is an anteromedial structure channelling the major commissure of the hemispheres *(Moldrich et al., 2010; Toyoda et al., 2010)*

Consistently with the development of the posterior neural tube, the ventral pattering of the telencephalon is mediated by SHH signalling. Initially expressed by the prechordal mesoderm, underling the prosencephalic neural plate, SHH becomes later expressed also by the ventral midline of the neural plate and establishes the ventral domain of the telencephalon *(Echelard et al., 1993; Rubenstein and Beachy, 1998)*. Indeed, mutation in the SHH signalling profoundly affects forebrain development. In particular, SHH-null mice do not form ventral telencephalic structures nor express ventral markers such as Dlx2, Gsx2, and Nkx2.1 *(Chiang et al., 1996; Fuccillo et al., 2004; Ohkubo et al., 2002; Rallu et al., 2002; Rash and Grove, 2007)*. Whereas, overexpression of SHH in the dorsal telecephalon can induce ectopic expression of ventral markers both in mouse and fish *(Macdonald and Barth, 1995; Ericson et al., 1995; Hauptmann and Gerster, 1996; Kohtz et al., 1998; Shimamura and Rubenstein, 1997)*. Moreover, since SHH is involved in cell proliferation and survival, SHH-null mice show underdeveloped brains and high cell mortality *(Ericson et al., 1995; Litingtung and Chiang, 2000; Ohkubo et al., 2002; Rowitch et al., 1999)*. In addition, SHH expression is essential for the correct formation of bilateral structures such as eyes and hemispheres; therefore, in both mouse and human, mutation in SHH

cause a condition where the forming hemisphere fail to separate, the holoprosencephaly.

The specification of the pallial domain is determined by the transcription factor Gli3. Although it is initially expressed in the entire forebrain, Gli3 becomes progressively restricted to the dorsal telecephalon *(Aoto et al., 2002; Corbin et al., 2003)*. Moreover, the Gli3-mutant mouse lacks both neocortex and hippocampus *(Grove et al., 1998; Kuschel et al., 2003; Theil et al., 1999; Tole et al., 2000)*. Notably, the phenotype of the SHH-null mouse can be rescued by Gli3 loss-of-function. In fact, SHH/Gli3-double mutant mice show normal specification of the ventral telencephalic structures *(Aoto et al., 2002; Rallu et al., 2002; Rash and Grove, 2007)*. Thus, SHH and Gli3 seem to establish the dorsoventral patterning of the telencephalon by mutually repressing each other.

In addition to SHH, the specification of the subpallium requires FGF signalling and the expression of FoxG1. In particular, FoxG1 appears to act downstream SHH; In fact, in both mouse and zebrafish, abrogation of FoxG1 expression results in the loss of the ventral telencephalic identity *(Danesin et al., 2009; Dou et al., 1999; Martynoga et al., 2005; Xuan et al., 1995)* and cannot be rescue by Gli3 loss-of-function Hanashima et al., 2007). Consistently, SHH overexpression does not rescue the phenotype of Foxg1-null mice, although Foxg1 is able, at least partly, to recover ventral development when SHH signalling is repressed *(Danesin et al., 2009)*. Furthermore, telencephalic development is completely abolished in Foxg1/Gli3 double mutant mice,

thus both Foxg1 and SHH are necessary for the development of the ventral and dorsal telencephalon, respectively *(Hanashima et al., 2007)*.

Indeed, FGF signalling plays an important role in both the antero-posterior and in the dorso-ventral patterning of the forebrain. In fact, as previously mentioned, FGF8 and Foxg1 mutually activates each other by creating a positive feedback loop that promotes the development of the ventral forebrain *(Martynoga et al., 2005; Paek et al., 2009; Shimamura and Rubenstein, 1997; Storm et al., 2003)*. Moreover, FGF8 and FGF3 double knockdown completely impairs ventral telencephalic development in zebrafish *(Shanmugalingam et al., 2000; Shinya et al., 2001; Walshe and Mason, 2003)*. Consistently, mice deprived of the two main FGF receptors FGFR1 and FGFR2 and FGF8-null or FGF8 hypomorphic mice share a similar phenotype *(Gutin et al., 2006; Storm et al., 2006)*. Notably, the phenotype of FGFR1/FGFR2 double mutant mice is not rescue by Gli3 loss of function *(Gutin et al., 2006)*. Instead, FGF8 overexpression partly restores ventral development in SHH-null mice (*Okada et al., 2008*).

It appears that both Foxg1 and FGF signalling act downstream the SHH-Gli3 network. In fact, SHH induces both Foxg1 expression and FGF signalling in the developing telecephalon by repressing the dorsal marker Gli3. Moreover, Foxg1 downregulation observed in SHH-null mice is rescued by Gli3 loss-of-function *(Rash and Grove, 2007)*. Similarly, SHH signalling maintains the expression of FGF3, FGF8, FGF15, FGF17, and FGF18 in the anterior medial telecephalon by repressing Gli3 *(Aoto et al., 2002; Kuschel et al., 2003; Rash*

and Grove, 2007; Theil et al., 1999). Overall, SHH signalling promotes ventral development by repressing Gli3, thus shielding foxg1 and FGF signalling, in the subpallium.

Early cortical patterning

The patterning along the anteroposterior axis of the cerebral cortex is mediated by the FGF factors produced by the ACP, the rostral signalling center. In particular, FGF8 forms a rostro-caudal gradient across neocortical epithelium. Moreover, if the expression of FGF8 by the ACP is tuned down, the anterior cortical areas are disrupted and the posterior ones result shifted forward *(Fukuchi-Shimogori and Grove, 2001)*. Coherently, ectopic electroporation of FGF8 in the posterior cortex creates a mirror duplication of the anterior cortical fields *(Fukuchi-Shimogori and Grove, 2001)*. Therefore, FGF8 acts as a morphogen and the ACP functions as the main organizer in the cortical area patterning *(Toyoda et al., 2010)*.

Early after neural induction, the entire neural plate expresses the transcription factor Pax6, which then becomes restricted to the pallium, while the subpallium expresses Nkx2.1 (*Inoue et al., 2000; Corbin et al., 2003)*. Initially, the domains of expression of the two transcription factors meet at the pallial-subpallial border *(PBS)*, while later the homeodomain transcription factor Gsx2 starts to be expressed at the interface *(Corbin et al., 2003)*. The opposite and partly overlapping gradients of Pax6 and Gsx2 define the position of the PBS *(Corbin et al., 2000; Stoykova et al., 2000; Toresson et al., 2000; Yun et al., 2001)*. Indeed,

Pax6 loss of function results in the ventral and lateral pallium expressing subpallial markers, such as Mash1, Gsx2 and Dlx2 *(Kim et al., 2001; Stoykova et al., 1996, 1997, 2000; Toresson et al., 2000; Yun et al., 2001)*.

Consistently, in Gsx2-null mice a portion of the subpallium acquires dorsal identity *(Corbin et al., 2000; Stoykova et al., 2000; Toresson et al., 2000; Yun et al., 2001)*. Moreover, the double knockout mice for Pax6 and Gsx2 only show minor disruption at the PBS, suggesting the mutual antagonistic function of these two transcription factors *(Toresson et al., 2000)*. Notably, Pax6 loss-of-function can rescue the dorsalized phenotype of the SHH-null mice, although lo a lesser extent compared to the loss of Gli3 *(Fuccillo et al., 2006)*. In addition, Gli3 is required for Pax6 expression *(Aoto et al., 2002; Kuschel et al., 2003; Theil et al., 1999)*. Finally, Gli3 and Pax6 interact with each other and with the transcription factor Emx2 in promoting pallial development *(Fuccillo et al., 2006)*. In fact, the expression of Emx2 in the cortical primordium is lost in the Gli3-null mice *(Theil et al., 1999)*, while Gli3 promotes dorsal expression of Emx2 via BMP and WNT signalling *(Theil et al., 2002)*.

As previously mentioned, the roof plate acts as a second organizer in the patterning of the neural tube secreting BMP and WNT factors essential for the acquisition of dorsal identity *(Chizhikov and Millen, 2005; Grove et al., 1998; Basler et al., 1993; Dickinson et al., 1995; Lee and Jessell, 1999; Liem et al., 1995, 1997; Shimamura and Rubenstein, 1997)*. In fact, the telencephalic roof plate originates two dorso-medial structures important in the patterning of the cortical epithelium: the choroid plexus and the cortical hem. The hem expresses the WNT factors

2a, 3a and 5a *(Grove et al., 1998)*, while the expression of several BMP factors comprises the adjacent hippocampal primordium and the choroid plexus, which, in particular, expresses BMP2, 4, 6 and 7 and the BMP signaling downstream targets Msx1 and Msx2, as well *(Furuta et al. 1997; Grove et al. 1998)*. Indeed, choroid plexus and cortical hem fail to form in mice where BMP signaling is blocked *(Hebert et al. 2003; Fernandes et al. 2007)*. Furthermore, BMP-soaked beads injected in forebrain of the developing chick disrupt ventral telecephalic development *(Golden et al., 1999; Spoelgen et al., 2005)*.

The loss of two WNT signaling downstream molecules, Lef1 and Lrp6, disrupts the development of the Dentate Gyrus, while the entire hippocampus is missing if the hem is removed or in WNT3a-null mice *(Galceran et al., 2000; Zhou et al., 2004; Yoshida et al., 2006, Lee et al., 2000b)*. Moreover, constitutive activation of canonic WNT signaling in the developing murine forebrain causes the expansion of the dorsal domain, whereas WNT signaling repression leads to reduced pallial development *(Backman et al., 2005)*. Finally, in chick, WNT signaling appears to be necessary and sufficient for the induction of dorsal telencephalic identity *(Gunhaga et al., 2003)*. Thus, early in neural development WNT signaling represses telencephalic specification and promotes posterior neural identities *(Heisenberg et al., 2001; Masai et al., 1997; van de Water et al., 2001)*, whereas later induces dorsal telencephalic identities *(Gunhaga et al., 2003; Backman et al., 2005)*. The interaction of Pax6 and Emx2 refines the position of the cortical hem and hippocampus within the caudomedial domain *(Kimura et al., 2005)*. In particular, Emx1

and Emx2 have a partly redundant function in specifying the hem and, consistently, the double knockout mice for Emx1 and Emx2 lacks both hem and hippocampus *(Shinozaki et al., 2004)*. Notably, Emx2 appears to be important both in establishing the domain of the hem and as an effector of hem-derived WNT signalling in the surrounding cortical epithelium *(Muzio et al., 2005)*.

Furthermore, the mutual repressive interaction between the FGF factors expressed by the ACP and the BMP factors of the hem further refines the anterior border of the hem/hippocampal domain *(Ohkubo et al., 2002; Shimogori et al., 2004; Storm et al., 2006)*. Indeed, FGF signaling appears to be dispensable for hem specification since the triple knockout mice for the three main FGF receptors *(FGFR1, FGFR2 and FGFR3)* show a telencephalon with dorsal fates correctly specified, although hypomorphic *(Paek et al., 2009)*. In addition, early *in utero* electroporation of FGF8 abolishes WNT expression in the dorsal midline and disrupt hem specification Shimogori et al., 2004. Finally, in the dorsal midline, the expression of Neurogenin (Ngn) and Hes genes regulates the border between hem and choroid plexus *(Imayoshiet al., 2008)*. In fact, Ngn is switched off in the choroid plexus, which starts expressing the Hes genes, while the hem maintains high levels of Ngn expression.

The antihem is a cortical signalling center positioned at the level of the pallial-subpallial border, flanking the cortical epithelium opposite to the hem. The location of the antihem is identified by the expression of different members of the EGF family (Tgfa, Nrg1,and

Nrg3), FGF7 and the WNT signalling antagonist Sfrp2 *(Assimacopoulos et al., 2003; Kim et al., 2001; Kornblum et al., 1997; Kawano and Kypta, 2003; Ladher et al., 2000; Rattner et al., 1997)*. Notably, the rostrolateral (high) to caudomedial (low) graded expression of Pax6 and the opposite gradients of Emx2 and Lhx2 in the cortical epithelium parallel, respectively, the position of the antihem, which extends rostrolaterally, and of the hem, located in caudomedial position *(Assimacopoulos et al., 2003; Grove et al., 1998; Mangale et al., 2008; Bishop et al., 2000; Nakagawa and O'Leary, 2001)*. Moreover, Pax6 and Foxg1 are required for the specification of the antihem *(Assimacopoulos et al., 2003; Kim et al., 2001; Dou et al., 1999; Muzio and Mallamaci, 2005)*. In fact, Foxg1 represses hem specification and Foxg1-null mice show expansion of dorsal fates, while the latero-ventral ones are missing *(Dou et al., 1999; Muzio, L. and Mallamaci A.J., 2005)*. On the contrary, Lhx2 expression represses antihem and hem fate; in fact, both structures expand at the expenses of the cortical epithelium in Lhx2-null mice *(Bulchand et al., 2001; Mangale et al., 2008; Monuki et al., 2001)*. Interestingly, when Lhx2 is removed only in a few patches of cells, those closer to the dorsal midline acquire the identity of hem, while the ones in lateral position, expressing both Foxg1 and Pax6, become antihem *(Mangale et al., 2008)*.

Neocortical development

The neocortex takes up the most part of the cerebral cortex, which includes also the paleocortex, formed by olfactory and piriform cortex, and the archicortex, including entorhinal cortex, subiculum and

hippocampus. Unlike the other regions, the neocortex shows a laminar pattern composed of six layers of neurons, each layer with its own distinct connectivity, morphology and function. In addition, the neocortex comprises different areas and functionally specialized cortical fields, which are closely interconnected with each other although each one is characterized by distinct cytoarchitecture, connections and pattern of gene expression *(O'Leary and Nakagawa, 2002; O'Leary et al., 2007; Rash and Grove, 2006; Sur and Rubenstein, 2005)*. Three of the main cortical areas process primary sensory information: the visual (V1), the somatosensory (S1) and the auditory (A1) areas. The fourth primary cortical area is the motor (M1) area, which controls voluntary movements. The olfactory information is pre-processed by the olfactory bulb and then sent to the olfactory cortex. Between the primary cortices there are several higher order cortical areas, specialized in further processing information related to specific features of a particular modality (e. g. movement perception, motor coordination).

Virtually all the glutamatergic neurons of the neocortex originate from Emx1-positive progenitors in the cortical ventricular zone (VZ). These progenitors give rise to the six cortical layers in an inside-out fashion; thus, the deep layer 6, 5 and 4 are generated first and, subsequently, the upper cortical layers 3 and 2 arise from the VZ and the intermediate progenitors of the subventricular zone (SVZ) *(Gorski et al., 2002; Kriegstein and Noctor, 2004; Mione et al., 1994; Molyneaux et al., 2007)*. The Cajal–Retzius (CZ) neurons, that populate layer 1, are generated in specific niches, such as hem, antihem, septum and subpallium, rather

than the VZ and then migrate tangentially spreading across the entire neocortex. Most of the GABAergic neurons of the neocortex, which makes up to 20% of the total neurons, originate in the ventral telencephalon (LGE and CGE) and migrate during development populating the entire pallium *(Ang et al., 2003; Marin and Rubenstein, 2003; Nery et al., 2002)*, although in primates a significant proportion of cortical interneurons are generated locally *(Letinic et al., 2002)*. Several transcription factors show overlapping and graded pattern of expression in the VZ and SVZ along the A/P and M/L axes, uniquely encoding the position and specifying the area identities of the cortical progenitors. Among these transcription factors of particular relevance in the cortical arealization are: Emx2, Sp8, CoupTF1 and Pax6 *(reviewed in: O'Leary, D.D. and Sahara O, 2008)*.

Several morphogens, secreted in a timely and localized fashion by different cortical patterning centers, are responsible for the fine regulation of these patterns of transcription. For instance, the FGF factors (FGF8, 17 and 18) secreted by the commissural plate (CoP), a structure derived from the anterior neural ridge, promote the expression of anterior cortical markers, such as Sp8, while repressing the expression of the posterior cortical markers Emx2 and COUP-TF1 *(Crossley and Martin, 1995; Garel et al., 2003; Storm et al., 2006)*. Consistently with its expression in the posterior cortical areas, Emx2 loss of function results in the expansion of the rostro-lateral cortex at the expenses of the caudo-medial (visual) areas, which, in turns, are greatly reduced in size *(Simeone et al., 1992; Bishop et al., 2000; Mallamaci et al., 2000a,2000b)*.

Moreover, conditional knockout of Sp8, normally expressed by progenitors in a high anterior- medial to low posterior-lateral gradient, results in an anterior shift of cortical markers, suggesting that Sp8 specifies identities of frontal/motor cortical areas *(Hamasaki et al., 2004)*. Interestingly, Sp8 is required for the maintenance of FGF8 expression in the CoP *(Sahara et al., 2007; Zembrzycki et al., 2007)*. Therefore, since FGF signalling expression greatly influences cortical area patterning, the shift in markers observed in the Sp8 conditional KO could either be due to a direct role of Sp8 in specifying the anterior cortical progenitors, or to a decreased secretion of FGF8 by the CoP. Consistently, loss of Emx2 results in the expansion of the FGF8/17 domain in the forebrain *(Fukuchi-Shimogori and Grove, 2003)*. Furthermore, Emx2 represses the ability of Sp8 to bind to the upstream elements in FGF8 promoter, thus suppressing the transcriptional activation activity of Sp8 and limiting the expression of FGF8 to the CoP *(Sahara et al., 2007; Zembrzycki et al., 2007)*. COUP-TFI is an orphan nuclear receptor expressed in a high posterior-lateral to low anterior-medial expression gradient by both progenitors and cortical neurons. Coup-TF1 conditional knockout by crosses to an Emx1-Cre line in early, E10, cortical progenitors results in a massive expansion of the frontal/motor areas at the expenses of most of the parietal and occipital cortex *(Liu et al., 2000)*. Thus, these results suggest that COUPTF1 is required to balance the patterning of the neocortex repressing the frontal/motor cortical identities in the parietal and occipital cortex *(Armentano et al., 2007)*. Finally, the autocrine secretion of FGF10 by cortical progenitors promotes their symmetric division, thus increasing their number and delaying differentiation

(Sahara and O'Leary, 2009). Consequently, manipulation of the FGF-signaling greatly influence both cortical arealization and brain size. *(Fukuchi-Shimogori and Grove, 2001; Garel et al., 2003; Storm et al., 2006; Sahara and O'Leary, 2009)*.

Hippocampal development

The hippocampus arises from the invagination of the dorsal midline of the telencephalon, adjacent to the cortical hem, at E8.5. The boundaries between the choroid plexus, cortical hem and hippocampus are defined early in development by the non-overlapping expression of molecular markers signatures. In fact, Msx1 and BMP4/7 are strongly expressed by the choroid plexus *(Grove et al., 1998, Bulchand et al., 2001)*, while the cortical hem expresses high level of WNT3a, WNT2 and WNT5, whose signalling is essential for the correct development of the hippocampus *(Grove et al.,1998)*. In particular, the analysis of the Gli3-mutant mouse is paradigmatic of the interplay of different signaling pathways in the development of the nervous system. In fact, the expression of Gli3 by the cranial mesenchyme represses SHH signaling in the dorsal telencephalon thus regulating also BMP and WNT expression. Indeed, in the Gli3-null mouse WNT3a expression by the cortical hem is compromised and the hippocampal development is defective. *(Grove et al., 1998; Grove and Tole, 1999; Lee et al., 2000)*. Consistently, experiments in which the cortical hem is ablated or hem-dependent WNT expression is abrogated showed the crucial role of the cortical hem in the hippocampal development. In addition, if the transcription factor Lhx2

is ablated in the neocortical cells surrounding the cortical hem, these acquire a cortical hem identity. Indeed, Lhx2 expression specifies the neuroepithelium toward a neocortical identity and represses alternative fates *(Bulchand et al., 2001; Mangale et al., 2008)*.

The hippocampus comprises three different fields: the Dentate Gyrus, the CA1 and CA3 layers. Each one of these regions has its own cellular composition and morphology, connectivity and expresses specific molecular markers. In particular, KA1 expression, a glutamate receptor subunit, is detectable as early as E14.5 in the CA3, while SCIP, a POU-domain transcription factor, is expressed in the CA1 starting from E15.5. However, the specification of the different hippocampal fields precedes the expression of any known marker. In fact, hippocampal explants harvested from E12.5 embryos correctly and autonomously upregulate the expression of the field-specific markers. *(Lee et al., 2000; Tole and Grove, 2001)*. The cortical hem is also the main source of Cajal Retzius cells (CZ). These are among the first neurons to appear at E10 and later migrate dorsolaterally populating the preplate and influencing the development of the hippocampal connections *(Del Rìo et al., 1997)* and the organization of the surrounding cortical tissues *(König et al., 1977, 1981; Del Rìo et al., 1995)*. Moreover, the CZ cells, arising also from the PSPB and the septum, secrete the glycoprotein Reelin, which is crucial for the correct neurogenesis and lamination of the cortex *(Zhao et al., 2004)*.

Likewise, hippocampal pyramidal neurons are generated starting from E10 in partially overlapping waves and gradients *(Bayer,*

1980); however, unlike cortical neurogenesis, in rodents new neurons are generated in the hippocampus long after birth. The pyramidal neurons of the CA1-3 originate in the VZ of the hippocampus and then migrate toward the pial surface on a glial scaffold *(Nadarajah et al., 2001)*, while the DG cells arise from a smaller and specialized region close to the fimbria, the dentate neuroepithelium *(Danglot et al., 2006)*.

Neurogenesis in the DG starts at E10 *(Deguchi et al., 2011)*, reaches a peak at E16 and continues in the first postnatal week *(Bayer, 1980)*. In addition, the generation of the first, deep layer neurons of CA1 and CA2 starts at E11 and peaks at E15 *(Stanfield and Cowan, 1979; Bayer, 1980)*, while CA3 neurons arise later (E12) and reach their maximum one day earlier (E14) *(Angevine, 1965)*. Upon leaving the VZ, migrating hippocampal neurons display an multipolar morphology *(Tabata and Nakajima, 2003)* and sojourn for 2-4 days in the subvetricular zone before continuing their migration *(Altman and Bayer, 1990b)*. Moreover, CZ cells play an important role in orchestrating neuronal migration. In fact, the DG cells originated in the dentate neuroepithelium, migrate tangentially in a sub-pial stream, attracted to the DG region by the Sdf1 factor secreted by CZ cells and become visible in the DG at E18. Just before birth, at E20, DG cells migrate radially and form the upper blade of the DG *(Barry et al., 2008)*. Finally, five days after birth (P5) both DG blades are formed and proliferating neuroblasts reside in the inner sub-granular zone of the DG.

In addition, interneurons residing in the hippocampus are generated between E12 and E13 in the medial and the caudal ganglionic

eminences (MGE and CGE, respectively) of the ventral telencephalon *(Pleasure et al., 2000; Wichterle et al., 2001; Nery et al., 2002; Tricoire et al., 2011)* and migrate toward the hippocampal primordium following similar routes of migration of the cortical interneurons. The first interneurons reach the CA1-CA3 fields at E16 and later, at E17, the DG primordium *(Manent et al., 2006)*. Consistently with their common ventral origins, Dlx1-null mice show almost complete loss of both hippocampal and cortical interneurons.

MicroRNAs in neural development

MiRNAs, small non-coding RNAs, are transcribed as primary miRNAs (pri-miRNAs) and then processed into precursor miRNAs (pre-miRNAs) and mature miRNAs with an average 22 nucleotides in length. Most miRNAs target the 3' UTR of mRNAs suppressing their translation *(reviewed by Ha and Kim, 2014; Krol et al., 2010)*; although both miRNAs binding to other regions of target mRNAs *(Broughton JP et al., 2016)* and small RNAs having positive effect on gene expression *(Vasudevan S; 2012)* have been reported. In addition, miRNAs play a critical role in animal development *(reviewed by Fu G. et al., 2013; Ines Alvarez-Garcia and Miska E.A., 2005; Stefani G. and Slack F.J., 2008)* and several human disease are linked to miRNAs aberrant expression *(reviewed by Tüfekci et al., 2014; Prosenjit et al., 2018)*.

In particular, miRNAs have been described regulating several processes occurring during vertebrate neural development *(Krol et al., 2010; Rajman M. and Schratt G., 2017)*, such as patterning and specification of neural progenitors, neurogenesis and plasticity of mature neurons *(Coolen and Bally-Cuif, 2009; Fineberg et al., 2009; Bian and Sun, 2011; Luikart et al., 2012; Schouten et al., 2012)*. For instance, miR-7a has an expression gradient opposed to Pax6 in the ventricular walls of the developing telencephalon, restricts Pax6 expression in the dorsal forebrain and controls the development of dopaminergic neurons in the olfactory bulb *(De Chevigny et al., 2012)*. Nurr1, a transcription factor important in the specification of dopaminergic neurons, is similarly regulated by miR-132 *(Yang et al., 2012)*. Consistently, some miRNAs help establishing specific cell types during neural development. In fact, inhibition of miR-181a and miR-125b impairs the differentiation of human stem cells differentiation in dopaminergic neurons *(Stappert et al., 2013)*, while miR-9 regulates FoxP1 expression in motor neuron development and altered miR-9 expression changes the columnar identities in developing chick spinal cords *(Otaegi et al., 2011)*. In addition, several studies have analysed global miRNA expression during *in-vivo* neurogenesis identifying time specific *(Barca-Mayo and De Pietri Tonelli, 2014; Lv et al., 2014; Miska et al., 2004; Nielsen et al., 2009; Yao et al., 2012)*, regionally restricted *(Anderegg et al., 2013)* and cell type-specific *(Paridaen and Huttner, 2014; Ghosh et al., 2014)* miRNAs and suggesting a post-transcriptional miRNA-mediated regulation of the switch from neurogenesis to gliogenesis in the radial glia.

Global loss of miRNA regulation via conditional knock-out (CKO) of Dicer shed light on the role of miRNAs in cortical and retinal development *(De Pietri Tonelli et al., 2008; Kawase-Koga et al., 2009; Nowakowski et al., 2011)*. Dicer CKO studies revealed profound effects on cortical histogenesis and layering; although early inactivation of Dicer in the developing brain generally leads to induction of apoptosis and extensive cell death, since several components of the DNA-damage response signal-transduction network are regulated by miRNAs *(Bailey et al., 2010)*. Early (E8) Dicer deletion under FoxG1 promoter leads to decreased expression of radial glia markers Nestin, Sox9 and ErbB2, abnormal migration of newborn neurons and expansion of Tbr2-expressing basal cortical progenitors *(Nowakowski et al., 2011)*. Consistently, loss of function of the Tbr2-targeting miRNA miR-92b results in an increase of Tbr2-positive neural progenitors, while miR-92b gain of function shows opposite effects *(Nowakowski et al., 2013)*. Similarly, Dicer CKO around E10 under Emx1 or Nestin promoters showed overproduction of early-born subcortical projection neurons and reduced number of late-born upper-layer callosal cortical neurons compared to control *(De Pietri Tonelli et al., 2008; Kawase-Koga et al., 2009)*. Moreover, Dicer removal in post-mitotic neurons did not impair cortical layering and only resulted in reduced dendritic development *(Davis et al., 2008)*. Thus, miRNAs are involved in fine-tune cell fate during corticogenesis and miRNAs loss-of-function affects different cell types and layers at different times.

Finally, during retinal development in *Xenopus* several key transcription factors specifying late retinal cell identity are regulated at the translational level. In fact, multipotent retinal progenitor cells express since early retinogenesis the transcript of the transcription factors Xotx5b, homolog of the mammalian homeobox gene Crx and specifying the late photoreceptor fate, Xotx2 and Xvsx1, homolog of Otx2 and Vsx2, respectively, and specifying bipolar cells fate *(Viczian et al., 2003; D'Autilia et al., 2006; Decembrini et al., 2006)*. However, the translation of these transcription factors is inhibited until later stages, when photoreceptor and bipolar cells are generated, by a cell-cycle dependent post-transcriptional mechanism mediated by miR-129, miR-155, miR-214, and miR-222 *(Decembrini et al., 2006)*. These four miRNAs are highly expressed in early retinal progenitors and progressively downregulated as retinogenesis procedes and the cell-cycle of the retinal progenitors lengthens *(Alexiades and Cepko, 1996, Decembrini et al., 2009; Pitto and Cremisi, 2010)*.

In conclusion, several miRNAs regulate the translation of key transcription factors involved in the ordered generation of the different types of neurons during corticogenesis and retinogenesis. In fact, competence of retinal progenitor in *Xenopus* is strictly regulated by a network of miRNAs, while Dicer loss-of-function in CKO mice strongly suggest miRNAs control of the competence of cortical progenitor cells as well. These results lead to the intriguing possibility that the transcripts of key genes specifying for different neuronal identities may be already present in early neural progenitors, conferring them

multipotency and priming them to differentiate into different kind of cells upon release from the translational inhibition *(Cremisi F., 2013)*.

Embryonic pluripotent stem cells

As previously described, pluripotency is the ability to generate all the cells of the developing embryo (including the germ line) and it is the defining feature of the cells of the inner cell mass (ICM) of the blastocyst. Although transient and ephemeral propriety of the early embryo, pluripotency can be captured and maintained *in vitro*. In fact, ICM cells from pre-implantation embryos can be harvested and expanded in culture as embryonic stem cells (ESCs) for an extended period retaining their pluripotency and self-renewal (*Evans and Kaufman, 1981; Wu, J. et al., 2016*). The pluripotent nature of mouse ESCs was defined through several functional assays, including the formation of chimeric animal with germline transmission after blastocyst injection, the ability to form teratomas *in vivo*, the multilineage differentiation capacity *in vitro* and the tetraploid complementation assay (*Evans and Kaufman., 1981; Martin G., 1981; Matsui et al., 1992*). By contrast, ESCs derived from the epiblast of the post-implantation embryos, which are termed epiblast stem cells (epiSCs), represent a more advanced developmental state, that is a "primed" state of pluripotency *(Brons, I. G. et al., 2007; Tesar, P. J. et al., 2007; Yali H. et al., 2012; Yoji K. et al., 2014; Jun W. et al., 2015)*. In fact,

although able to form chimeric blastocyst, epiSCs do not contribute to the germ line *(Brons, I. G. et al., 2007; Tesar, P. J. et al., 2007)*.

A few core regulatory genes are responsible for the maintenance of the pluripotent state and form the main hub of the highly interconnected pluripotency gene regulatory network *(Young R. A. et al., 2011; Ng H. H. and Surani M. A., 2011)*. Among these genes, OCT4, uniquely expressed in ES and primordial germ cells, is necessary for pluripotency both *in vivo* and *in vitro (Scholer, H. R. et al., 1989; Nichols, J. et al. 1998; Niwa, H. et al., 2000)*.

Sox2 is required for OCT4 expression and for the formation of the epiblast *(Avilion, A. A. et al., 2003; Masui, S. et al., 2007)*. Abrogation of OCT4 or SOX2 expression results in trophoectodermal differentiation, while their overexpression leads to the differentiation of ESC in mesendoderm or neural ectoderm, respectively *(Niwa, H. et al., 2000; Thomson, M. et al., 2011)*. NANOG is a core transcription factor for its pivotal role in establishing pluripotency in the ICM and its ability to enable LIF-indipendent pluripotency *in vitro (Mitsui, K. et al., 2003; Chambers, I. et al., 2003, 2007; Silva, J. et al., 2009; Suzuki, A. et al., 2006)*.

In addition, several studies showed that the overexpression of certain combinations of core pluripotency genes in somatic cells can override the epigenetic mechanism maintaining the cellular fate and restart the pluripotency machinery, thus obtaining induced pluripotent stem cells or iPSCs *(Takahashi, K. and Yamanaka, S., 2006; Gonzalez and Izpisua Belmonte, 2011)*.

We are able to derive and maintain ESCs activating the signalling pathways upstream the core transcription factors of pluripotency. In fact, ESCs were originally derived on a feeder layer of inactivated fibroblasts in presence of serum, thus supplying the cells with LIF, WNT and BMP factors *(Evans and Kaufman, 1981; Martin G., 1981; Young, R. A. et al., 2011)*. *In vivo* pluripotency is not a steady condition, rather a metastable state of the epiblast in the path toward terminal differentiation. Thus, to achieve unlimited self renewal capacity *in vitro*, we have to contrast the natural tendency of ESCs toward differentiation. In fact, the expression of the pluripotency transcription factors Oct4 and Sox2 leads to the activation of FGF4, which in turns promote the differentiation of ESC toward mesoderm and neuroectoderm via ERK signalling pathway *(Kunath, T. et al., 2007; Yuan, H. et al., 1995)*. The presence of LIF and BMP in the medium counteracts the pro-differentiation effect of the endogenous FGF4, thus stabilizing the pluripotent state of ESCs. In particular, LIF signalling is mediated by STAT3, which promotes self renewal of ESCs activating the downstream targets genes Klf4 and Tfcp2l1. Both these genes are required for selfrenewal and supports LIF-independent self-renewal when overexpressed *(Niwa, H. et al., 2009; Martello, G. et al., 2013; Ye, S. et al., 2013)*. Finally, STAT3 signalling inhibits mesodermal differentiaton, while BMP signalling and its downstream effectors, the Inhibitor of Differentiation (ID) proteins, suppress the differentiation toward neuroectoderm *(Chen, C. Y. et al., 2015; Ying, Q. L. et al., 2003)*.

The knowledge of the signalling pathways implied in establishing and maintaining pluripotency allowed us to devise a strategy to replace serum in stem cell culture. In fact, we can culture ESCs in a medium supplemented with PD0325901, a small molecule inhibitor of the pro-differentiation signalling MAPK-ERK, and CHIR99021, a glycogen synthase kinase 3 (GSK3) inhibitor *(Ying, Q. L. et al., 2008)*. In particular, both FGF4-ERK signalling and GSK3 inhibition activate Klf2, an essential gene of the pluripotency circuit *(Yeo, J. C. et al., 2014; Qiu, D. et al., 2015)*. Overall, ESCs cultured in dual inhibition (2i) medium show an uniform expression of pluripotency genes, efficient chimera formation and germline transmission, reduced expression of differentiation-associated genes and a global hypomethylation profile similar to the epigenetic profile of the naïve epiblast of the blastocyst *(Ying, Q. L. et al., 2008; Marks, H. et al., 2012; Boroviak, T. et al., 2014)*. By contrast, primed pluripotent stem cells (epiSCs) require fibroblast growth factor 2 (FGF2) and activin A signalling to self-renew *in vitro*. Moreover, epiSCs show lower expression of NANOG and Klf4, bivalent epigenetic marks at the regulatory elements of lineage-assosiated genes, female X-chromosome inactivation; and a poor contribution to blastocyst chimaeras *(Brons, I. G. et al., 2007; Tesar, P. J. et al., 2007)*. Finally, similarly to epiSCs, the *in vitro* self-renewal of human ESC rely on Activin A and FGF2 signalling, suggesting that human ESC are in a primed state of pluripotency as well *(Kojima, Y. et al., 2014; Wu, J. et al., 2015)*.

Neuralization of embryonic stem cells

When cultured in low-density, serum-free and feeder-free conditions, in absence of any exogenous growth factor, mESCs readily differentiate into NPCs, neural progenitor cells *(Tropepe et al., 2001, Ying et al., 2003)*. Thus, mESC behaviour closely matches the behaviour of dissociated animal cap experiments in *Xenopus*, supporting a model of default neural induction for the mammal as well *(Muñoz-Sanjuán I. and Brivanlou A. H., 2002; Smukler et al., 2006; Levine A. J. and Brivanlou A. H., 2007; Gaulden J. and Reiter J. F., 2008)*. That is, mES are fist committed toward an anterior neural fate and successively patterned by caudalizing factors to acquire a more posterior neural identity *(Stern, 2001)*. In fact, mESCs cultured at low density (to reduce the autocrine signalling) and in absence of exogenous posteriorizing factors (such as RA, WNT of FGF signalling) spontaneously acquire an anterior neural identity *(Pankratz et al., 2007, Watanabe et al., 2005. While the addition of growth factors to the medium steers the differentiation of mES toward midbrain/hindbrain (Kawasaki et al., 2000; Perrier et al., 2004)* and spinal cord *(Li et al., 2005; Wichterle et al., 2002)* fates. Moreover, consistently with the amphibian neural induction, the neural conversion of ESCs can be promoted blocking the endogenous BMP signalling which induces non-neural fates *(Pera et al., 2004; Tropepe et al., 2001; Ying et al., 2003; Chambers et al., 2009)*. Indeed, several studies, showed the importance of RA, BMP and WNT signalling in the acquisition of posterior neural identity in both murine and human ESC *(Nakamura et al., 2007; Watanabe*

et al., 2005 Bouhon et al., 2006; Ikeda et al., 2005; Kawasaki et al., 2000; Lee et al., 2000;,Mizuseki et al., 2003; Perrier et al., 2004; Salero and,Hatten, 2007; Watanabe et al., 2005; Wichterle et al.,2002). In addition, mESC-derived NPCs differentiationg *in vitro* first generate neurons and successively glial cells, showing the same temporal regulation of their *in vivo* counterpart *(Okada et al., 2004, Asano et al., 2009; Zhang et al., 2001)*. Finally, differentiating mESCs generate the different cortical cell types following the same timely regulated sequential neurogenic waves observed *in vivo (Eiraku et al., 2008; Gaspard et al., 2008; Bertacchi et al., 2013)*, showing the spatial-temporal conservation of the neural differentiation both *in vitro* and *in vivo (Shen et al., 2006)*.

Whether cultured in suspension as EB or as attached monolayer, differentiating ESCs give rise to Sox1+, Pax6+ and nestin+ neural rosettes closely resembling the early embryonic neural tube. *(Perrier et al., 2004)*. When dissociated and replated, ESC-derived neural rosettes give rise to nestin+, Sox1+, Sox2+, Pax6+, and Mushahi-1+ NPCs, which subsequently differentiate into a heterogeneous mixture of different subtypes of neurons (GABAergic, dopaminergic, serotonergic, and cholinergic), astrocytes, and oligodendrocytes *(Barberi et al., 2003; Zhang et al., 2001)*. Although protocols exist which allow to enrich this mixture of specific neural subtypes *(Barberi et al., 2003)*, the positional identity of these cells is often ignored. Indeed, specific neural subtypes such as the cholinergic neurons are present in different areas of the adult brain and show distinct gene expression profiles, connectivity patterns, electrophysiological proprieties and morphologies. Thus,

understanding how to obtain a precise subtype of neuron, patterned with the proper temporal and positional identity is pivotal and might have considerable repercussion on possible clinical applications.

As previously mentioned, the forebrain, comprising telencephalon and dienchephalon, arises from the anterior end of the neural tube where the caudalizing action of WNT and RA signalling are actively repressed. Indeed, mESC cultured as adherent monolayer in a chemically defined minimum medium supplemented with WNT and/or BMP signalling inhibitors acquire an anterior neural identity and expresses the forebrain marker FoxG1 *(Aubry et al., 2008; Ideguchi et al., 2010; Watanabe et al., 2005; Bertacchi et al., 2013, 2015)*, whereas the treatment with RA completely abolishes the induction of this gene. In particular, the treatment with WNT inhibitor increases the percentage of FoxG1/Pax6 double positive cells expressing the dorsal cortical markers Emx1+, while SHH treatment increases the number of Foxg1+ cells expressing Gsh2- and Nkx2.1 *(Watanabe et al., 2005; Bertacchi et al., 2015)*, which are markers of the medial and lateral ganglionic eminences, respectively.

The ganglionic eminences, transitory structures forming during development in the ventral telencephalon, give rise to the basal ganglia of the forebrain (striatum, substantia nigra, pallidum, and subthalamic nucleus), which are implied in different neurodegenerative diseases, such as Parkinson disease (dopamine producing neurons of the substantia nigra) and Huntington disease (striatal neurons). In general, most of the neurons originated in the ganglionic eminences belong to

the GABAergic subtype and express GABA, Gad6, Darpp32, Arpp21, calbindin, or calretinin *(Aubry et al., 2008)*. Accordingly, mESC cultured in medium supplied with WNT antagonist and then treated with SHH become GABAergic neurons, express Gad6 and secrete GABA upon stimulation *(Watanabe et al., 2005; Laeng et al., 2004; Aubry et al., 2008; Bertacchi et al., 2015)*.

ESC can be committed toward cortical fate making use of stromal feeder layers *(Ideguchi et al., 2010)* or cell aggregation *(Eiraku et al., 2008)*. However, these methods do not consent the identification of the signals responsible for ESC specification. Indeed, ESC cultured as monolayer in a chemically defined culture medium at a very low density acquire anterior forebrain identity, while the inhibition of SHH signalling allows to obtain dorsal telencephalic neurons *(Gaspard et al., 2008)*. However, other authors have shown that the inhibition of SHH signalling is dispensable at higher cellular densities *(Bertacchi et al., 2013, 2014, 2015)*. Indeed, several studies demonstrated that mouse and human ESCs cultured in a chemically defined culture medium, devoid of any added morphogen, differentiate into cortical pyramidal/projection neurons *(Anderson and Vanderhaeghen, 2014; Eiraku et al., 2008; Espuny-Camacho et al., 2013; Gaspard et al., 2008; Shi et al., 2012; van den Ameele et al., 2014; Vanderhaeghen, 2012; Michelsen et al., 2015; Bertacchi et al. 2014;2015; Terrigno et al., 2018a; 2018b)*. Finally, convenient manipulation of WNT signalling specifies differentiating murine and human ESC toward a medial dorsal telencephalic and hippocampal fate *(Terrigno et al., 2018a; Sarkar et al., 2018)*. Finally, FGF8 treatment of ESC-

derived dorsal telencephalic progenitors induces anterior motor cortical identity *(Terrigno et al., 2018b; Eiraku et al., 2008)*.

Clinical applications of pluripotent stem cells

ESC-derived neurons hold great promises for their clinical applications: such as the production of autologous neurons for the replacement of damaged neural tissues in neurodegenerative diseases, the repair of spinal cord lesions and the possibility to create *in vitro* models to assess the efficiency of drugs and therapies. Notwithstanding these potential applications, there are numerous challenges that will limit the clinical use of stem cells in the near future. In fact, ESC-derived neurons have to match the precise subtype, positional and temporal identity of the lesioned neural tissue. Besides this, concerns arise from the intrinsic tumorigenic potential of stem cells, primary due to the remaining of undifferentiated stem cells *(Hiromi K. et al., 2010; Satoshi N. et al., 2015)*. Despite these issues, several differentiation protocols using human ESC have proven to be safe for human transplantation, due to the longer differentiation time and, consequently, the lower percentage of residual pluripotent cells *(reviewed in Knoepfler P.S., 2009; Ben-David U. and Benvenisty N., 2011)*.

Indeed, several studies showed that ESC-derived neurons transplanted in different experimental models of brain damage can efficiently integrate and even promote functional recovery *(Chiba et al.,*

2004; Friling et al., 2009; Kim et al., 2002; Kriks et al., 2011; Lamba et al., 2009; Ma et al., 2012; Roy et al., 2006; Tabar et al., 2005; Yang et al., 2008; Michelsen et al., 2015, Espuny-Camacho et al., 2013; Terrigno et al., 2018a; Hargus et al., 2010; Wernig et al., 2008; Weick et al., 2010, 2011). In fact, matured hESC-derived neurons expressing the optogenetic receptor hChR2 functionally integrate in the host neural network after transplantation and can stimulate nearby host neurons *(Weick et al., 2010)*. Furthermore, follow-up studies showed that these neurons were able to modulate the activity of mouse cortical networks *in vitro (Weick et al., 2011)*.

Consistently, hChR2-expressing mES-derived motor neurons implanted in a mouse model of sciatic nerve damage, induced muscles twitching upon light stimulation *(Bryson et al., 2014)*. Finally, murine induced dopaminergic neurons (iDA) activated via chemogenetic DREDD receptor showed ulterior behavioural improvement *(Dell'Anno et a., 2014)* in PD mouse model. Intriguingly, optogenetic silencing of grafted dopaminergic neurons re-introduced the pre-transplantation behavioural deficit, mimicking the effect of a chemical re-lesioning.

Among the first clinical application of ESC to clinic, the Spinal Cord injury cell replacement therapy with hES-derived Oligodendrocyte progenitor cells proved to be effective in preclinical animal studies, promoting the remyelination of animal with acute spinal cord lesion *(Keirstead et al., 2005; N.C Manley et al. 2017)*; was successively declared safe for human testing by the FDA *(Alper J., 2009)* and it is currently in phase 1/2a of the clinical trial *(Manley NC et al., 2017; Priest CA et al., 2015)*. In addition, several other applications of ESC have

already been submitted for clinical trial approval, including clinical trials for eye disease, diabetes and heart disease *(Trounson, A. and McDonald, 2015; Ratcliffe, E., Glen, K. E., Naing, M. W. and Williams, D. J 2013; Kimbrel, E. A. and Lanza, R, 2015;)*. In particular, a phase 1 clinical trial involving 13 men with unilateral stroke was recently concluded: the men received a single intracelebral injection of CTX0E03, an immortalised human neural stem-cell line, showed no adverse events and a median improvement two years after the procedure of two points in the National Institutes of Health Stroke Scale (NIHSS) score *(Dheeraj K. et al., 2016; Borlongan C. V., 2016)*.

Ischemic stroke

In a stroke, regions of the brain experience sudden death due to lack of oxygen when the blood flow to the brain is lost by blockage or rupture of an artery. Stroke is the second leading cause of death worldwide, according to the World Health Organization *(Johnson W. et al., 2016)*; besides, it carries heavy social and economic burdens due to quality of life decay and familial impacts. Unfortunately, post-stroke rehabilitation is limited and only effective treatments and therapies are thrombectomy and infusion with tPA, tissue plasminogen activator, to breakdown blood clots in the acute phase *(Yamashita T. et al., 2011)*.

Because of the oxygen deprivation, the integrity of the blood-brain-barrier (BBB) is compromised following stroke. The BBB is an

important barrier formed by the interaction of neural, glial and vascular cells that regulates the transcellular molecular trafficking through the vascular endothelium *(Begley DJ et al., 2003; Abbott N. J. et al., 2006; Obermeier B. et al., 2013; Schoknecht K. et al., 2015)* and the leukocyte movements into and out of the central nervous system *(Ransohoff R.M. et al., 2012)*. The oxidative stress to the tight-junction proteins between the endothelial cells caused by reperfusion, that is the restoration of the blood flow following stoke, weakens the BBB *(Pop V. and Badaut J., 2011; Jiao H. et al., 2011)*, causing infiltration of immune cells *(Aktas O et al., 2007)*, secretion of inflammatory interleukins *(Kono H. and Rock K.L., 2008)* and eventually leading to complete vascular disruption *(Krueger M. et al., 2015)*. The ischemic lesion causes the stimulation of the innate immune response *(Kono H. and Rock K.L., 2008)*, polarizing the resident microglia cells toward the pro-inflammatory M1 phenotype. This in turn activates an inflammatory cascade, by secreting tumor necrosis factor-alpha (TNF-α), interleukin-1 beta (IL-1β) and reactive oxygen species *(Taylor R.A. and Sansing L.H., 2013)* and further exacerbates the damage to the CNS *(Gendron A. et al., 2002)*. Though post-stroke neuroinflammation contributes to the damage caused by the ischemic injury, it plays also an important role in promoting removal of debris and dying cells via phagocytosis *(Wattananit S. et al., 2016; Nathan C. and Ding A., 2010)*. Indeed, monocyte depletion in acute stroke impairs functional recovery *(Wattananit S. et al., 2016)*. Besides immune cells infiltration, serum proteins and fluids penetrate in the brain parenchyma through the damaged BBB causing vasoactive edema and amplifying the damage to the tissue *(Petrovic-Djergovic D. et al., 2016)*.

Moreover, the ischemic damage to the neurons causes failure in neurotransmitter reuptake, leading to excess extracellular glutamate and excitotoxicity *(Lipton P., 1999, Jin K.L. et al., 2006)*.

Although limited, spontaneous post-stroke recovery occurs *(Nakagomi T. et al., 2011; Jin K.L. et al., 2006; Yu T.S. et al., 2016)*. In particular, functional recovery and plasticity are strongly influenced by angiogenesis, the formation of new blood vessels from existing ones, in the ischemic penumbra, the tissue surrounding the core of the ischemic lesion *(Krupinski J. et al., 1994; Plate K.H. et al., 1999; Wei L. et al., 2001; Yu SW et al., 2007; Liu XS et al., 2007; Chen J. et al., 2003)*. Indeed, angiogenesis after ischemic lesion promotes blood supply, removal of debris and dead cells and produces attracting and homing diffusible signals, promoting endogenous neural stem cells proliferation and migration *(Arenillas JF et al., 2007; Wang YQ et al., 2009)*. Moreover, angiogenesis is coupled with increased endogenous neurogenesis *(Kernie S.G. and Parent J.M., 2010; Kokaia Z. and Lindvall O., 2003; Jin KL et al., 2006; Zhang R. et al., 2004)* and active proliferation of NSC in the SVZ and migration toward the site of vascular remodelling *(Thored P. et al., 2007)*. Concurrently, newborn NSCs can further stimulate angiogenesis via secretion of VEGF, vascular endothelial growth factor *(Lacar B. et al., 2012; Teng H. et al., 2008)*. Finally, ischemic insult induces proliferation of astrocytes, which play an important role in recovery, secreting neurotrophins and vascular growth factors *(Goss JR et al., 1998; Weidemann A et al., 2010)* and forming the glial scar, a glial formation in the stroke penumbra containing the lesion and inflammatory molecules,

promoting post-stroke revascularization *(Goss JR et al., 1998; Weidemann A et al., 2010; Huang L. et a., 2014; Roitbak T and Sykova E, 1999; Becerra-Calixto A and Cardona-Gomez GP, 2017)*.

Cell therapy in stroke

Indeed, the primary goal of cell transplantation therapies in stroke is functional replacement of the lost neural tissue. However, preclinical evidence suggests that transplanted NSCs improve post stroke outcome via by-stander effect due to the secretion of molecules promoting neuroprotection, immunomodulation and neoangiogenesis rather than actually replacing lost cellular circuits *(De Feo D. et al., 2012; Andres R.H. et al., 2011)*. Indeed, NSC-secreted brain derived neurotrophic factor (BDNF) is the major player in promoting neuroprotection and functional recovery following stroke *(Emanueli C., 2003; Lee HJ et al., 2010; Schabitz WR et al., 2007; Lim JY et al., 2008)*. Moreover, NSC-derived VEGF induces endothelial proliferation *(Leung DW et al., 1989; Gerber HP et al., 1998)* and has neuroprotective effect after ischemic injury *(Hayashi T et al., 1998; Kaya D et al., 2005; Sun Y et al., 2003)*. In addition, ciliary neurotrophic factors, glial cell-derived neurotrophic factors and other neurotrophins secreted by NSCs exert an important neuroprotective effect *(Huang EJ and Reichardt LF, 2001; Yuan M et al., 2013)*.

Neural stem cell transplantations in the acute phase, 48h, after stroke significantly decrease inflammation, BBB damage and

improve long-term outcome *(Huang L et al., 2014; Eckert A. et al., 2015; De Feo D. et al., 2012; Zhang T. et al., 2017; Smith HK and Gavins FN, 2012; Bacigaluppi M. et al., 2009; Chang DJ et al., 2013)*. In fact, NSCs transplanted early in the hippocampus of mice with media artery occlusion (MCAO) migrated toward the lesion and reduced the size of the infarcted tissue, BBB damage, microglia activation and secretion of pro-inflammatory interleukins, such as IL-6 and IL-1β *(Huang L et al., 2014)*. Consistently, transplantation of NSCs derived from human iPSCs 24h after ischemic insult decreased BBB leakage and IgG levels in the brain parenchyma *(Eckert A. et al., 2015)*. Indeed, several evidences suggest that NSCs can protect CNS from damage decreasing inflammatory molecules such as TNF-α, MCP-1, IL-1β, IL-6 and Iba-1 and dampening the inflammatory cascade *(De Feo D. et al., 2012; Smith HK, Gavins FN, 2012; Bacigaluppi M. et al., 2009)*. In addition, rats and mice receiving hNSCs transplant in the acute phase after stroke showed improved neurological outcome and functional recovery already two weeks after transplantation *(Huang L et al., 2014; Eckert A. et al., 2015; Ryu S et al., 2016; Sakata H et al., 2012)*.

Indeed, NSCs transplants facilitate post-stroke recovery also by improving angiogenesis and secreting VEGF, as showed by several studies *(Ryu S et al., 2016; Sakata H et al., 2012; Tang Y. et al., 2014)*. Furthermore, studies show that NSC-mediated functional recovery is partly due to production of newborn neurons or stimulation of endogenous neurogenesis *(Eckert A. et al., 2015 , Song M. et al., 2015; Tang Y. et al., 2014; Mine Y. et al., 2013; Cho T et al., 2002; Flax JD et al., 1998;*

Chu K. et al., 2003, 2004; Jeong SW et al., 2003; Zhang JJ et al., 2017). In fact, rodents receiving hNSC after stroke showed increased neuroblast proliferation in the ipsilateral SVZ and migration toward the lesion *(Mine Y. et al., 2013)*. Moreover, hNSC differentiated in astrocyte and reduced infarct volume *(Song M. et al., 2015, Tang Y. et al., 2014; Chu K. et al., 2003; Zhang JJ et al., 2017)*. Notably, also iPSC-NSCs transplanted several days after the ischemic insult (chronic stroke phase) showed higher VEGF levels and increased angiogenesis *(Chau M. et al., 2014; Moriyama Y et al., 2013)*. Similar results were obtained with CTX0E03, a human immortalized NSC line in rodents *(Pollock K. et al., 2006; Hassani Z. et al., 2012; Stroemer P. et al., 2009)* and men *(Dheeraj K. et al., 2016)*. Indeed, several preclinical post-stroke transplantation studies showed that hNSC differentiate in mature and electrophysiologically functional neurons, integrating in the host tissue and improving functional and behavioural recovery *(Oki K et al., 2012, Chau M. et al., 2014; Jin K. et al., 2011; Jin K et al., 2010; Hassani Z. et al., 2012; Stroemer P. et al., 2009)*. However, these studies show that several days after the transplant only a small number of neurons are generated by transplanted cells, which mostly expressed the neural progenitor marker Nestin rather than the neural marker TuJ-1 *(Eckert A. et al., 2015)*. Therefore, neural replacement is not the main component of the beneficial effect derived by NSCs grafting.

AIM OF THE RESEARCH

Aim of this work was to manipulate *in vitro* the endogenous morphogens involved in the early neural patterning of the Neural Tube (BMP, WNT, FGF) in differentiating mouse ESCs and characterize their effect on the positional identity of the ES-derived neurons. In particular, using this experimental approach, we assayed the role of WNT signaling in establishing isocortical rather than hippocampal identity, and the interaction between FGF signaling and miRNA-mediated RNA interference in regulating the arealization of embryonic cortex.

The modification of existing methods of *in vitro* neuralization and patterning of pluripotent cells, by fine-tuning the signaling pathways that normally orchestrate the acquisition of distinct types of neuronal identities during embryonic brain development, has allowed the production of neurons with specific identities *(Hansen et al., 2011; Lupo et al., 2014)*. In fact, there is growing evidence indicating that neural cells generated *in vitro* by mouse embryonic stem cells (ES) acquire distinct positional identities through the fine regulation of specific pathways of intracellular signaling *(Van den Ameele et al., 2014; Chuang et al., 2015; Lupo et al., 2014)*. Neural cells with a global gene expression

profile resembling naive embryonic cortical cells can be generated by inhibiting BMP and WNT signaling pathways that are otherwise endogenously active in neuralizing mouse ESCs *(Bertacchi et al., 2013, 2015)*.

Cortical area patterning is a developmental process generating different positional identities along the antero-posterior (A/P) and medio-lateral (M/L) axes of the dorsal telencephalon in mammals, and is achieved by the establishment of expression gradients of key transcription factors, such as Pax6, Sp8, Emx2, and COUP-TFI *(Greig et al., 2013; Sansom and Livesey, 2009; Alfano and Studer, 2013)*. In particular, the orphan nuclear receptor COUP-TFI plays a pivotal role during area patterning, as its cortical inactivation causes the most severe areal disorganization in postnatal neocortices described so far, leading to a massive expansion of the primary motor area at the expense of the somatosensory cortex *(Armentano et al., 2007; Alfano et al., 2014)*. Moreover, Fibroblast growth factor (FGF) 8 is a diffusible morphogen acting as a key organizer of the early neocortical area map *(Storm et al., 2006; Fukuchi-Shimogori and Grove, 2001; Assimacopoulos et al., 2012)*. In fact, FGF8 forms an anterior to posterior gradient by diffusing across the mouse neocortical primordium from a discrete source in the rostromedial telencephalon *(Toyoda et al., 2010)*. Thus, FGF8 regulates area identity by acting on downstream area mapping genes expressed in progenitors *(Sansom et al., 2005; Assimacopoulos et al., 2012)*. While FGF8 induces Sp8 expression anteriorly, it also downregulates Emx2 and COUP-TFI expression, that would otherwise promote the

development of posterior neocortical identity *(Borello et al., 2014; Sansom et al., 2005; Alfano and Studer, 2013)*. However, among the known mechanisms that mediate FGF8 signaling, the alteration of COUP-TFI gradient has the most striking consequences for area patterning *(Bertacchi et al., 2018)*. A crucial role of FGF8 is thus to repress COUP-TFI rostrally by establishing a low anterior to high posterior expression gradient in the neocortical primordium *(Garel et al., 2003; Storm et al., 2006; Alfano and Studer, 2013)*, but the molecular mechanisms of this inhibition are still not well understood. Aim of the project was the investigation of a miRNA-mediated molecular machinery accounting for the effects of FGF8 on COUP-TF1.

The ability to obtain virtually any particular type of neuronal identity starting from pluripotent cell cultures has generated new expectations of feasible and reliable protocols of neuronal cell transplantation for the potential treatment of many different neurodegenerative diseases. In fact, neurons suitable for transplantation must be able to integrate into the host tissue, produce the appropriate type of neurotransmitter and neurotransmitter receptors, and develop functional synapses with the host neurons. All these capabilities are normally displayed by *in vitro* produced neurons *(Espuny-Camacho et al., 2013; Michelsen et al., 2015; Yu et al., 2014)*. However, a crucial requirement for successful transplants is the ability of transplanted neurons to generate specific connections with functionally relevant targets.

Notably, so far, the regional identity of the neurons produced *in vitro* through the neuralization of pluripotent cells has mainly been established by their molecular characterization through variable degrees of analysis of their gene expression, ranging from the simple study of their neurotransmitter phenotype *(Eiraku et al., 2011; Shi et al., 2012; Shiraishi et al., 2017; Yu et al., 2014)* to a deeper investigation of their molecular nature by methods of global gene expression analysis *(Bertacchi et al., 2013, 2015a, 2015b; Edri et al., 2015; Espuny-Camacho et al., 2013; Van de Leemput et al., 2014; Yao et al., 2017)*. Even so, ascertaining the identity of a nerve cell produced *in vitro* by the comparison of its global gene expression profile to that of neurons *in vivo* is very useful but not sufficient. Indeed, the expression of markers of different positional identities in the CNS often depends on the developmental time of the analysis, thus making a given combination of markers specific to a type of neural cell only in a narrow time window.

Certainly, crucial aim for cell replacement protocols is the ability to produce the wanted type of neural cell to be replaced. However, the molecular identity of a neural cell by itself might not be predictive of its ability to extend appropriate projections and contact the right targets once transplanted *in vivo* and the adult brain is the favorite host structure for assaying this ability in transplantation experiments. Isocortex and hippocampus are main targets of neurodegenerative diseases, thus making them attractive candidates for cell replacement studies *(Iqbal et al., 2015; Poewe et al., 2017)*. The hippocampus is a natural niche of adult neurogenesis and a source of newly formed neurons that

are capable to form new connections in adult brain *(Eriksson et al., 1998; Van Praag et al., 2002)*. This makes hippocampus the region of choice to assay the ability of *in vitro* produced neural cells to make projections and to send them to appropriate targets. Eventually, the similarity of isocortex and hippocampus in terms of developmental origin makes the isocortex an ideal brain structure to be compared with hippocampus in transplantation studies.

In conclusion, reproducing *in vitro* the developmental repertoire of neural progenitor cells giving rise to different cortical areas offers a unique tool for studying the molecular signals regulating key genes of area patterning in a dish. Therefore, we aimed to assay the differential capability of neural cells obtained *in vitro*, which show a molecular identity of precursor cells of isocortex or hippocampus, to generate long range specific projections after transplantation in adult healthy or damaged brain. Indeed, the molecular identity acquired *in vitro* by neuralized ESCs dramatically affects their ability to form projections when transplanted in distinct brain regions.

In addition, we investigated the regulation of COUP-TFI protein and COUP-TFI mRNA expression in cultures of ES cell-derived neural cells. We first found that COUP-TFI protein levels are inhibited by the administration of FGF8, thus indicating the persistence of a molecular machinery coupling FGF8 signaling and COUP-TFI expression *in vitro*. Surprisingly, we observed that the inhibition of COUP-TFI levels by FGF8 occurred principally at the translational level and identified two main FGF8-induced microRNAs (miRNAs) targeting

the COUP-TFI 3'UTR. Finally, one of the *in vitro* characterized miRNAs conserved its ability to inhibit COUP-TFI during cortical development *in vivo*, indicating that our *in vitro* cellular model can be successfully adopted to gain insight into new developmental mechanisms required for proper neocortical area patterning.

RESULTS

Establishing isocortical or hippocampal identity via timely manipulation of WNT and BMP

As previously discussed, WNT and BMP signaling profoundly affects the fate of prosencephalic cells. In fact, during development, their repression is first required for acquiring a dorsal telencephalic identity. Subsequently, the dorsal midline of the telencephalic vesicle invaginates forming the median wall of the hem and the choroid plexus (Fig S1A). Secreted WNT factors from the hem are necessary for establishing the hippocampal identity in the adjacent presumptive cortex *(Lee et al., 2000; Machon et al., 2007)*. Therefore, we assayed the effect of inhibiting or activating the two signaling pathways during defined time windows of the ES cell neuralization protocol (Fig 1A; DIV: days of *in vitro* neuralization).

Neuralizing ESCs required combined WNT/BMP inhibition for acquiring a dorsal telencephalic molecular identity *(Bertacchi et al., 2015b; Yao et al., 2017)*. This is shown by the relative expression of antero-posterior (A/P) embryonic CNS markers (Fig 1B) in WNT/BMP double inhibited cells (WiBi cells) compared to control cells (Fig 1C). Notably,

double WNT/BMP inhibition was no longer required after DIV8 to induce the expression of the telencephalic markers FoxG1 and to repress the expression of the posterior markers Irx3, Otx2, En1 and Krox20. However, the reactivation of WNT signaling from DIV8 by CHIR treatment (CHIR 8 cells, Fig 1C) exerted a significant activation of Emx1 and Emx2 together with low expression of Irx3, Otx2, En1 and Krox20, and significant expression of FoxG1.

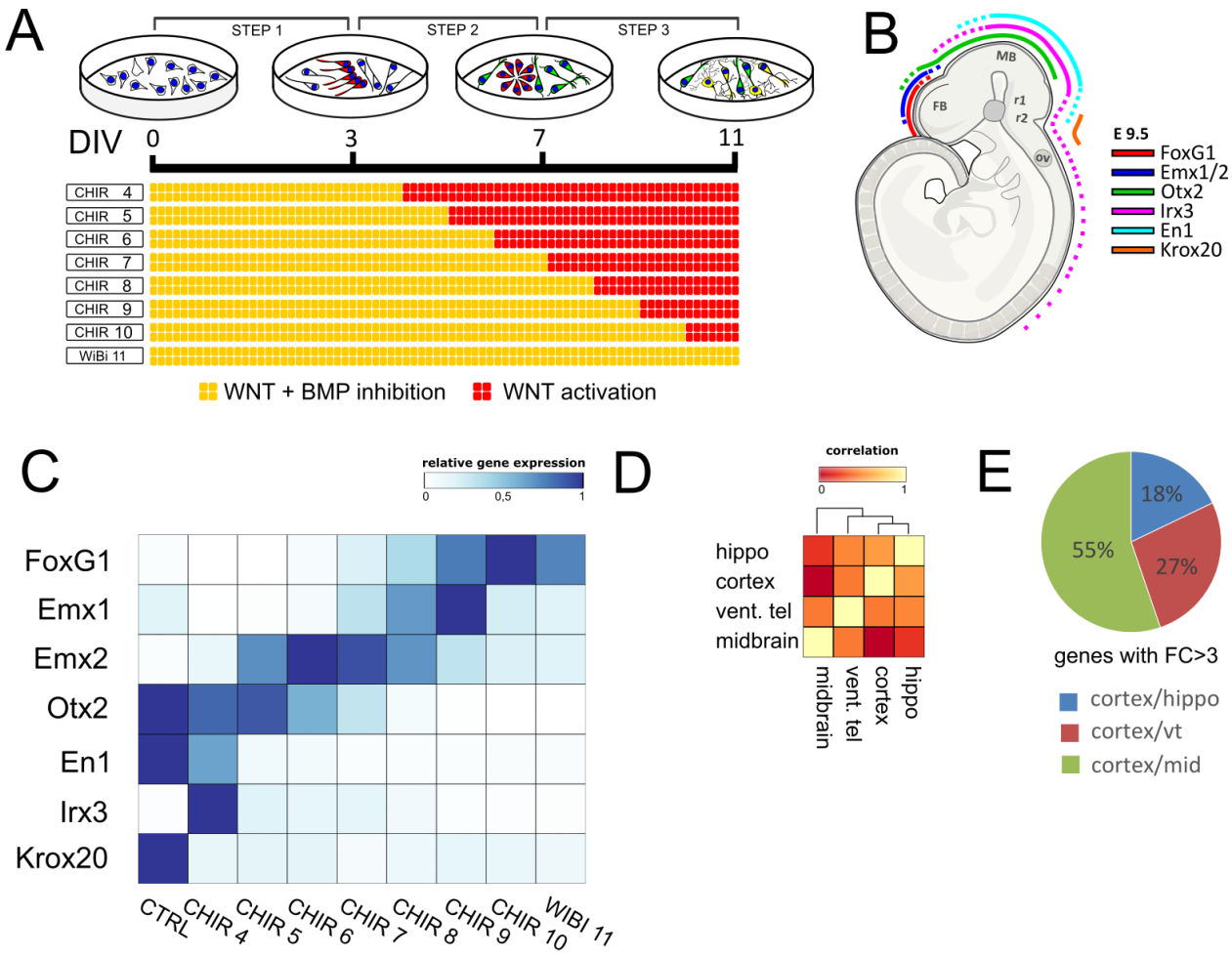

Figure 1. Timely regulation of WNT and BMP signaling affects the regional identity of ES cell-derived neurons

A, Scheme of the ES cell differentiation protocol. DIV, days of *in vitro* differentiation. **B**, Schematic drawing of an E9.5 embryo with the domains of expression of A/P markers. **C**, color map shows the mRNA fold change of the A/P markers in **B**, as evaluated by RT-PCR in ES cell-derived neurons. n = 3 independent experiments were pooled together and analyzed by qRT-PCR; each experiment contained n = 2 *in vitro* technical replicates. **D-E**, Global gene expression analysis of embryonic E15.5 regions: isocortex, hippocampus, midbrain and ventral telencephalon. Explants from three embryos were pooled together. **D**, Color map showing hierarchical clustering analysis of the distribution of Pearson correlation among transcriptome subsets of different embryonic brain regions. The subset of transcriptome analyzed consists of the 487 genes with the highest variance among samples (top 2%). Ctx, isocortex; hip, hippocampus; mes, mesencephalon; vt, ventral telencephalon. **E**, Pie chart reporting the % of genes with a 3 fold differential expression between isocortex and the other embryonic regions.

Accordingly, CHIR treatments beginning before DIV 8 (CHIR 4-7) posteriorized the identity of cells, while CHIR treatments after DIV8 (CHIR 9-10) were less effective in sustaining Emx2 expression. Emx1 and Emx2 are expressed in a similar caudal-rostral gradient in the E9.5 embryonic cortex, both are highly expressed in the developing archicortex and Emx2 expression is crucial for hippocampal development *(Fukuchi-shimogori and Grove, 2003; Theil et al., 2002; Yoshida et al., 1997)*. Moreover, CHIR treatment before DIV8 (CHIR 5-7) dramatically increased the expression of the markers of hem and choroid plexus Lmx1a and Ttr *(Imayoshi et al., 2008; Kuwamura et al., 2005; Millonig et al., 2000)*, while decreasing the dorsal telencephalic marker Lhx2 *(Monuki et al., 2001; Subramanian et al., 2009)* (Fig S1A-B).

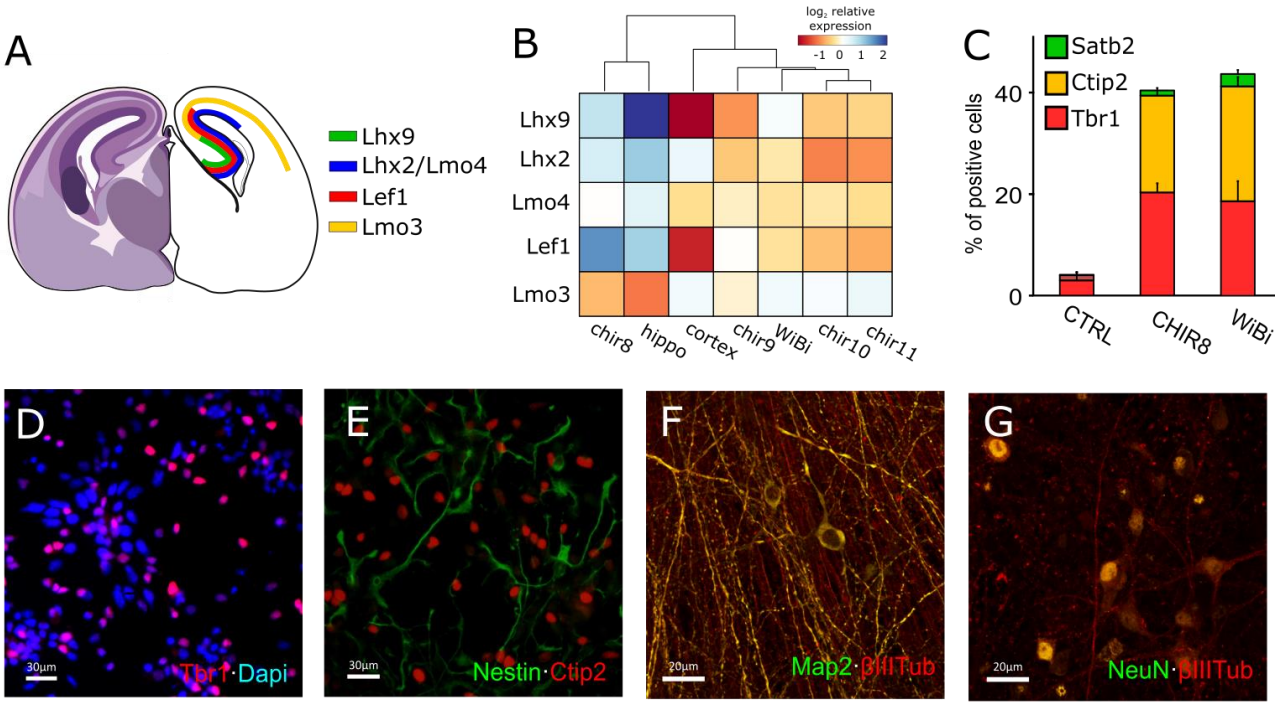

Figure 2 WNT signaling manipulations activate the expression of isocortical or hippocampal markers in neuralized ESCs

A, Schematic drawing of an E15.5 coronal section at the hippocampal level, showing the domains of expression of markers differentially expressed between isocortex and hippocampus. **B**, RT-PCR analysis of expression of the markers of hippocampal and isocortical identity shown in A, in ES cell-derived neurons. Color map show log2 mean-centered expression. n = 3 independent experiments were pooled together and analyzed by qRT-PCR; each experiment contained n = 2 *in vitro* technical replicates. **C**, Percentage of control (0.1% DMSO) and CHIR8 and WIBI cells positive for the dorsal telencephalic markers Satb2, Ctip2 and Tbr1. **D-G**, Immunocitodetection (ICD) of different neuronal markers in CHIR8 cells. Tbr1 and Nestin: DIV 13; Map2 and NeuN: DIV 25.

Isocortex and hippocampus are two dorsal telencephalic structures with common developmental origin and very similar profiles of gene expression. A main feature distinguishing them is the later development of hippocampus and its persistent neurogenesis in the adult. We performed gene expression profiling and compared the global gene expression of mouse E15.5 hippocampus, isocortex, midbrain and ventral telencephalon. Accordingly, we found higher correlation of hippocampus and isocortex compared to midbrain or ventral telencephalon (Fig 1D-E).

A few markers of positional identity are known to be differentially expressed between embryonic hippocampus and isocortex *(Abellán et al., 2014)* (Fig 2A). The analysis of these markers (Lhx2, Lhx9, Lmo3, Lmo4 and Lef1) suggested an hippocampal rather than a posterior isocortical identity of CHIR 8 cells (Fig 2B). In addition, CHIR-treated cells showed the expression of the dorsal telencephalic markers Tbr1, Ctip2 and Satb2 and Tbr2 (Fig 2C-E, S1C), as well as the expression of the neuronal terminal differentiation markers βIII Tubulin, NeuN and Map2 (Fig 2F,G). To further characterize the molecular identity of the cells in which WNT/BMP signaling was continuously inhibited (WiBi cells) or cells in which WNT/BMP signaling was reactivated from DIV 8 (CHIR 8 cells), we compared their global gene expression profiles with the profiles of embryonic cells by PCA and clustering analysis (Fig 3A,B). The 2nd and the 3rd components of PCA discriminated between E15.5 isocortex, striatum, hippocampus, midbrain and cells treated with WiBi CHIR at different times. While WiBi-treated cells located closer to

isocortex and striatum, CHIR-treated cells were closer to hippocampus (Fig 3A). Notably, the most significant loadings of the third component, that better separated hippocampus and isocortex, showed a significant clustering of WiBi and CHIR8 cells to E15.5 isocortex and hippocampus, respectively (Fig 3B). All in all, our results indicate that the differential activation from DIV 8 of one single signaling, WNT, induced a molecular identity of hippocampus (CHIR 8 cells) instead of isocortex (WiBi cells).

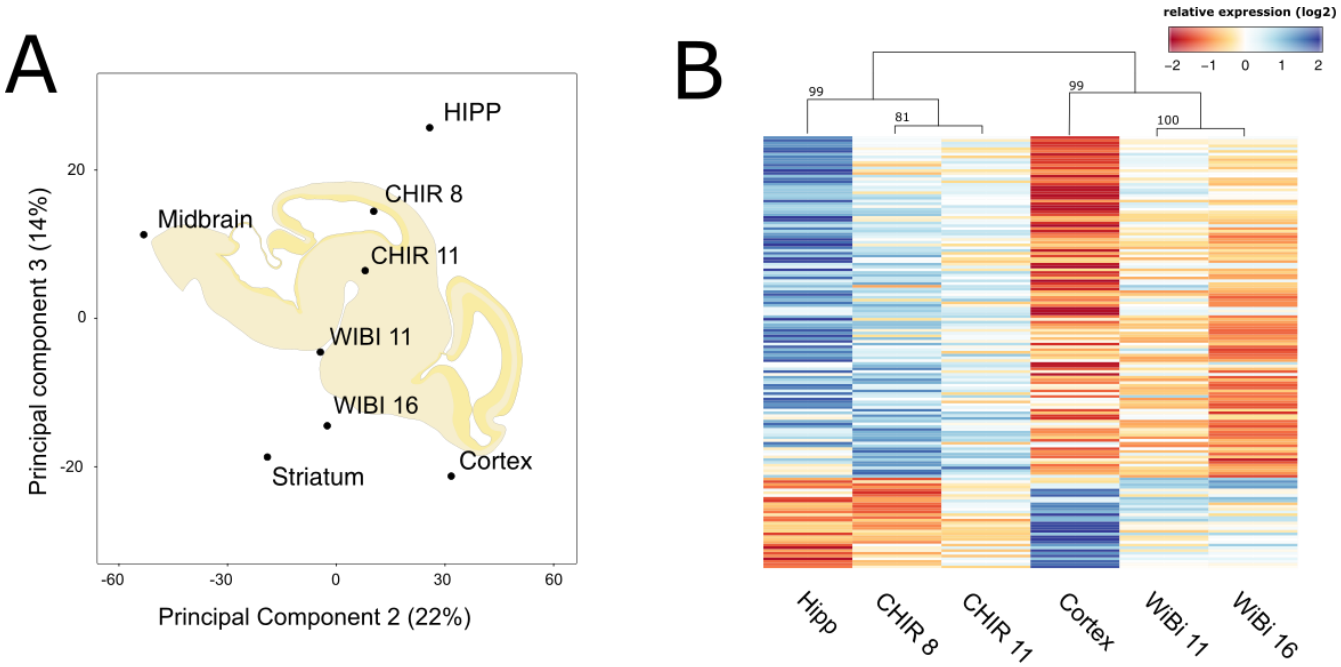

Figure 3 WNT signaling induction or repression induce, respectively, hippocampal or isocortical global gene expression profile in neuralized ESCs

A, PCA of the first quartile of most differentially expressed genes (n=3145) among WiBi cells, CHIR cells and E15 embryonic regions shown in labels (see Experimental Procedures). n = 3 independent cell cultures or embryonic explants for each treatment/embryonic region were pooled together. **B**, Color map and hierarchical

clustering (pearson correlation) of the top 5% (n=157) loadings of the third PCA component shown in A. Clustering scores were computed via multiscale bootstrap resampling (pvclust, see Materials and Methods). Scale indicates log2 mean-centered gene expression.

ESC-derived hippocampal cells send long range projections to Dentate Gyrus targets

We compared the behavior and projection pattern of the neural precursor cells produced via different WNT/BMP signaling manipulation after grafting *in vivo*. First, we labeled WiBi and CHIR8 cells by lentiviral transduction with prenylated forms of EGFP and mCherry. Before transplantation, cells were treated with DAPT and AraC to force their differentiation and negatively select dividing progenitors, respectively (see Materials and Methods). The two types of cells were first co-injected into the Dentate Gyrus (DG) of 2 months old mice (Fig 4A), because this is a niche of adult neurogenesis *(Eriksson et al., 1998; van Praag et al., 2002)* and it is also a permissive environment for the extension of new neuronal processes. One month after injection, both WiBi and CHIR8 cells persisted in the host tissue (Fig 4B), showing expression of the terminally differentiated neuronal marker NeuN (Fig S2B-C). Importantly, one month after grafting the proportions of NeuN/GFP and NeuN/Cherry double positive cells in the transplant remained unchanged, suggesting an equal survival ratio for both cell

types (Fig S2A). While isocortical cells were not able to extend long processes, only CHIR8 cells displayed abundant projections outside the graft, already one month after transplantation (Fig. 4C-G). These projections mainly contacted the ipsilateral CA3, CA1, subiculum and entorhinal cortex (Fig 4C-G). Fibers appeared to form potential synaptic contacts, as shown by staining with the vesicular glutamate transporter vGlut1 (Fig S2D).

Isocortical cells can send far-reaching projections when transplanted in adult motor cortex

When transplanted into adult motor cortex (Fig 5A), both WiBi and CHIR 8 cells persisted at least two months after injection and their ratio remained unchanged (Fig 5B, S2E-G). As in the case of transplantations in hippocampus, CHIR8 cells were able to efficiently extend projections, either inside the cortex (Fig 5C-E,F,H-I;K-L) or toward extra-cortical regions (Fig 5G, J, M). WiBi cells transplanted in adult motor cortex were also able to extend processes. However, they generated far-reaching processes less efficiently than CHIR8 cells one month after transplantation (Fig 5C-J).

Interestingly, two months after grafting WiBi cells were even more effective than CHIR8 cells in extending processes within the motor cortex (Fig 5K,L) and almost as efficient as them in sending axons to extra-cortical targets (Fig 5M).

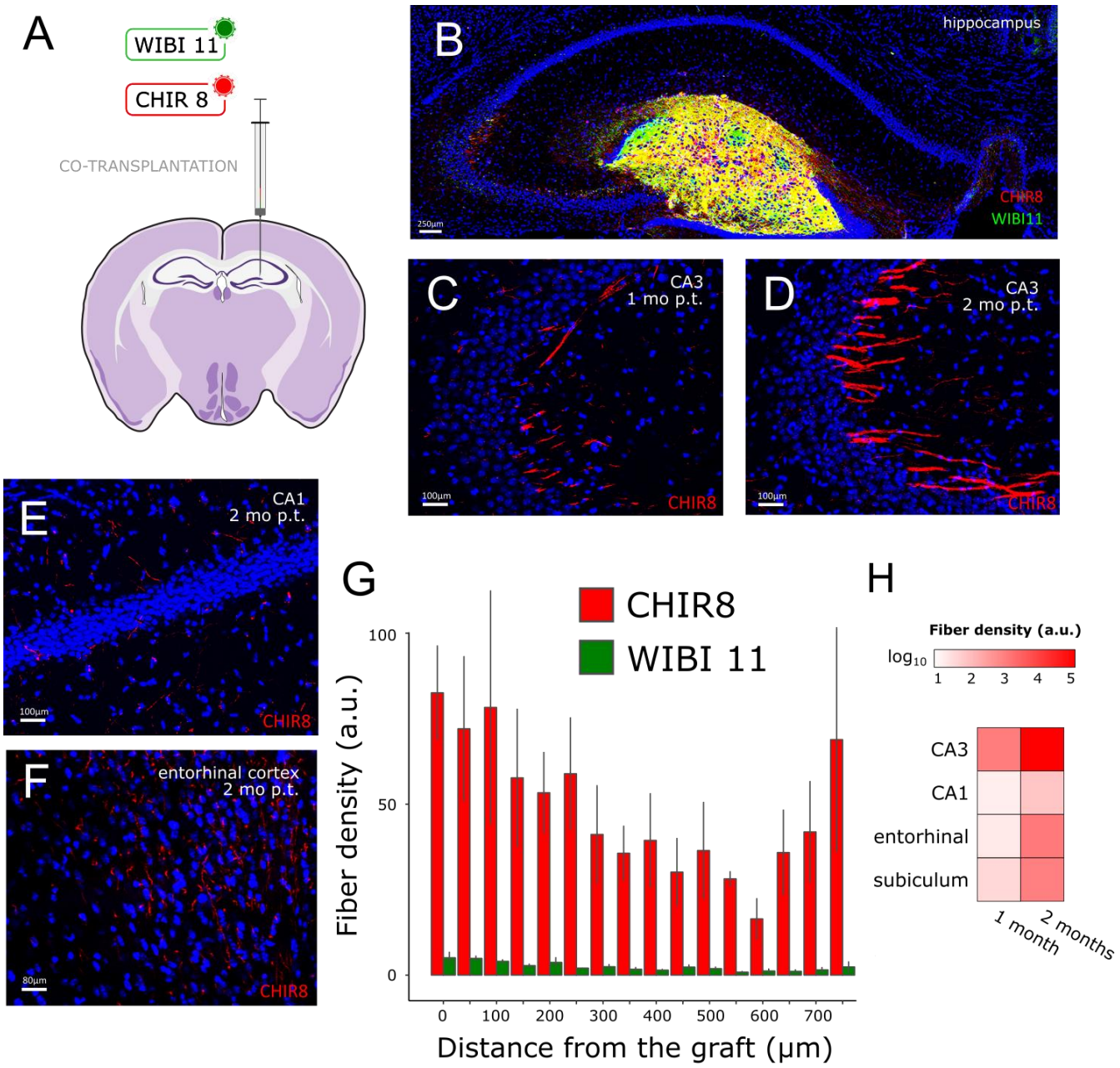

Figure 4 Cell transplantation in hippocampus

A, Method and site of cell grafting. **B**, ICD of CHIR8 (red) and Wibi cells (green) 3 months post-transplantation (mo p.t.) in hippocampus. Blue, Hoechst nuclear counterstaining. **C-F**, ICD of CHIR8 and Wibi fibers at different times post-

transplantation and in different regions, as indicated by labels. **G**, Density of Wibi and CHIR8 fibers at different distances from the graft, one month after transplantation. a.u., arbitrary units; error bars, SD. **H**, Heat map of CHIR8 fiber density in different hippocampal regions one and three months after cell grafting. N≥ 3 transplanted animals for each time point were analyzed.

Specifically, while WiBi and CHIR8 cells shared most of the cortical and subcortical targets, some regions such as the piriform cortex ($p < 0.01$), the auditory cortex ($p < 0.01$), the visual cortex($p < 0.05$), the entorhinal cortex ($p < 0.05$) and the hippocampal formation ($p < 0.01$) were mostly targeted by CHIR8 cells (Fig 5L-M and Fig 7), indicating cell-specific axonal outgrowth. We also analyzed other subcortical targets including the thalamus, midbrain and corticospinal tract, but we could not detect significant projections for either cell type. Altogether, these results indicated that cortical cells are slower than hippocampal cells in extending far-reaching axons when transplanted into the isocortex.

One important issue is whether the projection patterns of ES-derived neurons resemble those of hippocampal and cortical cells derived from mouse embryos. To this aim, we co-transplanted fetal (E 15.5) cortical and hippocampal neurons into the hippocampus (Fig S4A-F) or motor cortex (Fig S5A-F) of adult mice.

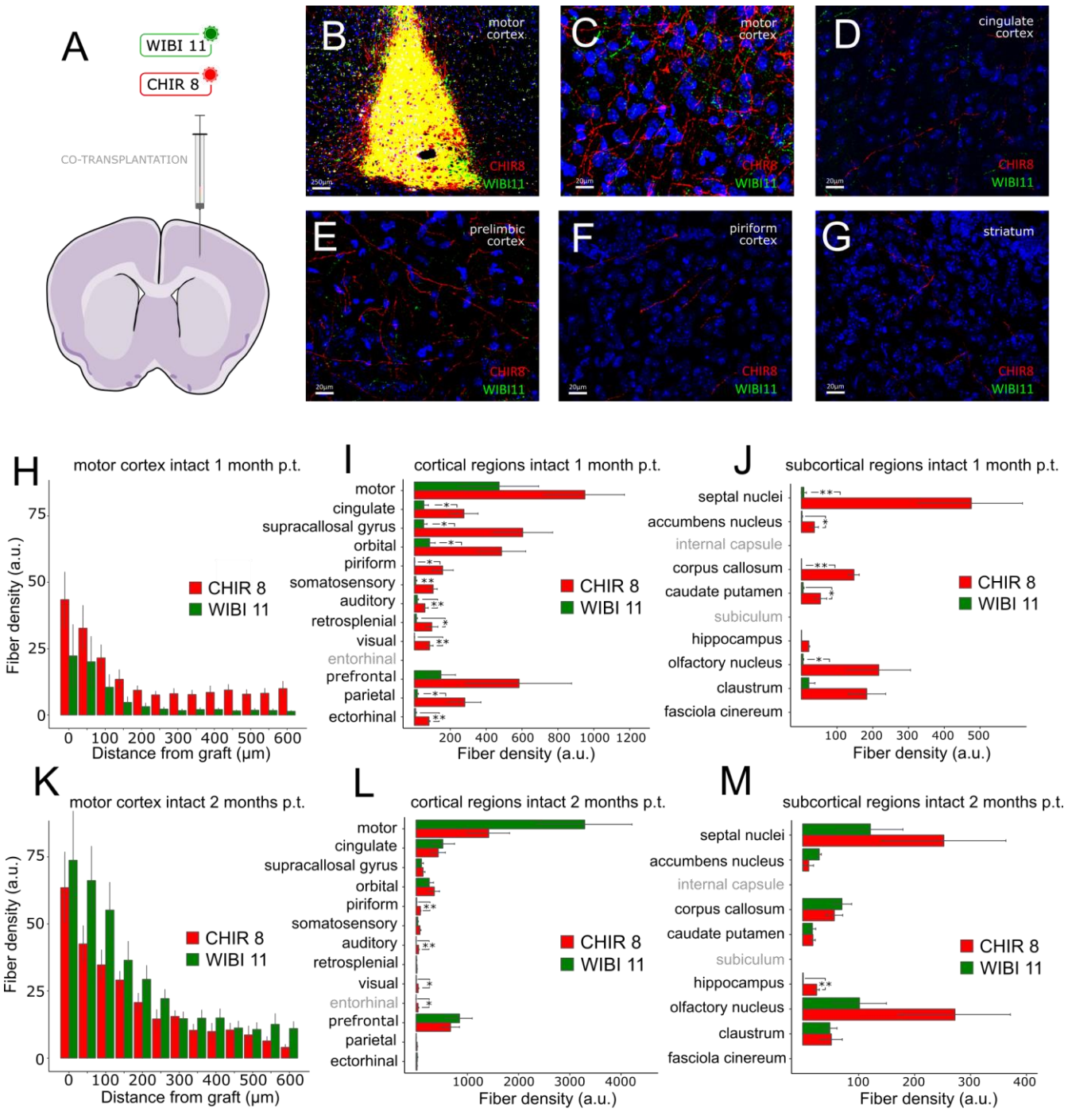
A
WIBI 11
CHIR 8
CO-TRANSPLANTATION
B
motor cortex
CHIR8
WIBI11
C
motor cortex
CHIR8
WIBI11
D
cingulate cortex
CHIR8
WIBI11
E
prelimbic cortex
CHIR8
WIBI11
F
piriform cortex
CHIR8
WIBI11
G
striatum
CHIR8
WIBI11
H
motor cortex intact 1 month p.t.
Fiber density (a.u.)
Distance from graft (µm)
CHIR 8
WIBI 11
I
cortical regions intact 1 month p.t.
motor
cingulate
supracallosal gyrus
orbital
piriform
somatosensory
auditory
retrosplenial
visual
entorhinal
prefrontal
parietal
ectorhinal
Fiber density (a.u.)
J
subcortical regions intact 1 month p.t.
septal nuclei
accumbens nucleus
internal capsule
corpus callosum
caudate putamen
subiculum
hippocampus
olfactory nucleus
claustrum
fasciola cinereum
Fiber density (a.u.)
K
motor cortex intact 2 months p.t.
Fiber density (a.u.)
Distance from graft (µm)
L
cortical regions intact 2 months p.t.
Fiber density (a.u.)
M
subcortical regions intact 2 months p.t.
Fiber density (a.u.)

Figure 5 Cell transplantation in normal motor cortex

A, Scheme of transplantation. **B** ICD of CHIR8 (red) and Wibi cells (green) 2 months after transplantation in healthy motor cortex. Blue, Hoechst nuclear counterstaining. **C-G**, ICD of CHIR8 and Wibi fibers at different times post-transplantation and in different regions, as indicated by labels. **H,K**, Density of Wibi and CHIR8 fibers at a different distances from the graft, one (H) and two months (K) after transplantation. **I,J,L,M**, WiBi and CHIR8 fiber density in cortical (I,L) and extra-cortical (J,M) regions, one (I,J) and two months (**L,M**) after transplantation; a.u., arbitrary units; error bars, SD . *$p < 0.05$; **$p < 0.01$ (two-tailed Student's t test). N≥ 3 transplanted animals for each time point were analyzed.

We found that embryonic cells displayed similar patterns of projection as compared to ESC-derived neurons, one month after transplantation. The main similarity concerned the differential projection pattern after transplantation into hippocampus. Indeed, only embryonic hippocampal, but not cortical cells, extended abundant projections and contacted CA3 via the Mossy Fiber pathway after grafting into the DG (Fig S4D-E).

Photothrombotic damage enhances long-range projections from transplanted isocortical cells

To assay the impact of a brain lesion on the projections of transplanted cells, we grafted WiBi and CHIR8 cells in a mouse model of ischemic stroke in the motor cortex. Cells were injected three days after inducing

photothrombotic damage (Fig 6A; see Materials and Methods) and their survival and pattern of axonal connectivity was analyzed one and two months after stroke (Fig 6B-N). Both WiBi and CHIR8 cells integrated into the host tissue and were detectable at least two months after transplantation (Fig 6B, S2E,H-i). As when transplanted in healthy motor cortex, CHIR8 cells efficiently extended axons into both cortical and extra-cortical regions, one month (Fig 6H-J) and two months (Fig 6K-M) after transplantation. However, WiBi cells formed intra-cortical projections more efficiently than CHIR8 cells already one month after grafting (Fig 6H,I). This was paralleled by an enhanced ability of WiBi cells to target subcortical regions one month after transplantation (Fig 6J).

However, two months after grafting, a refinement of axonal targeting occurred, making CHIR8 projections into septal nuclei and hippocampus more abundant than WiBi projections (Fig 6M, 7). Finally, the different behavior of WiBi and CHIR 8 cells was even more striking considering the total amount of fibers in all the regions analyzed (Fig 6N). Interestingly, CHIR8 cells appeared to reach a plateau in projection density already one month after transplantation and the total amount of fibers was not influenced by the ischemic insult, while WiBi cells projections increased with time and were specifically promoted by the lesion. We concluded that the photothrombotic damage further enhanced the process extension of WiBi cells, but CHIR8 and WiBi cells retained cell-autonomous ability to project toward specific cortical and extra-cortical targets.

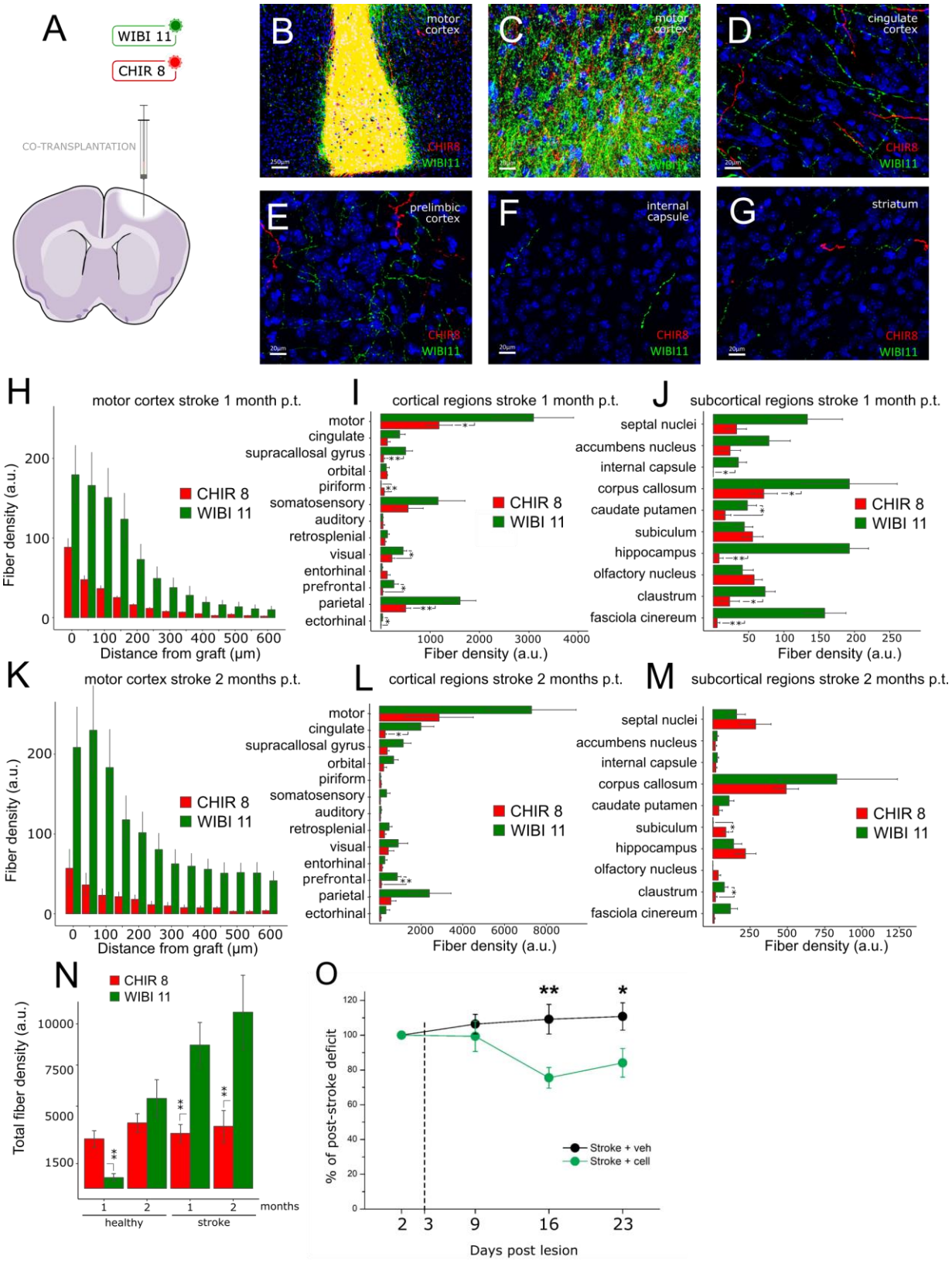
A
WIBI 11
CHIR 8
CO-TRANSPLANTATION
B motor cortex
C motor cortex
D cingulate cortex
E prelimbic cortex
F internal capsule
G striatum
CHIR8
WIBI11
H motor cortex stroke 1 month p.t.
Fiber density (a.u.)
Distance from graft (µm)
I cortical regions stroke 1 month p.t.
motor
cingulate
supracallosal gyrus
orbital
piriform
somatosensory
auditory
retrosplenial
visual
entorhinal
prefrontal
parietal
ectorhinal
Fiber density (a.u.)
J subcortical regions stroke 1 month p.t.
septal nuclei
accumbens nucleus
internal capsule
corpus callosum
caudate putamen
subiculum
hippocampus
olfactory nucleus
claustrum
fasciola cinereum
Fiber density (a.u.)
CHIR 8
WIBI 11
K motor cortex stroke 2 months p.t.
L cortical regions stroke 2 months p.t.
M subcortical regions stroke 2 months p.t.
N
Total fiber density (a.u.)
months
healthy
stroke
O
% of post-stroke deficit
Stroke + veh
Stroke + cell
Days post lesion

Figure 6 Cell transplantation in ischemic motor cortex

A, Method and site of transplantation. **B**, ICD of CHIR8 (red) and Wibi (green) cells 2 months after transplantation in photothrombotic motor cortex. Blue, Hoechst nuclear counterstaining. **C-G**, ICD of CHIR8 and WiBi fibers at different times post-transplantation and in different regions, as indicated by labels. **H,K**, density of Wibi and CHIR8 fibers at different distances from the graft, one (H) and two months (K) after transplantation. **I,J,L,M**, WiBi and CHIR8 fiber density in cortical (I,L) and extra-cortical (J,M) regions, one (I,J) and two months (L,M) after transplantation. a.u., arbitrary units; error bars, SD.**N**, total fiber density of WiBi and CHIR8 cells in healthy and ischemic brains, one and two months after grafting *$p < 0.05$; **$p < 0.01$ (two-tailed Student's t test). N≥ 3 transplanted animals for each time point were analyzed. **O**, Percentage of foot faults made with the contralesional forelimb in the gridwalk test. Values were normalized on the 2 days post-stroke value (initial deficit before transplantation). After the injection of WiBi cells (green, n=9) at day 3, mice showed a significant improvement in the motor performance compared to mice injected with vehicle (black, n=5) (Two way RM ANOVA followed by Holm-Sidak test: 16 days $p=0.004$, 23 days $p=0.015$).

We also asked whether cell grafting impacted motor performance in animals with ischemic damage. We choose to implant WiBi cells because since they showed better long-term integration than CHIR8 cells in our stroke model (Fig 6N, 7). Thus, mice received WiBi cells transplantation 3 days after experimental stroke and motor function was assessed longitudinally via the gridwalk test *(Lai et al., 2015; Alia et al., 2016)*. We found that while the motor deficit remained stable in the mice treated with vehicle solution, grafted mice showed a decline (starting from 16 days post-stroke) in the number of foot faults

made with the contralesional forelimb, indicating functional restoration (Fig 6O). However, we speculate that this very early response did not depend on the specificity of WiBi cell targets innervation as compared to CHIR8 cell innervation, because since the differences between the two types of transplants emerged later.

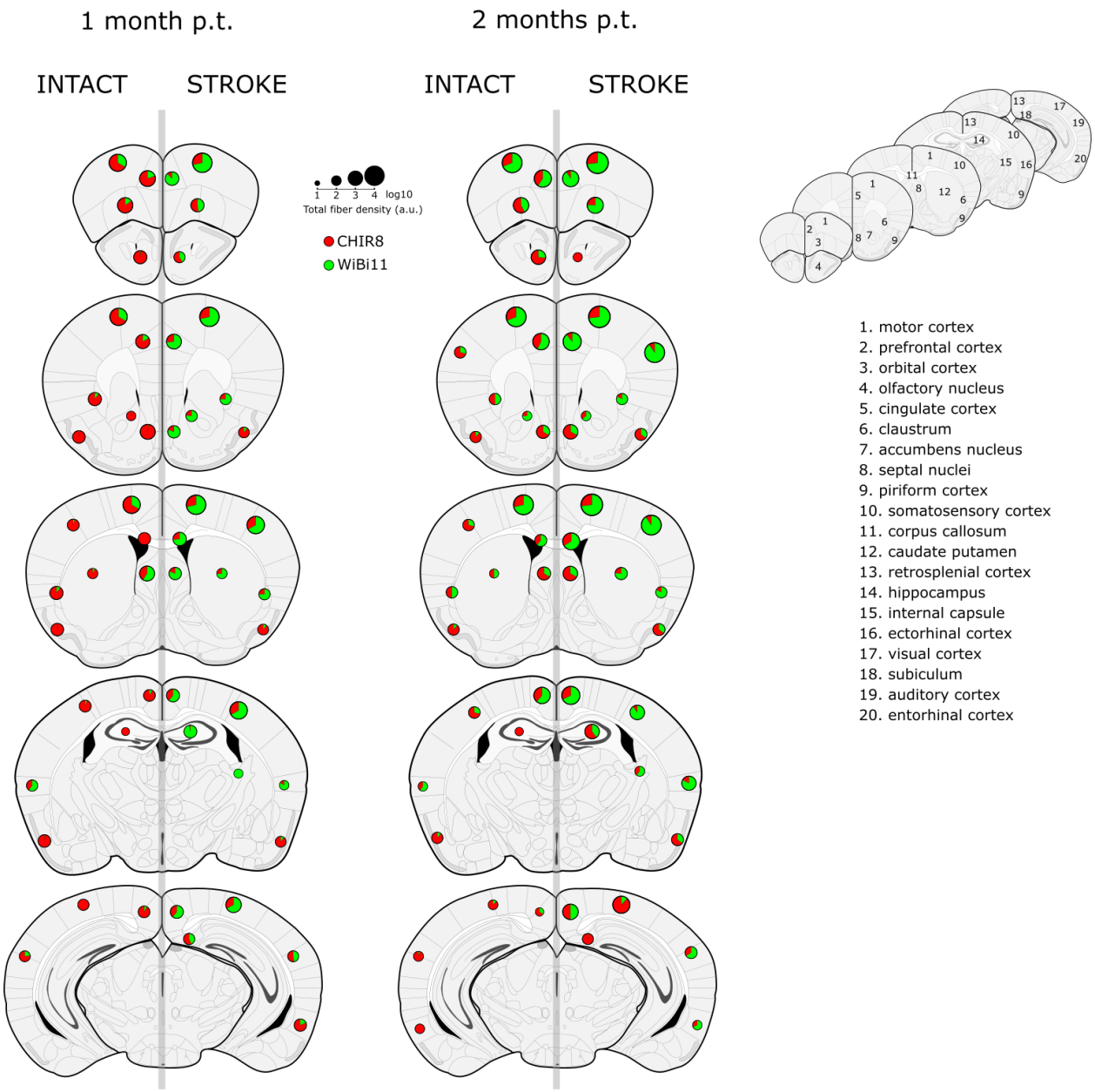

Figure 7 Cell-autonomous and environmental cues regulate axonal extension after grafting

Schematic showing the different cortical and subcortical regions inspected in the differential projection analysis: the total amount of fibers (size pie-chart, log10) and the proportions of CHIR8 and WiBi projections in each region, as reported in Figures 4-6. Isocortical and hippocampal cells co-transplanted in intact and ischemic motor cortex show different patterns of projection.

FGF8 regulates genes of cortical area patterning in a model of *in vitro* corticogenesis

While FGF8 downregulates the expression of forebrain genes and induces the expression of posterior markers during early phases of *in vitro* ES cell neuralization *(Chiba et al., 2005; Hendrickx et al., 2009)*, the combination of WNT/BMP inhibition on mouse ES (mES) cells drives neuralized cells towards a dorsal telencephalic identity after the first week of *in vitro* differentiation *(Bertacchi et al., 2015; Yao et al., 2017)*. Within committed dorsal telencephalic cells, FGF8 exerts then an opposite effect, promoting the acquisition of rostral area identity, hence acting as an anteriorizing cortical factor. We exploited the plasticity of our *in vitro* system to evaluate the effect of FGF8 signaling on cortical area mapping genes. Intracellular FGF8 signaling was activated by FGF8 treatment starting from the 8th day of *in vitro* neuralization (DIV8) of mESCs previously corticalized via WNT/BMP inhibition (WiBi) (Fig. 8A). To confirm that FGF8 signaling was not affecting telencephalic

identity, RT-PCR analysis of general markers of A/P identity was performed at DIV11 on WiBi- and FGF8-treated cells (Fig. 8B). FGF8-treated cells express high levels of the anterior markers FoxG1, Emx2 and Pax6 and low levels of the posterior markers En1 and Krox20, similarly to cells treated only with WiBi and E16 embryonic mouse cortex (Fig. 8B; *Bertacchi et al., 2013; 2015*). Consistently, control cells neuralized in minimal medium and E16 midbrain cells show an opposite trend (Fig. 8B). Moreover, activation of FGF8 signaling from DIV8 does not impair the subtype-specific cortical markers CTIP2 and SATB2 *(Leone et al., 2008)*, indicating that the previously acquired cortical identity is not compromised by late FGF8 treatment (Fig 8C-D).

Next, we assessed the expression of a broader plethora of genes involved in early regional identity to further evaluate the *in vitro* effect of FGF8 activation on early area patterning. Differentially expressed genes between FGF8- and WiBi-treated cells were correlated to genes differentially expressed between anterior and posterior embryonic cortices (Fig 8E-F).

Since the cortical neuroepithelium normally shows distinct profiles of genes expressed in gradient at E11.5 (Hey1, FGF15, FGF18) and at E13.5 (Epha3, Klf3, Efr1, Spry2, PTN), we used two separate times of *in vitro* differentiation, DIV11 and DIV13. We found a significant correlation ($r_s=0,75$; $p<10^{-5}$) between FGF8-treated cells and embryonic anterior cortex, and between WiBi cells and embryonic posterior cortex, respectively, indicating that FGF8 signaling can regulate the activation of A/P cortical genes *in vitro* similarly to what observed *in vivo*.

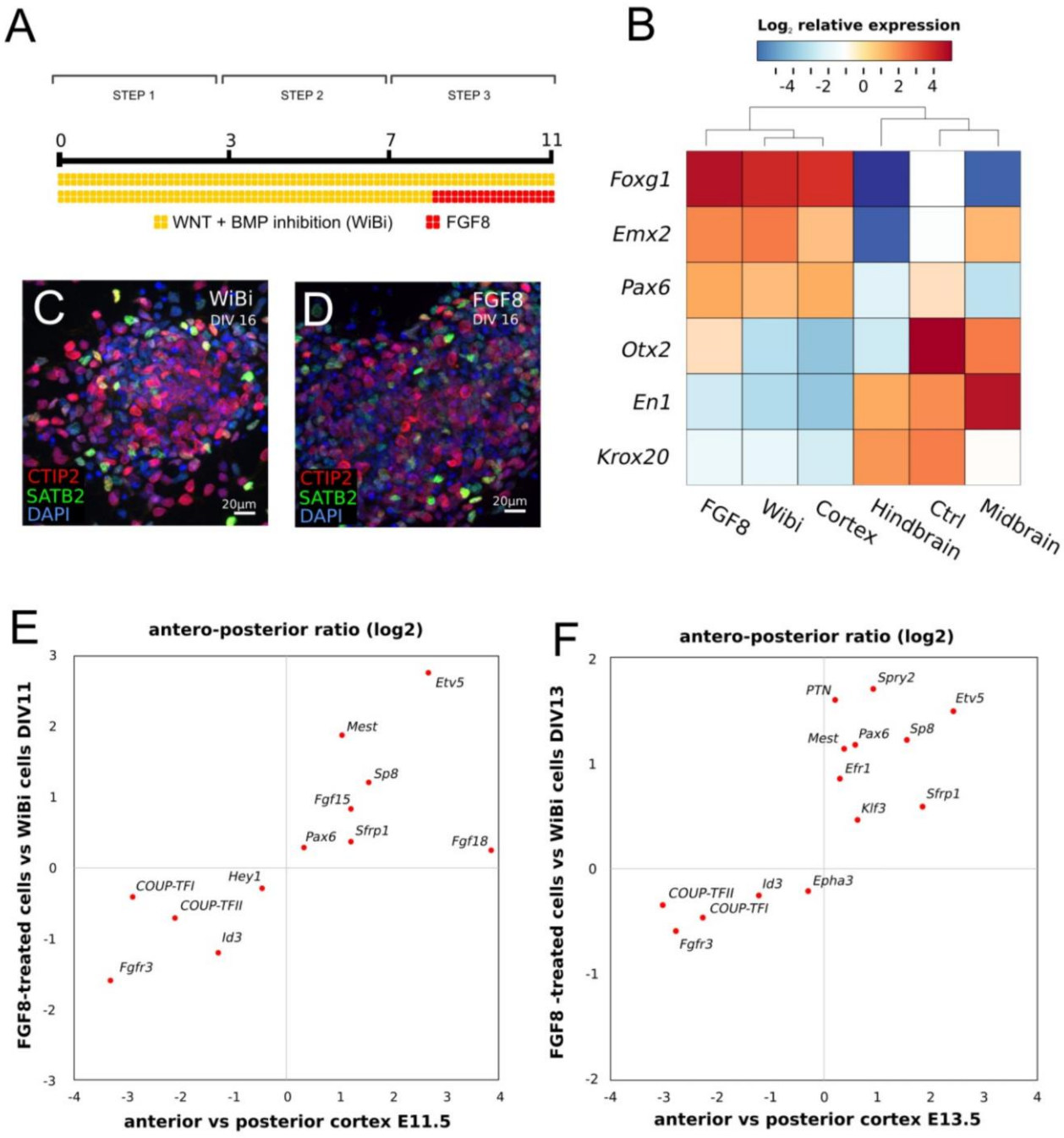

Figure 8 FGF8 induces anterior cortical identity *in vitro*

A, Differentiation protocol with WNT and BMP double inhibition (WiBi, yellow) and FGF8-treatment (FGF8, red). **B**, Color heat map showing hierarchical clustering and mRNA relative fold-change of A/P neural markers, evaluated via RT-PCR, in

mouse ES cell-derived neurons (WiBi, FGF8 and Ctrl) at DIV11 and in different regions of the E16 embryonic mouse brain (Cortex, Hindbrain, Midbrain). Ctrl, mouse ESCs neuralized without WiBi. Color map shows log 2 mean-centered expression. N=3 independent experiments were pooled together and analyzed by RT-PCR; each experiment contained n=2 *in vitro* technical replicates. **C-D**, Immunocytodetection (ICD) of pan-cortical markers CTIP2 (red) and SATB2 (green) in WiBi (C) and FGF8 (D) neurons ad DIV16. **E-F**, mRNA fold change bi-plot of A/P cortical markers at E11.5 (E) or E13.5 (F) in WiBi versus FGF8 treated cells (vertical axis) and anterior versus posterior mouse fetal cortex (horizontal axis). RT-PCR was performed on RNA from n=3 independent cultures pooled together, each with 2 *in vitro* technical replicates.

Finally, the inhibition of endogenous FGF signaling by treating corticalized cells with the MEK inhibitor PD0325901 *(Barrett et al., 2008)* from DIV8 to DIV11 exerts an opposite effect on A/P cortical markers (Fig. S6A), suggesting that endogenous FGF ligands *(Bertacchi et al., 2015)* might be responsible for modulating A/P markers already in WiBi control cells.

FGF8 inhibits COUP-TFI translation by acting on its 3'UTR

Among the several FGF8 targets involved in areal patterning, the transcriptional regulator COUP-TFI, a key player of posterior/sensory cortical identity, is inhibited by FGF8 in anterior/motor cortex *(Garel et al., 2003; Storm et al., 2006)*. We thus assessed whether FGF8 could regulate COUP-TFI also *in vitro* by treating mES-corticalized cells with either FGF8 or FGF inhibitor.

Notably, FGF8-treated cells show a marked decrease in the number of cells expressing COUP-TFI (Fig. 9A-C), or alternatively an increase in COUP-TFI levels in presence of the FGF inhibitor (Fig. S6A-D). After 48hr of FGF8 treatment, we noticed that FGF8 efficiently represses COUP-TFI protein but not COUP-TFI transcript levels, which are nevertheless downregulated 96hr later (Fig. 9D-E). This indicates that FGF8 might act first and more efficiently on COUP-TFI translation than COUP-TFI transcription, and suggests a mechanism involving COUP-TFI regulation via its 3'UTR.

To directly investigate a possible role of the COUP-TFI 3'UTR in inhibiting COUP-TFI translation, we prepared a lentiviral vector (Fig. 9F) capable of over-expressing just the 3'UTR (Fig. 9G-N). This construct was transduced into corticalized cells and the expression of COUP-TFI protein (Fig. 9G-H) and COUP-TFI mRNA (Fig. 9I) was analyzed 48hr later.

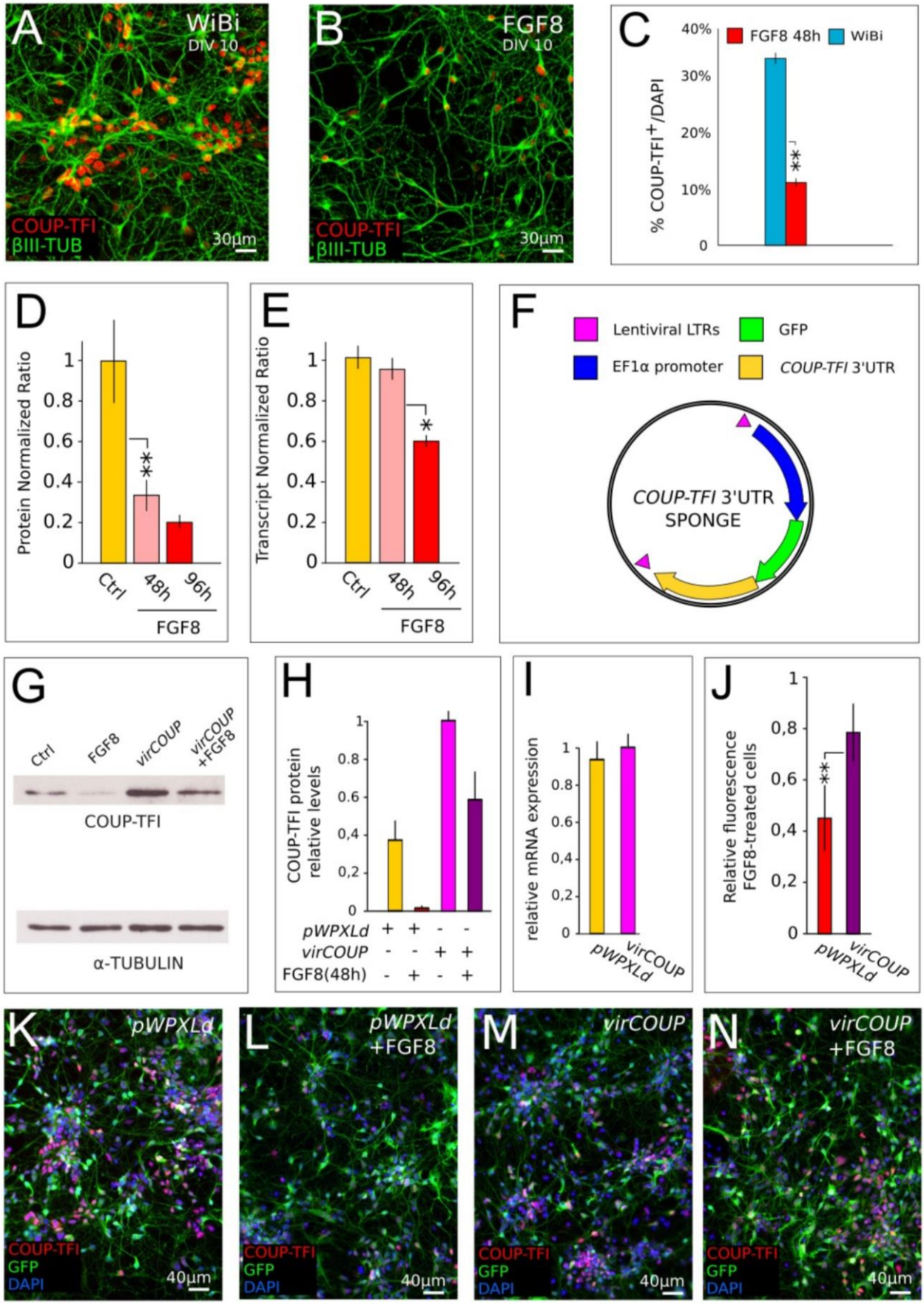
A
WiBi
DIV 10
COUP-TFI
βIII-TUB
30µm
B
FGF8
DIV 10
COUP-TFI
βIII-TUB
30µm
C
FGF8 48h
WiBi
% COUP-TFI+/DAPI
40%
30%
20%
10%
0
**
D
Protein Normalized Ratio
Ctrl
48h
96h
FGF8
**
E
Transcript Normalized Ratio
Ctrl
48h
96h
FGF8
*
F
Lentiviral LTRs
GFP
EF1α promoter
COUP-TFI 3'UTR
COUP-TFI 3'UTR
SPONGE
G
Ctrl
FGF8
virCOUP
virCOUP +FGF8
COUP-TFI
α-TUBULIN
H
COUP-TFI protein relative levels
pWPXLd
virCOUP
FGF8(48h)
I
relative mRNA expression
pWPXLd
virCOUP
J
Relative fluorescence FGF8-treated cells
pWPXLd
virCOUP
**
K
pWPXLd
COUP-TFI
GFP
DAPI
40µm
L
pWPXLd +FGF8
COUP-TFI
GFP
DAPI
40µm
M
virCOUP
COUP-TFI
GFP
DAPI
40µm
N
virCOUP +FGF8
COUP-TFI
GFP
DAPI
40µm

Figure 9 FGF8 inhibits COUP-TFI translation acting on the 3'UTR

A,B, Immunofluorescence (IF) of COUP-TFI (red) and β-III TUBULIN/TUJI (βIII-TUB, green) in control cells (A) and after 48hr of treatment with FGF8 (B) at DIV10. **C**, Percentage of COUP-TFI-positive cells in control cells and cells treated with FGF8 for 48hr. Error bars, SEM; n= 3 independent cultures. **D**, Quantification of COUP-TFI protein levels via Western Blot analysis after 48hr and 96hr of FGF8 treatment. **E**, COUP-TFI transcript levels in control and FGF8-treated cells after 48hr and 96hr analyzed via RT-PCR. **F**, Schematics of the lentiviral "sponge" vector carrying the COUP-TFI 3'UTR. **G-I**, Representative Western blot (G) and densitometric analysis (H) of COUP-TFI protein levels in cells transduced with the lentivirus carrying the COUP-TFI 3'UTR (virCOUP) or the control empty construct (pWPXLd) and treated with FGF8 for 48hr. (I) COUP-TFI transcript levels analyzed via RT-PCR in control cells (pWPXLd) or cells over-expressing COUP-TFI 3'UTR (virCOUP). **J**, Relative COUP-TFI fluorescence intensity (24hr FGF8-treated versus vehicle) in cells transduced with the virCOUP or control vectors. n=2 independent cultures; error bars, SEM. **K-N**, ICD of COUP-TFI and GFP in cells transduced with virCOUP (M,N) or control vector (K,L) and treated with FGF8 for 24hr (L,N). For RT-PCR in E,I, n = 2 *in vitro* technical replicates were pooled together and n = 3 independent cultures were performed. Densitometric analysis in D, H was performed on n = 2 biological replicas; At least 4 to 8 wells of 24-well plates were pooled in each replica to compensate for differences in cell seeding.* $p \leq 0.05$, ** $p \leq 0.01$.

Notably, COUP-TFI 3'UTR over-expression reduces the inhibitory effect of FGF8 treatment on COUP-TFI translation, as evidenced by Western Blot protein quantifications (Fig. 9G-H), without affecting transcript levels at the same time-point (Fig. 9I). Moreover, COUP-TFI protein levels are higher in GFP-expressing cells treated with FGF8 and transduced with the COUP-TFI 3'UTR vector when compared

to cells treated with FGF8 and transduced with a control vector (Fig. 9J-N). This indicates that cis-acting inhibitory signals, located within the 3'UTR, exert their action at cellular levels. Taken together, these data suggest that over-expression of the COUP-TFI 3'UTR acts as a "sponge" buffering some trans-acting inhibitory signals induced by FGF8.

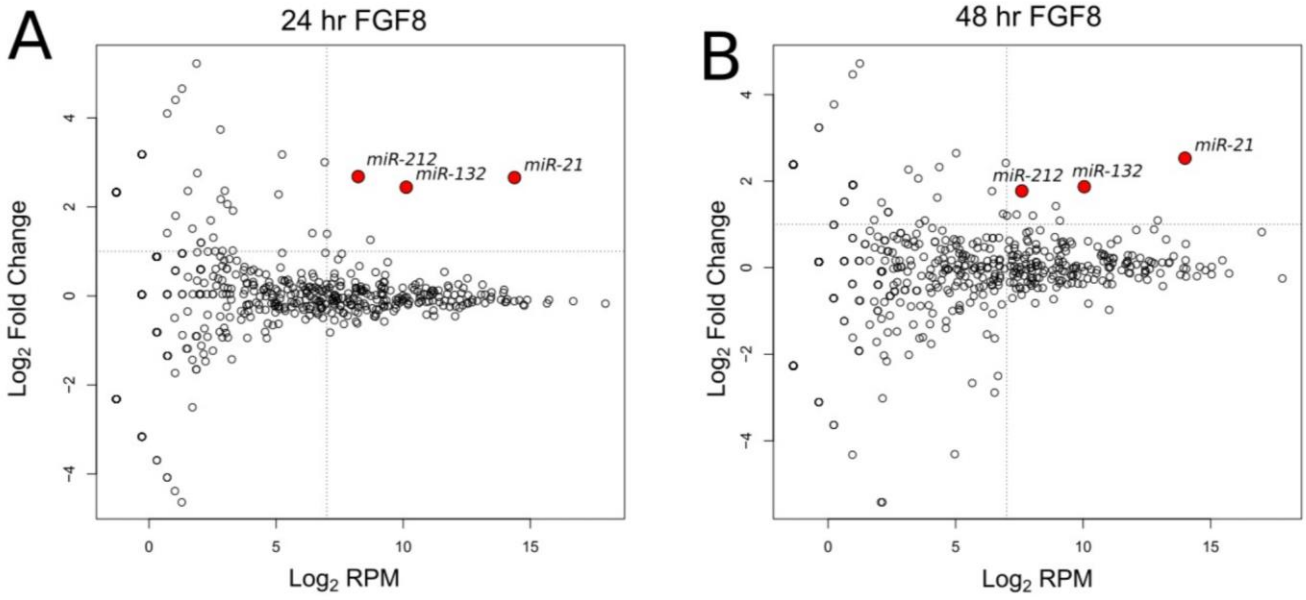

C

24 hr FGF8

miRNA	logFC	logCPM	FDR
miR-132	2.50	10.11	3E-07
miR-212	2.71	8.19	9.7E-07
miR-21	2.74	14.37	0.00211

48 hr FGF8

miRNA	logFC	logCPM	FDR
miR-132	1.86	10.03	8.83E-06
miR-335-5p	1.45	8.92	1.45E-05
miR-21	2.58	14.03	0.00108
miR-212	1.74	7.63	0.0017
miR-148a	1.11	12.91	0.0017
miR-674	1.25	8.03	0.0060
miR-335-3p	1.22	7.4	0.0182

D

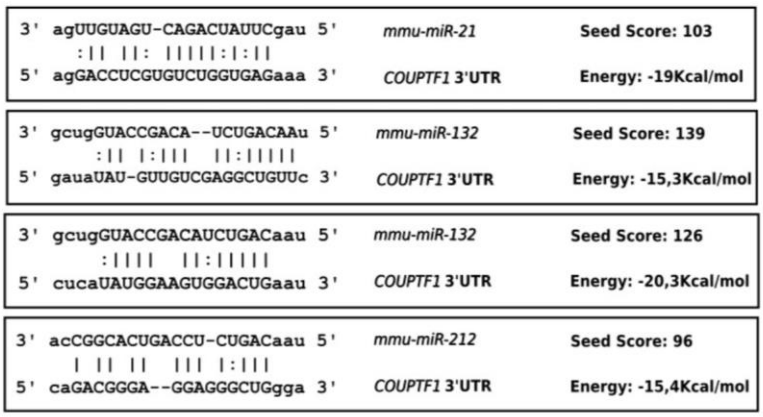

Figure 10 FGF8 activates miRNAs targeting the COUP-TFI 3'UTR in silico

A,B, Biplot showing the mean expression levels (log2 RPM) vs fold change (log2) for each microRNA detected, measured after 24hr (A) or 48hr (B) of FGF8 treatment. **C**,

Lists of the miRNAs significantly enriched after 24hr and 48hr of FGF8-treatment. Labeled in red are the miRNAs predicted to bind the COUP-TFI 3'UTR and significantly enriched at both time-points. **D**, Putative binding sites of miRNAs predicted to target the COUP-TFI 3'UTR. "Seed score" and "binding energy" were evaluated using miRanda algorithm (see Experimental Procedures).

The FGF8-induced miRNA miR-21 inhibits COUP-TFI translation *in vitro*

To investigate whether FGF8 could induce the expression of any miRNAs in mES corticalized cells, we analyzed the miRNA global expression profiles of cells after 24 or 48hr of FGF8 treatment. After 24hr, only a few miRNAs show a significant increased expression (FDR<0.05) when compared to those obtained after 48hr of treatment (Fig. 10A,B, respectively). We focused only on the miRNAs significantly induced at both time points and with higher expression levels: miR-132, miR-21 and miR-212 (Fig. 10C). Interestingly, the three miRNAs show high in silico binding affinity on the COUP-TFI 3'UTR, as predicted by the miRanda bioinformatics tool *(Betel D et al., 2008)* (Fig. 10D).

As the three miRNAs represent good candidates for the embryonic regulation of COUP-TFI expression during corticogenesis, we directly tested their function by inhibiting their action. miR-132 and miR-212 are organized in a transcriptional cluster and share the same seed sequence and putative targets *(Wanet et al., 2012)*. To inhibit the function of both miR-21 and miR-132/miR-212, we targeted their seed

sequences by transfecting locked nucleic acid (LNA)-based antisense oligonucleotides in corticalized mESCs *(Stenvang J. et al., 2012)*. We found that inactivating both miR-21 and miR-132/miR-212 *in vitro*, the ratio of cells expressing COUP-TFI in cultures treated with FGF8 significantly increases when compared to scramble LNA control transfections (Fig. 11A-C). This indicates the involvement of miRNAs in mediating FGF8-dependent inhibition of COUP-TFI *in vitro*.

However, the induction of the three miRNAs by FGF8 *in vitro* might not reflect the actual *in vivo* mechanisms of COUP-TFI regulation. To this purpose, we investigated whether they were differentially expressed in anterior and posterior regions of the embryonic mouse cortex at E11.5, a developmental time in which the A/P COUP-TFI expression gradient is well defined *(Armentano et al., 2007)*. If these miRNAs were involved in COUP-TFI translational inhibition, we would expect higher expression in anterior cortical regions where COUP-TFI expression is normally low. Among the three miRNAs, only miR-21 is significantly ($p<0.05$) more expressed in the anterior than posterior cortex, whereas miR-132 and miR-212 show no regionalized expression (Fig. 11D). Moreover, miR-21 expression is significantly increased in E11.5 COUP-TFI null cortices, which have expanded rostral features *(Armentano et al., 2007; Alfano et al., 2014)*, whereas miR-132 and two unrelated control cortical miRNAs (miR-181 and miR-222) are not affected (Fig. 11E), indicating that miR-21 is linked to anterior cortical identity.

Since miR-21 shows the most promising expression pattern and miR-132 has two predicted binding sites with high affinity, we focused on these two miRNAs and investigated whether they could interfere with the expression of COUP-TFI, Sp8 or FGF8. Transfection of mature miR-21 in DIV8 cells affects only COUP-TFI transcript level at DIV10, leaving Sp8 and FGF8 mRNA expression unchanged, whereas miR-132 over-expression has no effect on the expression of the three genes (Fig. 11F) Finally, the analysis of Ki67-positive dividing progenitors at DIV11 after the transfection of mature miR-21 at DIV8, showed no effect on neural progenitor proliferation *in vitro* (Fig. S7), in line with unchanged Sp8 and FGF8 expression. Taken together, our data suggest that miR-21 might be the most relevant miRNA for establishing COUP-TFI graded expression and that this effect would be exerted downstream of FGF8.

Specificity of miR-21 interaction with the COUP-TFI 3'UTR

To further decipher the functional specificity of miR-21 and miR-132 on the COUP-TFI 3'UTR, COUP-TFI protein levels were assessed after mature miRNA lipofection at DIV8. miR-21 transfected cells have significantly lower protein levels than cells lipofected with miR-132 or controls (Fig. 12A-E), in accordance with the mRNA analysis by RT-PCR (Fig 11F).

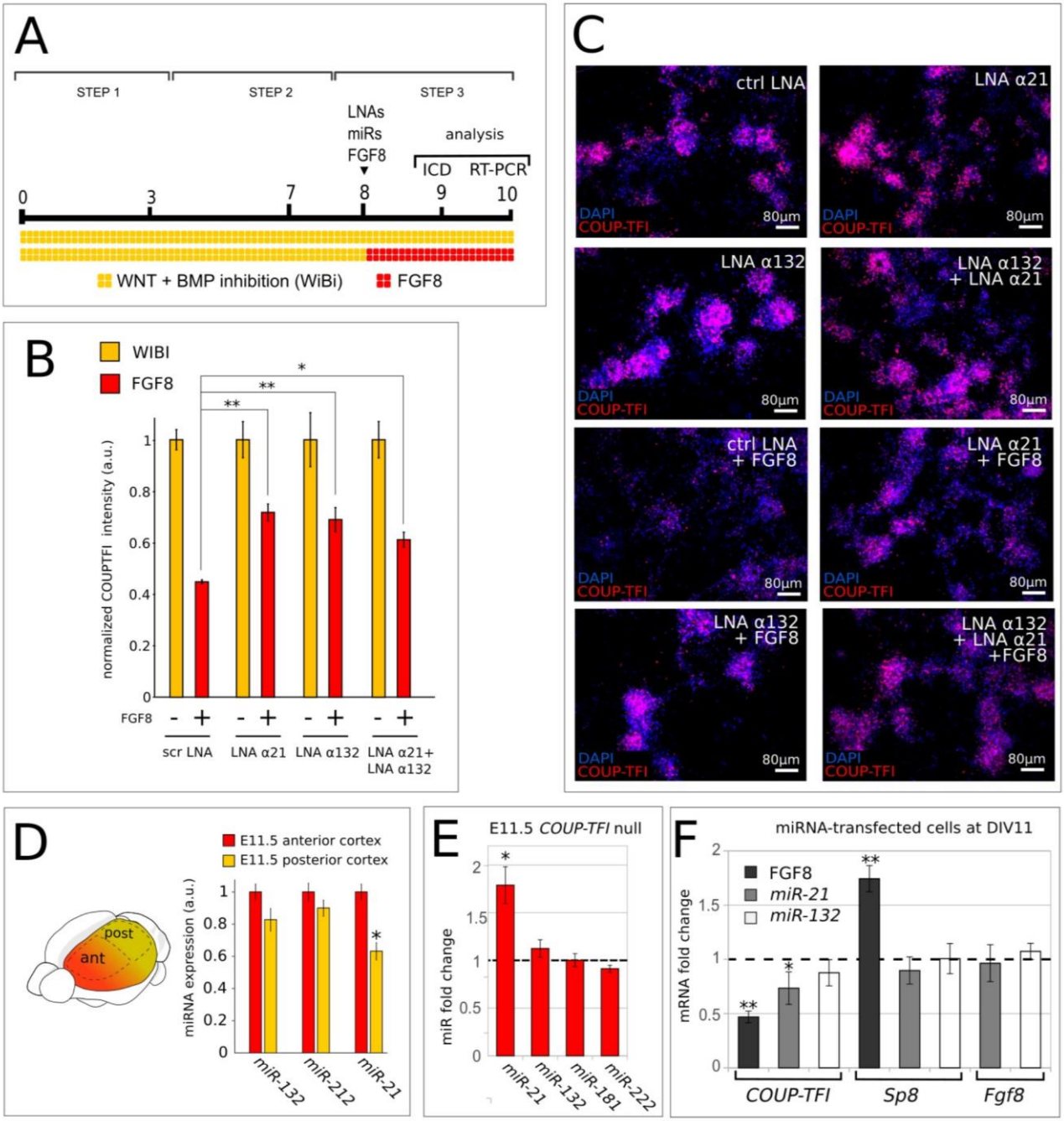

Figure 11 FGF8-induced miRNAs repress COUP-TFI expression *in vitro*

A, Schematics of the cell sample preparation for the LNA experiment. **B**, Normalized COUP-TFI fluorescence intensity (see Materials and Methods) in cells transfected with LNA against miR-21, miR-132/212 or scramble LNA and treated with FGF8 for

24hr. Error bars correspond to SEM. Statistical significance was obtained via the one-way ANOVA ($p<0.005$), followed by the t-test with Bonferroni correction (*$p\leq0.05$, **$p\leq0.01$). **C**, Immunocytodetection of COUP-TFI (red) in cells transfected with LNA against different miRNAs (α, in labels) and treated with FGF8 for 24hr. **D**, Normalized levels of miR21, miR132 and miR212 in anterior or posterior E11.5 mouse embryonic cortex dissected as shown in the left cartoon and analyzed by RT-PCR. **E**, RT-PCR analysis showing fold changes in miRNA expression in E11.5 COUP-TFI null normalized to WT cortices. **F**, RT-PCR mRNA analysis of DIV11 progenitors *in vitro* after transduction with miRNAs or treatment with FGF8. RT-PCR in E, F was carried out with RNA from n=3 independent cultures pooled together with n=2 *in vitro* technical replicates. *$p\leq0.05$, **$p\leq0.01$, Student T-test.

Next, we investigated miR-21 and miR-132 specificity by mutating the seed sequence of their predicted binding sites in COUP-TFI 3'UTR (Fig. S8) and compared the effects of different mutations via EGFP reporter assay in transfected HEK293T cells. Both miR-21 and miR-132 significantly inhibit EGFP reporter translation in the presence of WT seed but are ineffective when seeds are mutated, thus confirming their specificity of action (Fig. 12F).

Finally, we assayed the EGFP WT 3'UTR vector in DIV8 corticalized cells and observed a significant inhibition of EGFP signal 48 hr after FGF8 treatment (Fig. 12G-L), thus indicating that the effect of FGF8 on COUP-TFI translation is most likely direct and mediated by signals in the 3'UTR. Moreover, transduction of both miR-21 and miR-132 mutated vectors in FGF8-treated cells shows intermediate EGFP levels, but only the mutation of the miR-21 binding site significantly decreases the inhibitory effect of FGF8 compared to WT (Fig. 12L). Taken

together, these data confirm a preferential role of miR-21 in mediating the inhibitory effect of FGF8 on COUP-TFI in corticalized cells.

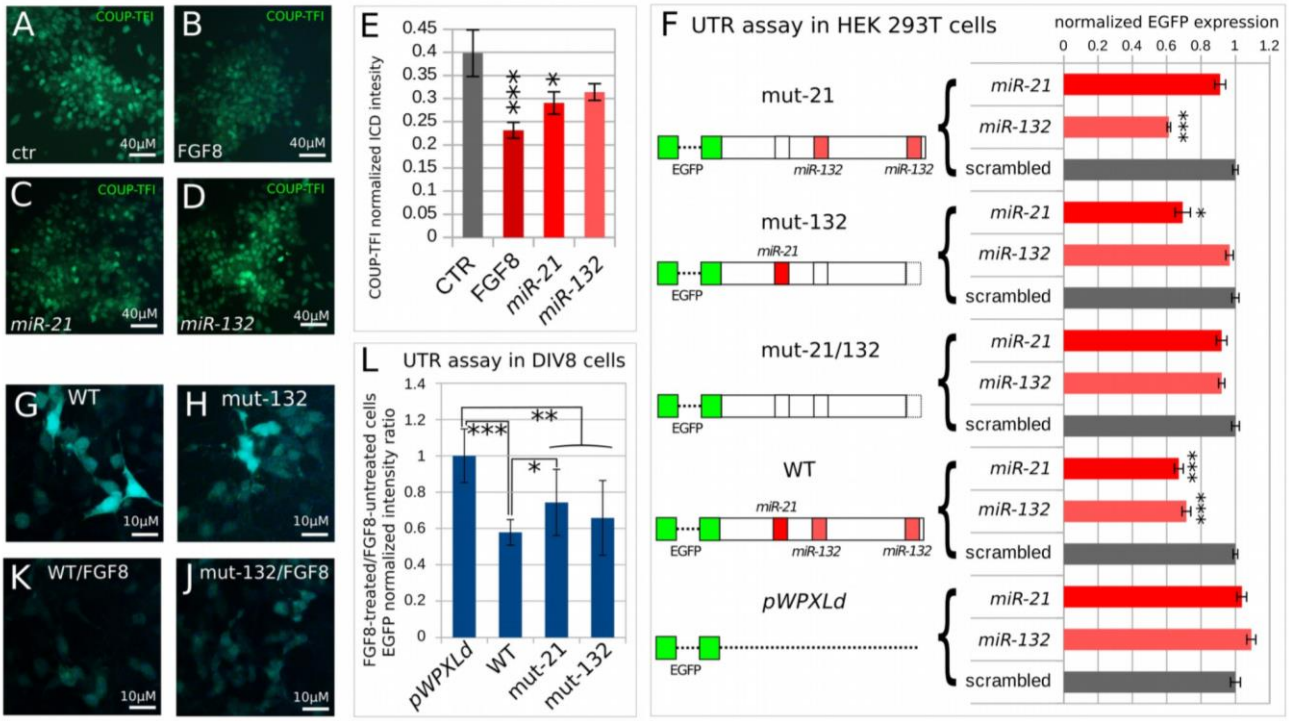

Figure 12 mir-21 and miR-132 selective binding to the COUP-TFI 3'UTR

A-D, examples of cells transfected with control (ctr) miRNA, miR-21 or miR-132 at DIV8, cultured to DIV11 in normal or FGF8-containing medium, as indicated in the images, and then immunostained with COUP-TFI antibody at DIV11. **E**, Quantification of COUP-TFI protein levels of transduced cells in (A-D). Relative intensity of COUP-TFI antibody fluorescence was normalized with respect to DAPI signal. Error bars, SEM. *p≤0.05, ***p≤0.001, Student T-test, n=2 independent cultures. **F**, Effect of the mutation of miRNA seed on the translation of reporter constructs carrying EGFP after their transfection in HEK 293T cells and EGFP imaging 24hr after transfection. Fluorescence intensity values were normalized with respect to cells transfected with control miRNA, containing a scrambled sequence. **G-J**, DIV10 cells after lentiviral transduction of EGFP reporter constructs as in F and

48h of culture in normal medium (G, H) or in medium containing FGF8 (K, J). **L**, Effect of the mutation of miRNA seed on the translation of reporter constructs carrying EGFP after their transduction in DIV8 cells and EGFP imaging 48hr after transduction. Values show the ratio of fluorescence between cells cultured without FGF8 and cells treated with FGF8 from DIV8 to DIV10, after normalization to the ratio of control cells transduced with pWPXLd. EGFP intensity evaluation shown in F, L was calculated as EGFP/DAPI pixel intensity ratio in cells from n=2 independent cultures. Error bars, SEM. *p≤0.05, **p≤0.01, ***p≤0.001, Student T-test.

Complementary expression of miR-21 and COUP-TFI protein and their interaction *in vivo*

To evaluate the *in vivo* role of miR-21 on COUP-TFI regulation, we compared miR-21 and COUP-TFI expression in E12.5 mouse embryonic cortices. Mature miR-21 shows decreasing A/P and M/L expression gradients (Fig. 13A-D), which are complementary to the increasing A/P and M/L COUP-TFI protein gradient (Fig. 13E-H), and in line with the RT-PCR-based expression analysis (Fig. 11D). This suggests that miR-21 could regulate COUP-TFI expression also *in vivo* by interacting with its 3'UTR.

To test this hypothesis, Michele Bertacchi (Institute of Biology Valrose, Université Côte d'Azur) first over-expressed a construct encompassing the COUP-TFI 3'UTR linked to a GFP reporter (Fig. 14A) and then inactivated miR-21 action by *in vivo* lipofection using specific LNA oligonucleotides (Fig. 14B). In utero electroporation (IUE) of the

COUP-TFI 3'UTR plasmid into E12.5 embryos (Fig. 14A) increases COUP-TFI levels in GFP-electroporated progenitors after 48 hr (Fig. 14D, F, G), when compared to the contralateral non-electroporated cortex or to control GFP-electroporated brains (Fig. 14C, E, G). IUE of the COUP-TFI 3'UTR plasmid carrying a mutated miR-21 binding site does not affect COUP-TFI protein level (Fig. S9). Thus, similarly to the *in vitro* data (Fig. 9), an abundance of the exogenous COUP-TFI 3'UTR might act as a "sponge", competing with its endogenous counterpart by sequestering available miRNA and hence counteracting COUP-TFI inhibition.

To further support miR-21 action in COUP-TFI inhibition, Michele lipofected E12.5 cortices with LNA-based antisense oligonucleotides against miR-21 (Fig. 14B) and tested COUP-TFI protein levels. Notably, we found increased levels in the lipofected E14.5 anterior embryonic cortex (Fig. 14I,K,M) compared to the contralateral non-lipofected hemisphere (Fig. 14H,J,M), or to the side lipofected with a scramble non-specific LNA (Fig. 14L and S10A-D), indicating that blocking miR-21 action affects COUP-TFI translation *in vivo*. No significant differences in COUP-TFI levels were found between treated and non-treated E12.5 medial and posterior cortices (Fig. 14M), consistent with a higher concentration of miR-21 in anterior versus posterior cortex (Fig. 13A-D). Together, these data confirm a key role of miR-21 in inhibiting COUP-TFI levels *in vivo*.

Overall, our *in vivo* approaches support the *in vitro* data and strongly suggest that miR-21 is a key component in mediating the FGF8

action of COUP-TFI anterior inhibition by cooperating in the establishment of its low anterior to high posterior expression gradient observed in embryonic cortices.

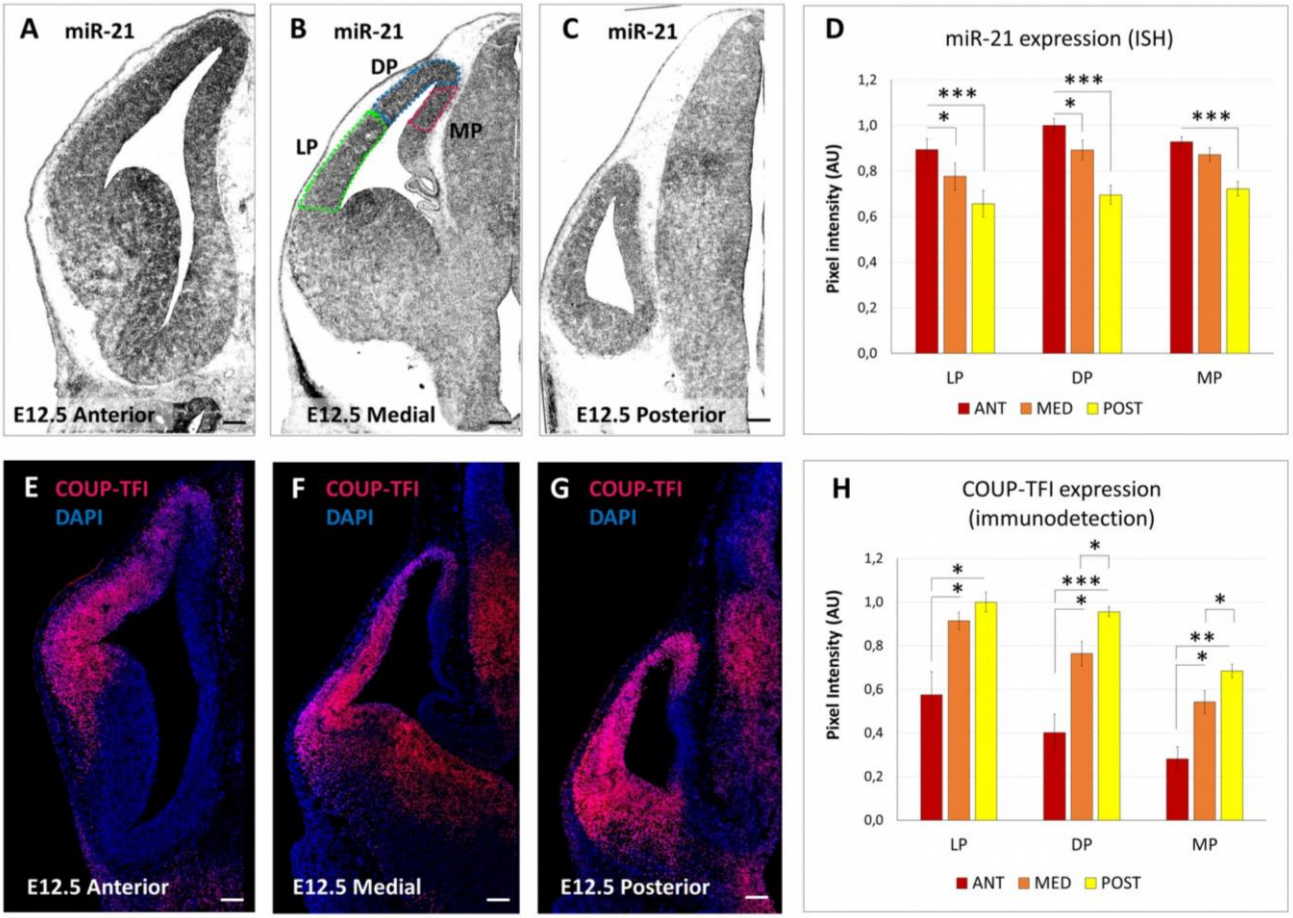

Figure 13 miR-21 and COUP-TFI are expressed in complementary gradients in the embryonic cortex

A-C, In situ hybridization of miR-21 in E12.5 mouse brain sections at anterior (A), medial (B) and posterior (C) levels along the A/P brain axis. Scale bars: 100 μm. **D**, Normalized COUP-TFI intensity (ImageJ, Pixel intensity analysis) in different pallial regions as schematized in (B). Measurements were performed on at least 3 sections coming from the anterior, medial and posterior regions of three E12.5 brains, in

different dorso-ventral areas as indicated (LP: lateral pallium; DP: dorsal pallium; MP: medial pallium). Error bars, SEM. Statistical significance obtained by the Student T-test (*p≤0.05, ***p≤0.001). **E-G**, Immunofluorescence of COUP-TFI (red) on E12.5 brain sections at different A/P levels as in (A-C). Nuclei counterstaining (blue) was obtained with DAPI. Scale bars: 100 μm. **H**, Normalized COUP-TFI fluorescence intensity (ImageJ, Pixel intensity analysis) in different pallial regions, as indicated. Measurements were performed as in D. Error bars, SEM. Significance obtained by the Student T-test (*p≤=0.05, **p≤0.01, ***p≤0.001).

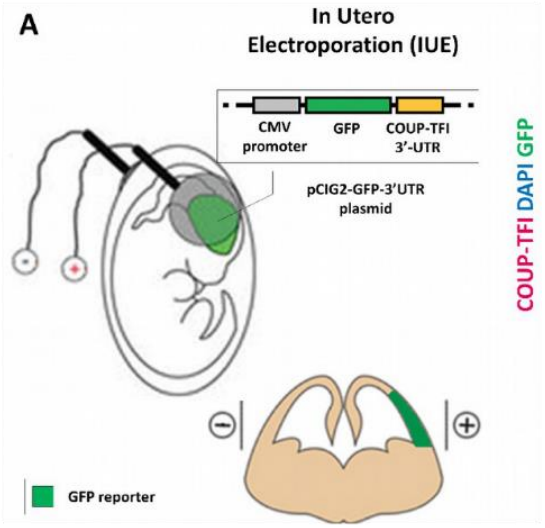

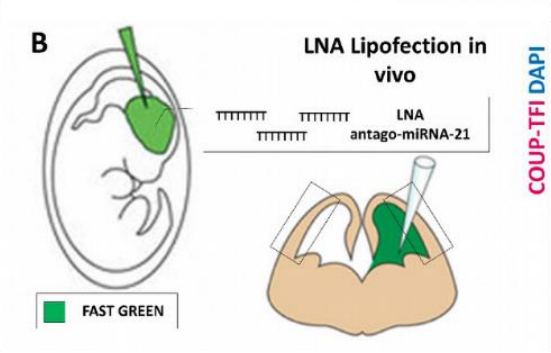

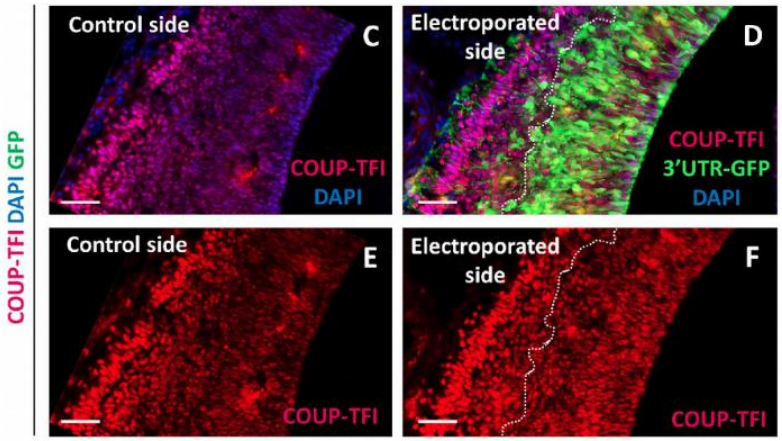

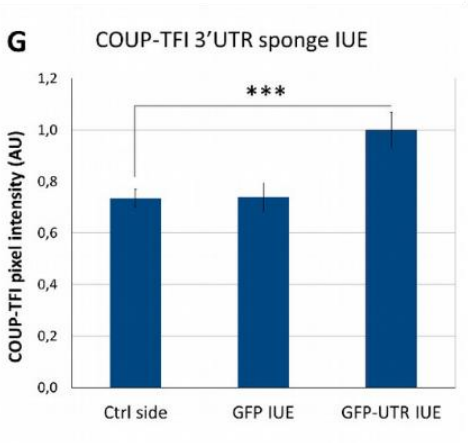

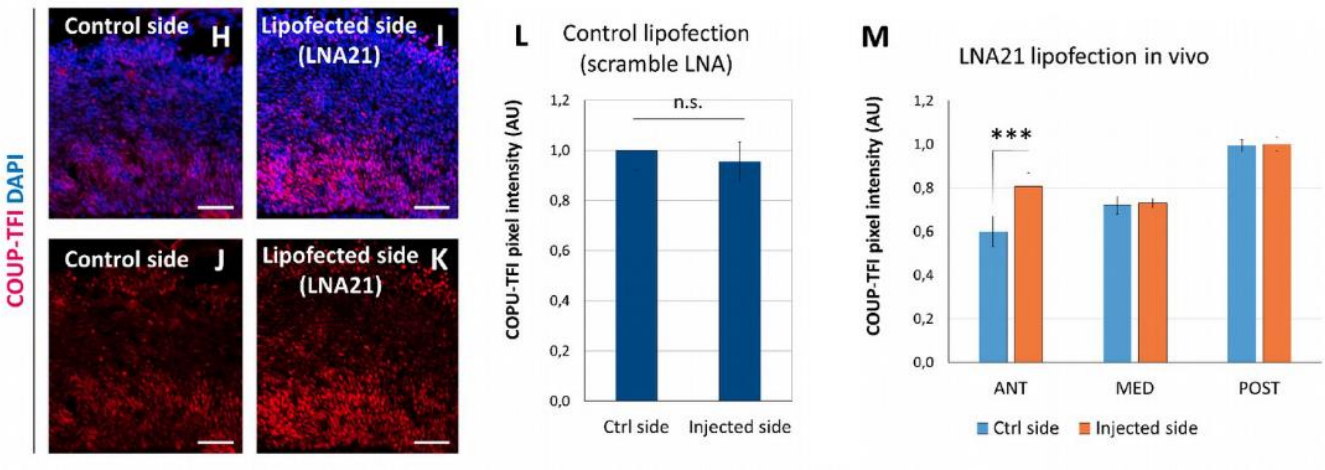

Figure 14 miR-21-mediated control of COUP-TFI translation *in vivo*.

A, Schematics of the in utero electroporation (IUE) experiment. The pCIG2-IRES-GFP-3'UTR "sponge" plasmid was injected into one telencephalic hemisphere and electroporated in neural progenitors, as described in Experimental Procedures. To target the lateral/dorsal pallium of one hemisphere, the electrodes were placed as schematized. Brains were collected 48hr later and processed for IF. The electroporated area was recognizable by GFP expression. **B**, Schematics of the LNA experiment in utero. Brains were injected with Lipofectamine/LNA mixture at E12.5 and collected 48hr later for IF. The injected side (visualized by adding Fast green to the LNA mixture) was compared to the contralateral un-injected side. **C-F**, IF of COUP-TFI (red) and GFP (green) in brain sections electroporated with the "sponge" plasmid at E12.5 and analyzed at E14.5. The lateral/dorsal pallium of the electroporated hemisphere (D, F) was compared to the contralateral control hemisphere (C, E). Nuclei counterstaining (blue) was obtained with DAPI. Scale bars: 50μm. **G**, Pixel intensity quantification (ImageJ) of COUP-TFI fluorescence in electroporated or control cortices. The staining was quantified only in the ventricular (VZ) and subventricular zones (SVZ), where cortical progenitors reside, as electroporated cells need more than 2 days to reach the cortical plate. Error bars, SEM.; t-test (***$p \leq 0.001$). **H-K**, IF of COUP-TFI (red) in brain sections after miR-21 inhibition by means of LNA lipofection in utero. The neural progenitor regions of

the lipofected hemisphere (I, K) were compared to equivalent regions of the contralateral control hemisphere (H, J). Nuclei counterstaining (blue) was obtained with DAPI. Scale bars: 50μm. **L**, Pixel intensity quantification (ImageJ) of COUP-TFI fluorescence in cortices lipofected with control scramble LNA, compared to non-lipofected brains. Corresponding images are shown in Fig.S10 A-D. Error bars, SEM.; t-test (n.s.= non-significant). **M**, Pixel intensity quantification (ImageJ) of COUP-TFI fluorescence in cortical areas as shown in H-K. The staining intensity was quantified at different levels along the A/P axis of E14.5 brains, as indicated. A significant difference was found only in the injected side of anterior regions (Error bars, SEM.; t-test; ***$p \leq 0.001$).

DISCUSSION AND CONCLUSIONS

Manipulation of WNT and BMP signaling: recapitulate cortical and hippocampal development *in-vitro*.

We compared the connectivity of two types of neural cells generated *in vitro* after their transplantation in intact or lesioned regions of the adult mouse brain. Our results indicate that the different molecular identity acquired by the cells after treatment with a single molecule (CHIR99021) in a very precise time window, profoundly affected their connectivity and their ability to integrate into different host environments. We showed that the timely manipulation of WNT signaling during mouse ES cell neuralization generated neural precursor cells with a isocortical or hippocampal molecular identity. The reactivation of WNT signaling soon after the expression onset of early dorsal telencephalic markers initiated a hippocampal program of differentiation, while prolonged WNT/BMP inhibition induced an isocortical identity.

A number of studies focused on the signaling required *in vitro* to steer the positional identity of neural precursor cells. Both mouse

and human ES or IPS cells expressed markers of dorsal telencephalic identity upon inhibition of WNT signaling, or combined WNT/BMP inhibition, during *in vitro* neuralization *(Bertacchi et al., 2015b; Chambers et al., 2009; Espuny-Camacho et al., 2013; Mariani et al., 2012; Shi et al., 2012)*. However, many of the markers used to ascertain the positional identity of *in vitro* differentiated cells - e.g. Emx2, Foxg1, Tbr1, Ctip2, Satb2 - are co-expressed by cortical and hippocampal precursors or neurons *(Bulfone et al., 1995; Fukuchi-shimogori and Grove, 2003; Gyorgy et al., 2008; Hébert and McConnell, 2000; Nielsen et al., 2010)* and the exact identity (isocortical versus hippocampal) of the neurons generated *in vitro* in these studies could not precisely be established. Gage and colleagues *(Yu et al., 2014)* showed that the expression of DG markers could be induced in neural precursor cells generated by human IPS cells that were initially deprived of WNT/BMP signaling and then exposed to exogenous WNT/BMP. Moreover, they showed that the neurons generated in this way were able to functionally integrate into mouse DG after grafting, suggesting that WNT/BMP signaling was required to induce a hippocampal identity in precursor cells that were previously committed to a general telencephalic identity. However, a direct comparison of these cells with different ones, focusing on the capacity to integrate and extend neurites in distinct environments, was not performed.

We aimed to precisely identify the molecular identity of our *in vitro* generated neural progenitor and precursor cells. The analysis of specific markers of hippocampal vs isocortical differentiation, and the

comparison of the global gene expression profiles of *in vitro* differentiated cells and of a number of embryonic regions, allowed us to identify a mechanism that is sufficient to refine the dorsal telencephalic positional differentiation. Our results indicate that in a specific time window, which corresponds to DIV8 of our protocol of neuralization, cells can acquire either an isocortical or a hippocampal molecular identity, depending on the degree of WNT signaling at that time. Markers that show graded expression levels between the embryonic hippocampus (Lhx9, Lhx2, Lef1, Lmo4) and isocortex (Lmo3) were differentially expressed by WiBi and CHIR8 cells. Moreover, the global gene expression profiles of WiBi and CHIR8 cells clustered with embryonic isocortex and hippocampus, respectively. WNT signaling de-inhibition before DIV8, or later than DIV9, failed to induce a hippocampal gene expression profile, indicating the existence of a time window of cellular competence for the induction of hippocampal identity.

Isocortical and hippocampal ESC-derived neurons: different axonal outgrowth and targeting.

It is known that hippocampal cells, together with olfactory bulb cells, are the only CNS cells able to undergo efficient adult neurogenesis in mammals *(Eriksson et al., 1998; van Praag et al., 2002)*. Conversely, adult cortical cells are not able, in physiological conditions, to generate new

neurons, although they share common origin and similar molecular identity with hippocampal cells *(Magavi et al., 2000)*. In this study, we compared WiBi and CHIR8 cells for their ability to generate new processes in different *in vivo* environments. To this aim, we compared their pattern of connectivity by differential labeling them with fluorochrome-carrying lentiviral vectors and co-transplanting them into different adult brain regions. This is a novel approach to the study of the neurogenic potential acquired *in vitro* by neuralized pluripotent cells.

Both WiBi and CHIR8 precursors survived and fully differentiated in mature neurons after grafting in adult hippocampus and isocortex. However, they showed different capacity of axonal projection. In intact hippocampus, only grafted hippocampal cells were able to extend long-range projections, while isocortical cells failed in sending far-reaching processes. At least a subpopulation (about 30%) of CHIR8 cells displayed markers of DG granule cells, such as Calb1, and contacted proper targets of adult DG neurons such as CA3. This axonal projection became more robust over time, as shown by the dramatic enhancement of fiber density 2 months vs. 1 months after transplant (Fig 4H). Finally, the fact that similar results were obtained transplanting primary cultures of fetal hippocampal or cortical neurons suggests that the different behavior of CHIR8 and WiBi cells might indeed be due to the specific, respectively, hippocampal and cortical identity acquired *in vitro*.

Likewise fetal cells of the embryonic motor cortex, ES-derived isocortical cells transplanted into either intact or

photothrombotic motor cortex failed in sending projections to thalamic nuclei and midbrain, according to previous observations *(Michelsen et al. 2015)*. In addition, a significant number of processes were found in the internal capsule of photothrombotic brains one month after stroke. Based on these observations, we might speculate that our cells acquired a motor identity. However, we cannot exclude that they might simply have maintained a general isocortical identity and that a further specification step would have been required for generating also thalamic and midbrain projections. Their layer identity remains to be assessed but we speculate that a majority of them differentiated as deep-layer neurons, because at the time of their transplantation they were mostly expressing Tbr1 and Ctip2 markers (Fig 2C).

The results obtained after transplantation in photothrombotic motor cortex indicate that the normal cortical environment retains some cues inhibiting the extension of new processes from WiBi cells and that such cues are somehow removed after the photothrombotic damage. However, it is interesting to note that, after a first early phase when WiBi processes were much denser than CHIR8 process both in cortical and extra-cortical regions one month after grafting, two months after the density of CHIR8 fibers into hippocampus and septal nuclei was significantly higher than the density of WiBi processes. We speculate that, in addition to a differential capacity of axonal extension, WiBi and CHIR8 cells hold some ability in selecting specific targets of innervation that is refined over time. This is also supported by the observation that WiBi processes were less dense

than CHIR8 processes in healthy motor cortex and callosum one month after graft, but they increase dramatically at two months. These data suggest that isocortical and hippocampal cells display different degrees of axonal pruning/plasticity in specific brain regions.

Altogether, our observations indicate that the distinct molecular identities acquired by CHIR8 and WiBi cells paralleled their different behavior after transplantation and suggest that WiBi and CHIR8 cells might be very similar to naive isocortical and hippocampal precursor cells, respectively. Furthermore, this interpretation is supported by the similar projection patterns established by fetal hippocampal and cortical neurons co-transplanted under the same experimental conditions as WiBi/CHIR8 cells (see Fig. S4-S5).

Fetal hippocampal cells grafted into the adult mouse hippocampus survived and successfully contacted the correct hippocampal layers and typical hippocampal target regions as the septum and the entorhinal cortex *(Shetty and Turner, 1996; Zaman and Shetty, 2001)*. In addition, also mouse and human neurons generated *in vitro* by pluripotent cells were successfully grafted into mouse hippocampus *(Yu et al., 2014)* or hippocampal slice *(Hiragi et al., 2017)*. Consistently, we observed a very similar pattern of connectivity after transplantation of both fetal or ESCs-derived neurons in hippocampus.

The pivotal role of the molecular identity acquired *in vitro* for establishing proper connections.

A number of experiments of grafting into mouse isocortex of either fetal cells or neural precursors originated *in vitro* by pluripotent cells have been performed. Overall, these studies show that embryonic or fetal neural precursors transplanted in the intact adult hippocampus integrate efficiently in the host circuitry and contact the correct target in the host tissue displaying specific patterns of long-range projections, whereas the intact adult cortical parenchyma appears to be poorly permissive with the transplanted cells *(Avaliani et al., 2014; Fricker-gates et al., 2002; Gage et al., 1995; Guitet et al., 1994; Rosario et al., 1997; Sheen et al., 1999; Shetty and Turner, 1996; Shin et al., 2000)*. Indeed, this behavior suits well with the natural capability of the hippocampal niche, unlike the cortical environment, to support adult neurogenesis. In addition, several studies reported that experimentally-induced cortical damage (e.g. aspiration, experimental ischemia or chemically-induced neurodegeneration) resulted in functional integration and higher connectivity of the transplanted cells, thus suggesting the existence of inhibitory cues in the healthy isocortex removed by the lesion *(Espuny-Camacho et al., 2013; Falkner et al., 2016; Gaillard et al., 2007; Michelsen et al., 2015; Tornero et al., 2013)*. Our results, which are consistent with these observations, indicate that the inhibitory effect of the intact cortical environment affects isocortical but not hippocampal cells, both fetal or

originated by ESCs, although the signals mediating such inhibition are currently unknown.

The possibility to successfully transplant neural precursors originated *in vitro* from ES or iPS cell into damaged isocortex has opened new opportunities for therapeutic approaches for cortical stroke. Here we showed that transplanted cells were able to establish potential synaptic connections with the host, as indicated by axonal varicosities stained with vGlut1 (Fig S2D, L). Moreover, grafting WiBi cells promoted some functional restoration of forelimb function after ischemic damage to the motor cortex. Improvements in motor output were already apparent as early as 16 days after stroke, suggesting that, in addition to network rewiring due to axon extension by the transplanted cells, bystander effects (e.g., relase of trophic factors, modulation of inflammation etc.; *George and Steinberg, 2015; Lee et al., 2008; Chen et al., 2003; Borlongan et l., 1998; Modo et al. 2002*) likely play a key role in the observed recovery. Finally, We speculate that the specificity of innervation that we found for WiBi and CHIR8 cells could might could affect later processes of motor recovery. These and other functional aspects of cell transplantation in ischemic motor cortex are currently under investigation.

Our results highlight the importance of the type of molecular identity acquired by the cells during their *in vitro* neuralization to establish proper connections. When transplanted into photothrombotic motor cortex, WiBi cells, more efficiently than CHIR 8 cells, sent far reaching processes toward the surrounding cortical regions

(somatosensory, cingulate, prefrontal) and some sub-cortical regions (internal capsule, caudate putamen, claustrum) typically targeted by resident cortical projection neurons. Although our observations clearly indicate a functional difference between WiBi and CHIR 8 cells, we can not anticipate how their differential connectivity after grafting could relate to their different molecular identity. The analysis of genes differentially expressed between hippocampal and isocortical cells originated by ESCs *in vitro* showed clusters of biologically related pathways with high enrichment score comprising ECM-cell interaction (the most enriched), cell-cell interaction, PI3K-Akt signaling pathway and WNT signaling. Notably, ECM-cell interaction is the most enriched pathway also in the analysis of genes differentially expressed between embryonic isocortex and hippocampus (Table S1). We speculate that changed expression of some of the genes belonging to this category could account for the specificity of connectivity of WiBi and CHIR8 cells.

In conclusion, our *in vitro* system proved useful to finely dissect the molecular pathways generating cell diversity in CNS development. *In vivo* grafting in distinct adult brain regions revealed an intrinsic functional diversity of neural precursor cells generated *in vitro*, which might have a crucial impact for cell replacement therapies. Our findings support the importance of *in vitro* systems in addressing developmental biology issues and pose the bases for more focused assays of isocortical or hippocampal cell replacement.

FGF8 regulates cortical area-patterning by inhibiting COUP-TF1 translation via *miR-21*

We found that corticalized mouse ESCs express significant levels of COUP-TFI and that FGF8 treatment can inhibit COUP-TFI during a precise time of the neuralization protocol. This well reproduces what normally happens during early corticogenesis, in which FGF8 downregulates anterior COUP-TFI expression in progenitor cells *(reviewed in Alfano and Studer, 2013)*. We showed that the mechanisms of COUP-TFI inhibition exerted by FGF8 *in vivo* can be reproduced *in vitro* and that FGF8 can initiate a genuine program of anterior positional identity specification in a cell culture system. Our experiments not only confirmed the reliability of our *in vitro* approach but also revealed an unexpected mechanism of post-transcriptional regulation, acting through the 3'UTR of COUP-TFI also *in vivo*. FGF8 signaling initially decreases COUP-TFI protein levels without affecting COUP-TFI mRNA, and this effect is blocked by over-expressing its 3'UTR, which likely acts as a scavenging sponge for FGF-induced miRNAs. Our data demonstrate that miR-21 represents one of the key mediators in the FGF8-dependent COUP-TFI inhibition *in vitro* and *in vivo*. Overall, we propose that cell culture systems can mimic the differentiation of specific neuronal types and be used in unraveling molecular mechanisms of cortical positional patterning.

Despite resembling their physiological counterparts, simple cell culture systems lack the endogenous morphogenic gradients normally present *in vivo*, such as FGF8. However, this can be an advantage when performing functional experiments aiming to identify the mechanisms involved in the formation of graded responses to a known signal. Indeed, by comparing the miRNAome of early cortical progenitor cells in the presence or absence of FGF8, we found few miRNAs immediately induced by FGF8. Only three miRNAs predicted to target the COUP-TFI 3'UTR were significantly induced by 24hr of FGF8 treatment (miR 21, miR132 and miR 212). Consistently, FGF signaling was reported to induce miR-132 expression in endothelial cells *(Anand et al., 2010)*, indicating that multiple tissues share a molecular mechanism of miR-132 activation by FGF. In our study, all three miRNAs were able to inhibit COUP-TFI translation in ES corticalized cells, but only miR-21 is expressed in a gradient complementary to COUP-TFI in embryonic cortices. This does not imply that miR132 and miR-212 have no effect on COUP-TFI expression, but that, possibly, miR-21 is the most effective one in modulating cortical COUP-TFI gradient expression, whereas miR132 and miR-212 might fine-tune COUP-TFI in other contexts and/or temporal windows.

As COUP-TF members are orphan nuclear receptors, in which no ligands have been characterized so far, it is plausible that their expression depends on regulatory feed-forward and feedback loops involving miRNAs in several developmental and differentiation processes *(Eendebak at al., 2011)*. Indeed, several papers unraveled a co-

regulation between COUP-TFII (also Nr2f2) and miR-302 in ES cell differentiation *(Rosa and Brivanlou, 2011; Hu et al., 2013; Wang et al., 2014; Kang et al., 2015)*, or COUP-TFII and other miRNAs in various forms of cancer *(Lichtfield and Klinge, 2012; Qin et al., 2014)*. However, very little was known about the regulation of COUP-TFI expression by miRNAs during neural development. One paper predicted a series of miRNAs, which could target COUP-TFI during inner ear development, and uncovered a co-regulatory interaction between COUP-TFI and miR-140 on KLF9 expression *(Chiang et al., 2013)*. This interaction seems not to work in the cerebral cortex, indicating that miRNAs might regulate COUP-TFI expression in a cellular-dependent context. Finally, miR-17/106 might act as critical regulators of the neurogenic-to-gliogenic transition in which both COUP-TF genes are also involved, however no direct regulation between COUP-TFs and miR-17/106 has been described *(Naka-Kaneda et al., 2014)*. On the contrary, our results reveal a specific role of miR-21 in regulating COUP-TFI protein expression in early cortical progenitor cells. Therefore, this is the only study, to our knowledge, demonstrating a fine regulation of COUP-TFI expression by a miRNA, miR-21, during neocortical area patterning. Finally, it would be interesting to find out whether either miR-21 or other miRNAs regulate or are controlled by other transcription factors involved in cortical area specification.

In conclusion, our observations indicate that molecular mechanisms regulating genes of cortical patterning are maintained in isolated cells *in vitro*, allowing the use of cell culture models for studies

of cortical areal development. At the same time, they open new opportunities for therapeutic approaches, in which the differentiation of pluripotent cells into a motor rather than a sensory cortical neuron is required for cell transplantation experiments in a damaged/degenerated cerebral cortex.

MATERIALS AND METHODS

Mouse ESCs differentiation and transfection

Murine ES cell lines E14Tg2A (passages 25-38) and 46C (transgenic Sox1-GFP ESCs, kindly provided by A. Smith, University of Cambridge, UK; passages 33-39) were cultured on gelatin-coated tissue culture dishes at a density of 40000 cells/cm2. ES cell medium, which was changed daily, contained GMEM (Sigma), 10% Fetal Calf Serum, 2mM Glutamine, 1mM sodium Pyruvate, 1mM non-essential amino acids, 0.05mM β-mercaptoethanol, 100 U/ml Penicillin/Streptomycin and 1000 U/ml recombinant mouse LIF (Invitrogen). Chemically defined minimal medium (CDMM) for neural induction consisted of DMEM/F12 (Invitrogen), 2mM Glutamine, 1mM sodium Pyruvate, 0.1mM non-essential amino acids (NEAA), 0.05mM β-mercaptoethanol, 100 U/ml Penicillin/Streptomycin supplemented with N2/B27 (no vitamin A; Invitrogen).

The protocol of ES neuralization consisted of three steps. In Step-I, dissociated ESCs were washed with DMEM/F12, seeded on gelatin-coated culture dishes (65000 cells per cm2) and cultured in CDMM plus 2.5μM WNT inhibitor (53AH, Cellagen Technology) and 0.25μM BMP inhibitor (LDN193189, Sigma) for 3 days. In Step-II, ES cell

were dissociated and seeded (65000 cells per cm2) on Poly-ornithine (Sigma; 20 μg/ml in sterile water, 24 hours coating at 37°C) and natural mouse Laminin (Invitrogen; 2.5 μg/ml in PBS, 24 hours coating at 37°C). Cells were cultured for 4 additional days in CDMM Plus WNT/BMP inhibitors, changing the medium daily. Serum employed for Trypsin inactivation was carefully removed by several washes in DMEM/F12. In Step-III, cells were dissociated and seeded (125000 cells per cm2) on Poly-ornithine and Laminin coated wells. Subsequently, isocortical culture were kept in CDMM Plus WNT/BMP inhibitors for four (WiBi 11) additional days, whereas hippocampal culture (CHIR8) were grown in CDMM supplemented with CHIR 3μM (Santa Cruz Biotechnology). On the eleventh day of differentiation *in vitro* DMEM/F12 was replaced with Neurobasal and NEAA were removed from the CDMM to avoid glutamate-induced excitotoxicity. FGF8-treated cells (FGF8) were grown in CDMM supplemented with FGF 100ng/mL (R&D), replaced daily. MEK inhibitor (PD0325901, Calbiochem, 1μM; Barrett et al., 2008) was added daily to block FGF signaling. On the eleventh day of differentiation *in vitro*, DMEM/F12 was replaced with Neurobasal and NEAA were removed from the CDMM to avoid glutamate-induced excitotoxicity.

LNA miRNA transfection was performed using Lipofectamine 2000 (Invitrogen) according to manufacturer's instructions (miRCURY LNA miRNA Inhibitors, Exiqon). Briefly, each LNA (5nmol) was resuspended in TE buffer (10mM Tris pH 7.5 or 8.0, 1mM EDTA) to a concentration of 50uM. Cells were then transfected

O/N at 37°C and 5%CO2 in 24 well plates using 80nM LNA and 2.5uL/well of Lipofectamine 2000 in a final volume of 0.5mL/well Optimem. Since LNA concentration higher than 100nM resulted toxic for the cells, we used less than half the concentration (40nM) in the experiments in which two LNAs were co-transfected.

Mature miRNAs (miRNA mimics, supplied by Shanghai GenePharma) were transfected in 24 well plates at 60 nM final concentration using 2 μl of Lipofectamine 2000 in 0.5mL Optimem for 4-6 hr. mmu-miR-21a-5p mimic was assembled by annealing 10' at RT uagcuuaucagacugauguuga-uu sense strand RNA and ucaacaucagucugauaagaaa-uu antisense strand RNA. For mmu-miR-132-3p mimic, uaacagucuacagccauggucg-uu sense strand and cgaccauggcuguagacugaaa-uu antisense strand RNAs were used. Scramble control mirna had uucuccgaacgugucacgu sense strand and acgugacacguucggagaa antisense strand. When co-transfected with lentiviral vectors carrying WT or mutated COUP-TFI 3'UTR in HEK 293 T cells, miRNA mimics were used at 30nM final concentration and mixed with 500ng of lentiviral vector DNA.

Cortical and hippocampal primary cultures

Cortical and hippocampal tissues from E15.5/E16.5 embryos were dissociated in HBSS (Invitrogen) with trypsin 0.25% (Invitrogen) for 15' at 37 °C. Enzymatic activity was stopped with twice the volume of DMEM plus FCS 10% and 100U/ml DNase (Sigma). Cells were seeded in Neurobasal medium (2mM Glutamine, 1mM sodium Pyruvate, 0.05mM β-mercaptoethanol, 100 U/ml Penicillin/Streptomycin

supplemented with B27) at a concentration of 150000 cells per cm2 in Poly-ornithine/Laminin coated wells. After 24h (DIV 1) cells were infected with either the pWPXLd-memGFP or the pWPXLd-memCherry lentivirus for 6hs at 37°C. After 48hs (DIV 2) cells were dissociated for grafting and qualitative gene expression analysis.

Gene expression analysis

RT-PCR and Immunocitodetection (ICD) analyses were carried out as previously described *(Bertacchi et al., 2013)*. Primary antibodies used for ICD included NeuN (1:1000; Millipore), Tbr1 (1:1000; Millipore), MapII (1:400; xx), Ntub (1:1000, Sigma), CTIP2 (1:1000; Abcam), SATB2 (1:400; Abcam), COUP-TFI (Abcam ab60059, 1:1000), KI-67 (ThermoFisher, 1:1000) and TUJ1 (β-III-TUBULIN, 1:1000; Covance). Alexa Fluor 488 and Alexa Fluor 546 anti-mouse, anti-rabbit or anti-chicken IgG conjugates (Molecular Probes, 1:500) were used as secondary antibodies.

Total and small RNA was extracted with NucleoSpin RNA II or small RNA columns (Macherey-Nagel). RNA quantity and RNA quality were assessed with Nanodrop and gel electrophoresis. For each sample, 200ng of total RNA was reverse-transcribed, using Eurogentec cDNA synthesis kit for mRNAs and Qiagen miR-script kit for miRNAs. RT-PCR was performed using iTaq Universal SYBR Green Supermix (Bio-rad) on Rotor-Gene 6000 (Corbett). Amplification take-off values were evaluated using the built-in Rotor-Gene 6000 relative quantification analysis function, and relative expression was calculated with the 2-ΔΔCt method, normalizing to the housekeeping gene β-Actin or U6 for mRNAs or miRNAs, respectively. Standard errors were

obtained from the error propagation formula, as described in *(Nordgård et al., 2006)*.

Microarray hybridization and data analysis

Embryonic tissues were dissected from n = 3 mouse embryos (Sv129s6 strain, Taconic) at embryonic day (E)12.5. Cells were detached by trypsinization, washed and resuspended in PBS, 2% FBS, 2mM EDTA and kept on ice. Total RNA was extracted with NucleoSpin RNA II columns (Macherey–Nagel). RNA from three different sets of experiments was pooled. RNA quality was assessed with Agilent Bioanalyzer RNA 6000 Nano kit; 50 ng of RNA were labelled with LowInput QuickAmp Labeling Kit One-Color (Agilent Technologies), purified and hybridized overnight onto Agilent SurePrint G3 Mouse Gene Expression Array (8x60K, grid ID 028005), according to the manufacturer's instructions. Agilent Microarray scanner G2564C was used for slide acquisition and spot analysis was performed with Feature Extraction software (Agilent). Data were background-corrected and normalized between arrays by means of Bioconductor package Limma *(Smyth, 2005)*. Principal component analysis (PCA) and hierarchical clustering were performed both on the first-quartile or on the top 2% genes (n=487) displaying the higher variance among samples. In the hierarchical clustering analysis, p.value were computed via multiscale bootstrap resampling (rep=1000) using the R package "pvclust" *(Suzuki and Shimodaira, 2006)*. Pathways enrichment analysis was performed using DAVID (v. 6.8) *(Huang et al., 2007)* and the R package

"RDAVIDWebService" *(Fresno and Fernández, 2013)* on the most differentially expressed genes (Fold change ≥ 3) between the samples.

Lentiviral vector construction and use

Vector carrying a membrane-localized GFP and mCherry were constructed swapping the original GFP in the pWPXLd vector (Addgene number 12258) with, respectively, the prenylated GFP in pME-EGFPCAAX and mCherry in pME-mCherryCAAX *(Tol2kit, Kwan et al., 2007)* using the restriction sites MluI/XmaI. The entire COUP-TFI 3'UTR (748bp) was obtained from the genomic BAC library RPCI-23 (Source Bioscience, Genome Cube) and amplified via PCR using a forward and reverse primer carrying, respectively, an XmaI and KpnI restriction site at their 5' (FW: attcccgggactttgggtgtttcccaccc, rev: taaaggtacctttgctaaattcttttatttttgtttaa). The vector carrying the COUP-TFI 3'UTR (virCOUP) was constructed swapping the original WPRE sequence in the pWPXLd vector (Addgene number 12258), with the amplicon carrying the COUP-TFI 3'UTR using the restriction sites XmaI/KpnI. The ligated vector was then sequenced to ensure the correct cloning of the 3'UTR. Mutations of the predicted binding sites of mmu-miR-21a-5p (miR-21) and mmu-miR-132-3p (miR-132) in the 3' UTR of COUP-TFI were obtained by PCR using Q5® High-Fidelity DNA Polymerase (NEB). The seed sequence of miR-21 at +245 and that of miR-132 at +389 (Fig. S8) were replaced with a Not I restriction sequence. To this aim, upstream and downstream halves of mutated 3'UTR were generated by PCR using the external forward or reverse primer reported above in combination with a mutated internal reverse or forward

primer, respectively. The mutated internal primers used for miR-21 site were miR-21_mut_fw caccaagcggccgcgatttggaagagaggaccatgag and mir-21_mut_rev cacaggcggccgcacgaggtccttttttctttcctttccaatgtac. The mutated internal primers used for miR-132 site at +389 were miR-132_mut_fw cagtatgcggccgcaatcctatgtagaaacatacactgaacattgttattc and mir-132_mut_rev cagctagcggccgcttccatatgagtagttttctgtacagaatatatcc. Upstream and downstream mutated halves were then digested with Not I enzyme, ligated and used as a template for PCR together with external forward and reverse primers. PCR products were finally restricted with XmaI/KpnI, purified and inserted in pWPXLd vector. The seed sequence of miR-132 at +651 was deleted by PCR. For this purpose, the 3'UTR with the mutated miR-132 site at +389 was used as a template, and fw: attcccgggactttgggtgtttcccaccc and rev taaaggtacccgacaacatatatcgcactcattataagaagc as primers. The deleted fragment obtained was then restricted with XmaI/KpnI, purified and cloned in pWPXLd vector. Lentiviral vectors were produced transfecting 293 T cells with 150 nM polyethylenimine (PEI) reagent (Sigma) and either pWPXLd-memGFP or pWPXLd-memCherry plasmids, together with the Δ8.91 packaging and a VSV-G envelope expressing plasmids *(Zufferey et al., 1997)* in a ratio of 20 μg:15 μg:5 μg, respectively, per single 100-mm dish. Transfection medium was discarded 24 hours after transfection and viral particles were collected at 48 h and 72 h, pooled and frozen at −80 °C.

miRNAome profiling

For each point, 2 biological replicates, each consisting of a pool of 3 cell cultures, were analyzed. Total RNA was extracted with miRNeasy Mini Kit (Qiagen). The small-RNA library was prepared using 1 μg of total RNA per sample and the TruSeq Small RNA Sample Preparation (Illumina) following the manufacturer's instructions and sequenced on Illumina HiSeq 2000 platform, running in 50-bp single-read mode using sequencing chemistry v3, and then demultiplexed in a FASTQ format using CASAVA v.1.8 (Illumina). Library adaptors were trimmed and reads were mapped to the mouse genome (NCBI37/mm9) with miRExpress *(Wang et al., 2009)*. miRNA reads were annotated using the miRBase mouse reference (mirbase.org, V19). Normalization was performed as counts per million (CPM) and differential expression was evaluated with the R package EdgeR *(Robinson et al., 2010; Bioconductor)*.

In silico analysis of 3'UTR putative binding sites

For the identification of potential binding sites in the COUP-TFI 3'UTR, we employed the miRanda algorithm *(Betel et al., 2008; Enright et al., 2003; microrna.org)*, which takes into account both the seed complementarity score and the thermodynamic stability of the binding between miRNAs and 3'UTRs (Fig 10F), setting as thresholds a minimum score of 100 and a maximum energy of −15 kcal/mol.

Western Blot

Sample lysis was performed using RIPA buffer (50mM Tris-HCl pH 7.6, 1 % NP40, 0.5 % deoxycholic acid, 150mM NaCl, 1mM EDTA, 1mM

PMSF, 1 % SDS) supplemented with Complete Protease Inhibitor Cocktail (Roche), lysates were then incubated for 30 min on ice and sonicated three times for 10 sec each on medium power in order to reduce viscosity. The supernatant was harvested by centrifugation (10 min at 13,000 RPM, 4 °C) and quantified with a Micro BCA Protein Assay Kit (Thermo Scientific). Samples were then denatured with LDS Sample Buffer (Thermo Scientific) and heated for 10 min on a thermal block at 99 °C. The total protein extract (10 to 20µg) was resolved on 10 % acrylamide gels, transferred on a nitrocellulose membrane (Hybond-c Extra, GE Healthcare), blocked with 5 % milk proteins in TBST (50mM Tris pH 7.6, 150mM NaCl, 0.05 % Tween-20), and incubated for 1hr at RT with primary antibodies: COUPTFI (1:2000; homemade antibody) and α-Tubulin (clone B-5-1-2; 1:5000; Sigma-Aldrich; T6074). The membrane was washed three times with TBST (15 min each) and probed with an HRP-conjugated secondary anti-mouse or anti-rabbit antibody for 1 h (Santa Cruz Biotechnology; sc-2005 and sc-2030, respectively). After three more washes, the signal was revealed by means of an enhanced chemiluminescence kit (G&E Healthcare) on a BioMax XAR Film (Kodak). Densitometric analysis of the blots was performed with either ImageJ (imagej.nih.gov) gel analysis function or the ChemiDoc Imaging Systems Software (Bio-Rad).

In vitro immunocytodetection (ICD) and imaging

Cells prepared for immunocytodetection experiments were cultured on Poly-ornithine/Laminin coated round glass coverslips. Cells were fixed using 2% paraformaldehyde for 10-15 minutes, washed twice with PBS,

permeabilized using 0.1% Triton X100 in PBS and blocked using 0.5% BSA in PBS. Primary antibodies used for microscopy included CTIP2 (1:1000; Abcam), SATB2 (1:400; Abcam), TUJ1 (1:1000; Covance), GFP (GFP-1020, Aveslab) and COUP-TF I (1:2000). Primary antibodies were incubated 2hr at room temperature; cells were then washed three times with PBS (10' each). Alexa Fluor 488 and Alexa Fluor 546 anti-mouse, anti-rabbit or anti-chicken IgG conjugates (Molecular Probes, 1:500) were incubated 1hr at RT in PBS containing 0.1% Triton X100 and 0.5% BSA for primary antibody detection, followed by three PBS washes (10' each). Nuclear staining was obtained with DAPI. Immunofluorescence microphotographs were processed and analyzed with ImageJ 1.48p software (https://imagej.nih.gov/ij/index.html), measuring integrated pixel intensity. COUP-TFI signal quantification was performed on 3 biological replicas per group and on 10 different randomly chosen fields for each sample. Analysis of COUP-TFI expression was performed by applying first an appropriate threshold for each channel in order to remove background signal, then normalizing COUP-TFI pixel intensity on the nuclear staining (DAPI). EGFP reporter activity in HEK 293T and ES-neuralized cells was evaluated as EGFP/DAPI pixel intensity ratio. 10 different randomly chosen fields of 2 biological replicas per group were analyzed.

Immunofluorescence on frozen brain tissue

Mouse embryonic brains were dissected and fixed in 4% PFA at 4°C for 2hr in agitation, then washed in PBS1X and dehydrated in 30% Sucrose O/N at 4°C. Brains were then embedded in OCT and stored at -80°C.

Cryostat tissue sections (14 μm) were processed for immunodetection, as described for *in vitro* ICD, with the only difference that antigen retrieval unmasking was performed at the beginning of the staining, by boiling slides twice in sodium citrate 85 mM, pH6.

RNA in situ hybridization (ISH)

miRNA-21 antisense and control scramble probes (Exiqon) were used following manufacturer's instruction. Brains for ISH were fixed O/N with PFA 4% at 4°C, dehydrated in 30% Sucrose and embedded in OCT resin, then stored at -80°C. ISH was carried out on 14 μm-cryosections as follows. Defrosted and air-dried brain sections were treated with RIPA buffer (150nM NaCl, 1% NP-40, 0.5% Na deoxycholate, 0.1% SDS, 1mM EDTA, 50mM Tris, pH 8.0) for 10 minutes, then post-fixed 15 minutes in 4% PFA at room temperature. Pre-hybridization and hybridization of the sections with Exiqon probes were performed in the following solution: 50% formamide, 5X SSC, 5X Denhardts solution (Invitrogen), 500μg/ml Salmon sperm DNA (Ambion), 250 μg/ml Yeast t-RNA. The Exiqon probe was added in the hybridization solution at a concentration of 0.5μl for 300μl/slide. Different temperatures were tested for optimal hybridization, ranging from 4°C to 37°C; best results were obtained with cold temperature (4°C). The day after, slides were washed twice for 1 h at 4°C in the following solution: 50% formamide, 2X SSC, 0.1% Tween 20. Then, the samples were equilibrated in MABT solution and blocked in MABT / 10% sheep serum. The hybridized probes were detected by overnight incubation at 4°C with an anti-DIG antibody (1:2.000; Roche). Finally, sections were washed several times in

MABT, then equilibrated in B3 buffer (100mM Tris, pH 9.5, 50mM MgCl2, 100mM NaCl, 0.1% Tween-20). The staining was obtained incubating the slices in NBT/BCIP solution (Roche) at room temperature (or O/N at 4°C). Two quick washes with B3 buffer supplemented with Tetramisole (0.5 mg/ml; Sigma) were performed before staining to reduce background.

In utero electroporation (IUE)

In utero electroporation was performed on E12.5 mouse brains, by trying to target the latero-dorsal regions of the telencephalic dorsal pallium. The electroporations were performed using a Tweezertrode electrode (diameter 7 mm; BTX) connected to a NEPA21 Type-II electroporator (NEPA GENE). The following parameters were used: four 35 V pulses, P(on) 50 ms, P(off) 1s and 5% decay rate. The "sponge" plasmid was produced by cloning the PCR-amplified COUP-TFI 3'UTR DNA sequence into the XhoI and NotI sites of a pCIG2-IRES-GFP plasmid *(Heng et al., 2008)*. The "mutated sponge" (where miR-21 seed was substituted by a scramble sequence, see Fig. S9A) was obtained by inserting the mutation with apposite primers (5'-caacttgcttaaaatgaaaaaaaaaaaaaaaaaaagaacgatttg-3'; 5'-ttttcattttaagcaagttgacgaggtccttttttctttcctttcc-3') then amplifying the mutated UTR sequence with NotI site containing primers (5'-ataagaatgcggccgcgactttgggtgtttcccacccaat-3'; 5'-ataagaatgcggccgcttttgctaaattcttttatttttg-3') and finally cloning it in the pCIG2-IRES-GFP plasmid. The 1X DNA solution for IUE was injected in one of the two brain telencephalic vesicles prior to the application of

electric current and consisted of endo-free TE buffer, 1X Fast Green and the plasmid at a final concentration of 1mg/ml. The original pCIG2-IRES-GFP plasmid was electroporated at the same concentration as the control. For LNA lipofection experiments, the injected solution consisted of 3 μl Lipofectamine 2000 (Invitrogen), 0.4μl Fast Green and 2μl LNA antagomiR. In this case, since the transfection was mediated by Lipofectamine, no electric field was applied following the injection into telencephalic vesicles.

Stroke induction

The photothrombotic lesion was induced as previously described *(Lai et al., 2015; Alia et al., 2016)*. Briefly, animals were anesthetized with Avertin (20ml/kg, 2,2,2 tribromoethanol 1.25%; Sigma-Aldrich, USA) and placed in a stereotaxic apparatus. After a midline scalp incision, the bone was carefully dried and cleaned. A Rose Bengal solution (0.2 ml of a 10mg/ml solution in PBS; Sigma Aldrich) was injected in the peritoneum. After 5 min, the brain was illuminated through the intact skull for 15 min using a cold light source (ZEISS CL 6000) linked to a 20X objective that was positioned 0.5 mm anterior and 1.75 mm lateral from Bregma, i.e. in correspondence with the caudal forelimb area *(Tennant et al., 2011; Vallone et al., 2016)*. At the end of the surgery, the skin was sutured and mice were allowed to awaken from anesthesia.

In vivo grafting

ESCs were differentiated into isocortical (WiBi 11) and hippocampal (CHIR 8) neurons, as previously described. On day 9, WiBi- and CHIR-

treated neurons were transduced, respectively, with a lentivirus carrying a membrane-bound form of GFP and mCherry for 6 hours at 37°C. To eliminate undifferentiated ES and cycling cells, gamma-secretase inhibitor 10μM (DAPT, Sigma) was added to the culture medium on day 14 and 15 and Aracytin 5μM (AraC) on day 15. After 16 days of differentiation, ESCs were dissociated and resuspended at a concentration of 150'000 cells/μL in DMEM/F12 supplemented with 10% FCS. In co-transplantation experiments, WiBi- and CHIR-treated cells were pooled and injected together in equal proportions. A volume of 1μL of cell suspension was injected in 2 months old mice using a Hamilton syringe (gauge 29). For the hippocampal grafting, mice (n=5) were transplanted into the DG (2 mm posterior and 1.5 mm lateral from Bregma, depth 1.7 mm). The transplantation in the motor cortex of healthy (n=6) mice was performed at the same coordinates of the experimental photothrombotic lesion (i.e., in correspondence with the caudal forelimb area), at a depth of 0.7 mm. In the ischemic mice (n=6) two injections were performed 3 days after the experimental stroke: one in the center of the ischemic lesion and the other in the periphery of the ischemic core at -1.3 mm posterior and 1.75 mm lateral from Bregma. An additional group of stroke animals were injected with vehicle (i.e. cells medium, n=5) or WiBi cells (n=9) using the same two coordinates as described above. They were used for the behavioral assessment of motor deficits after ischemia using the gridwalk test (see below).

Gridwalk Test

To evaluate the motor performance after stroke, animals were allowed to walk freely on an elevated grid (32 x 20 cm, with 11 x 11 mm-large openings) for 5 minutes, video-recording the task. Subsequently, the videos were analyzed off-line by means of a custom-designed Graphical User Interface implemented in Matlab *(Lai et al., 2015)* by an experimenter blinded to the experimental group. Correct steps and foot-faults, i.e. steps not providing body support, with the foot falling into grid hole were assessed and the percentage of foot faults for each limb was then calculated, as previously described *(Lai et al., 2015)*. The test was performed at 2, 9, 16 and 23 days post stroke.

Axonal projection imaging and quantification

For immunohistochemistry, brains were collected after transcardial perfusion of deeply anaesthetized mice with PBS (5 min) followed by 4% PFA, 30–40 min. Brains were then post-fixed in 4% PFA overnight, at 4 °C, and sectioned on a microtome into 50μm coronal sections, which were kept free-floating for further processing. Brain slices were incubated in a blocking solution with 1 hour min (10% bovine serum albumin; 0,3% Triton X-100) before applying the primary antibodies Rat anti-mCherry (1:1000; Life Technologies), Goat anti-GFP (1:800; Abcam), for overnight incubation at 4 °C. After washing, slices were incubated with species-specific secondary antibodies conjugated to 488 and Cy3 (Jackson ImmunoResearch) used at 1:500 for 2 h at room temperature. Nuclear staining was performed with (1:500) Hoechst 33342 (Sigma); 5

min at room temperature) and coverslips were mounted on glass slides with Vectashield (Vector Labs).

Images were acquired with epifluorescence microscope (Axio Imager. Z2, Zeiss) equipped with Apotome.2 (Zeiss) at resolutions of 1350 × 1024 pixels and a 40 × ec-plan-neofluar oil objective (1.3 NA). The differential projection analysis was performed on three animals for each group; for each experimental animal, and for each region analyzed, z-stack images (2.5 μm z-step size) of 3 different sections were acquired with the ZENpro software (Zeiss) and then processed with ImageJ 1.48p software (https://imagej.nih.gov/ij/index.html). Analysis of the transplanted cells was performed by applying an appropriate threshold for each channel in order to remove background signal and obtain a binary image of the projections/cell bodies. For each experimental animal, the size of the transplant was measured as the average area of the three sections, in the series, with greatest cross-section of the graft. Projection density for each image and each channel was then calculated as total number of pixel above threshold normalized on the average area (expressed in millions of pixels) of the graft from which the fibers originated. In the quantification of projections surrounding the grafts, for each animal and for 3 different sections, longitudinal multi-tile z-stacks at a resolution 1024 * 4096 were acquired in the immediate proximity of the graft; the images were then thresholded, as previously shown, and the fiber density was calculated as the total number of pixel above threshold for each bin (50μm), normalized on the size of the graft and projected onto the major axis of the image.

SUPPLEMENTAL MATERIALS

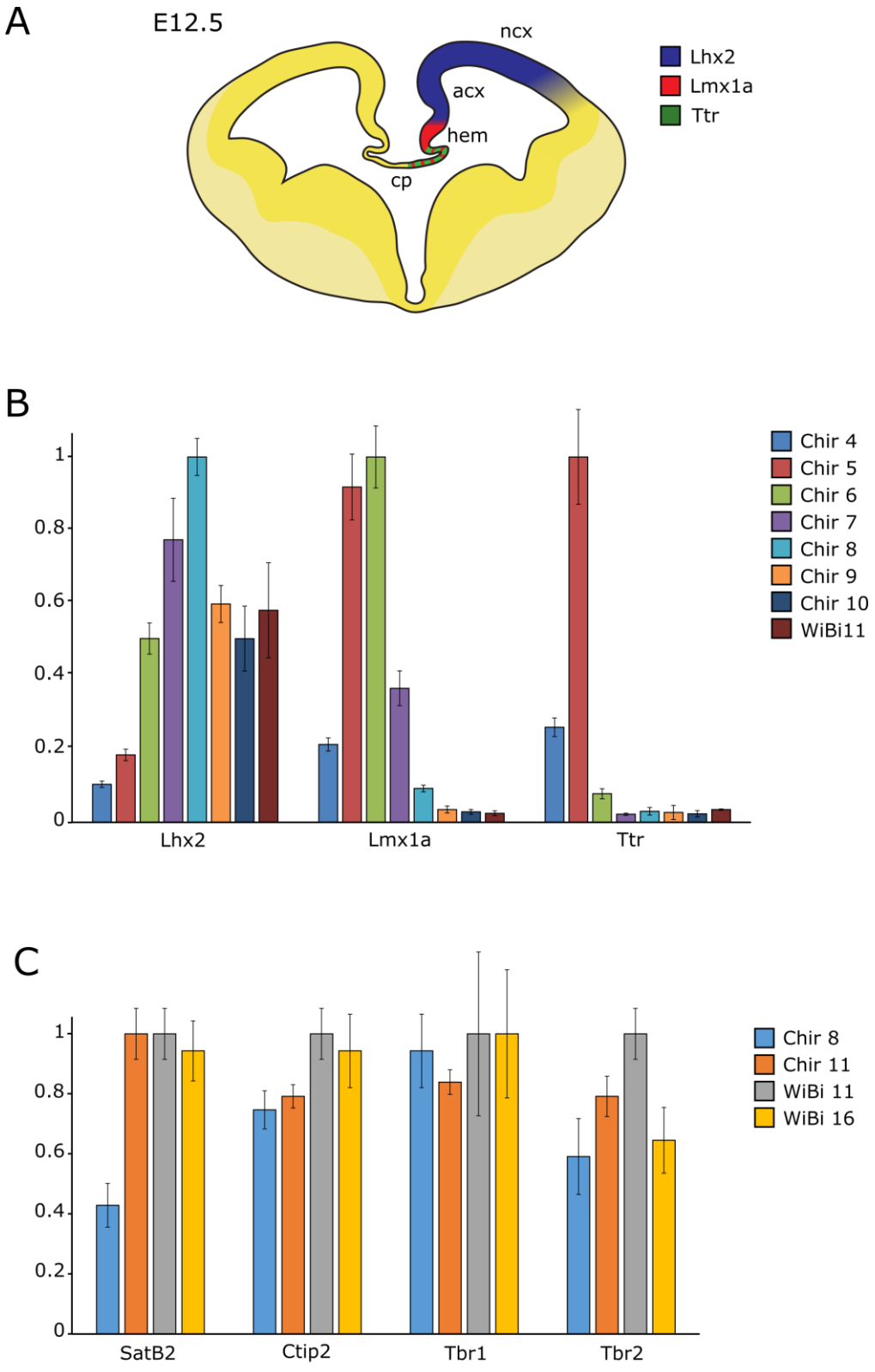
A
E12.5
ncx
acx
hem
cp
Lhx2
Lmx1a
Ttr
B
1
0.8
0.6
0.4
0.2
0
Lhx2
Lmx1a
Ttr
Chir 4
Chir 5
Chir 6
Chir 7
Chir 8
Chir 9
Chir 10
WiBi11
C
1
0.8
0.6
0.4
0.2
0
SatB2
Ctip2
Tbr1
Tbr2
Chir 8
Chir 11
WiBi 11
WiBi 16

Figure S1 Markers of hem, choroid plexus and dorsal telencephalon

A, Hippocampal organizer, cortical hem and choroid plexus arise from the median wall of the telencephalon. Drawing depicts a coronal section of the E12.5 mouse embryonic brain and the expression of the markers of hem and choroid plexus Lmx1a and Ttr, and the dorsal telencephalic marker Lhx2. cp, choroid plexus; hem, cortical hem; acx, archicortex; ncx, neocortex. **B**, mRNA fold change of the choroid plexus markers Lmx1 and Ttr and the dorsal telencephalic marker Lhx2, as evaluated at DIV 11 by RT-PCR in cells treated with CHIR at different time points. Expression levels of each gene has been normalized on the maximum value in the series. **C**, Quantification via RT-PCR of the pan-cortical markers Satb2, Ctip2, Tbr1 and Tbr2 in cells at DIV16 (C).

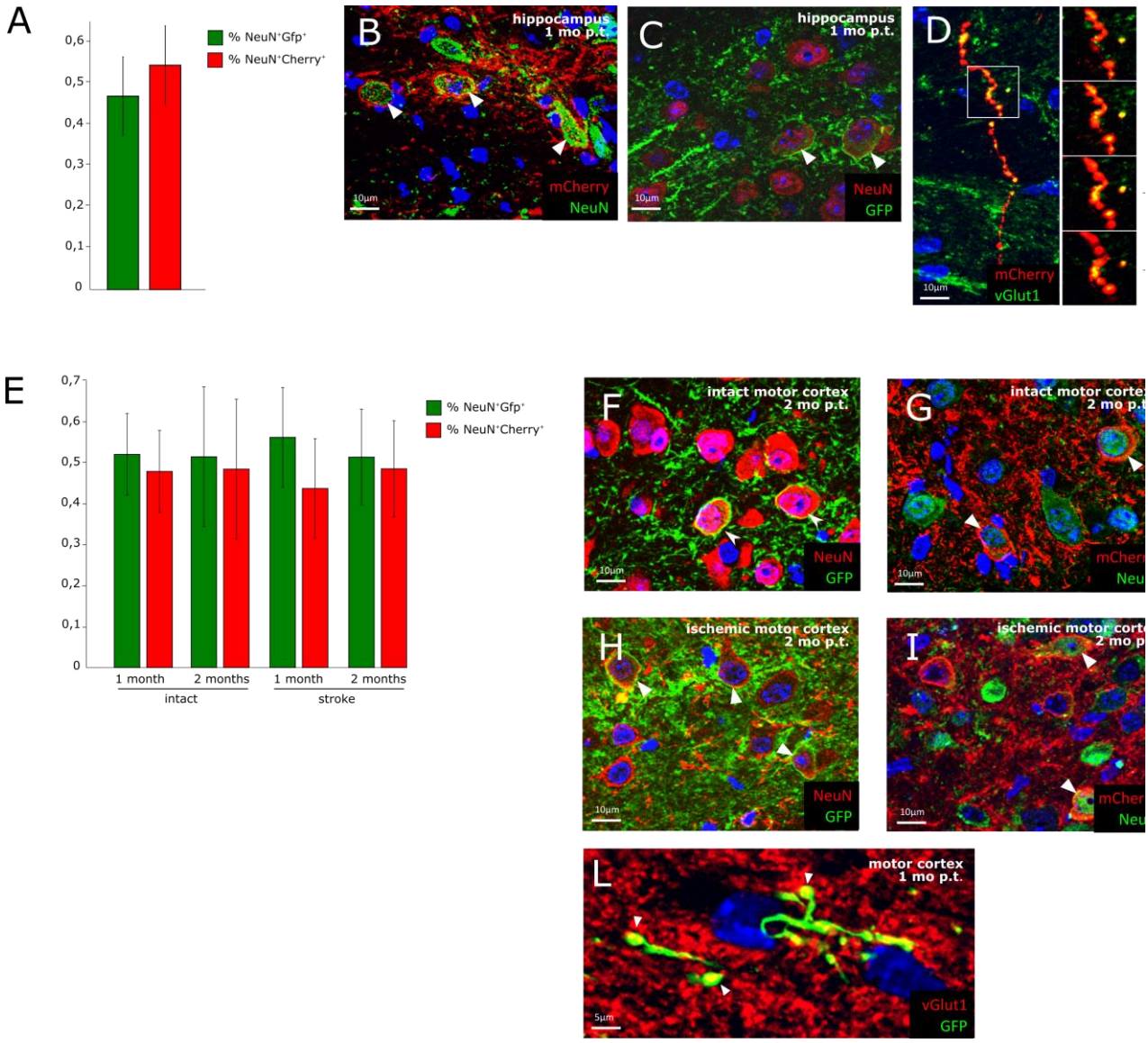

Figure S2 Staining for NeuN and synaptic markers in transplanted cells

A-C) Quantification and immunohistochemistry of NeuN+/mCherry+ and NeuN+/GFP+ double positive cells (arrowheads) in hippocampus 1 month post transplantation (p.t.). **D**, Deconvoluted ICD of CHIR8 fibers (mCherry, red) and vGlut1 (green) in the hippocampus 1 month p.t. (left) and zoom-in of the indicated ROI showing co-localization of vGlut1 and mCherry in each optic plane (right). **E-I**)

Quantification and immunohistochemistry of NeuN+/mCherry+ and NeuN+/GFP+ double positive cells (arrowheads) in intact and ischemic motor cortex 1 and 2 months after grafting. L) Optic section showing ICD of WiBi fibers (GFP) with vGlut1-positive axonal varicosities (arrowheads) in the motor cortex of an ischemic brain 1 month p.t.

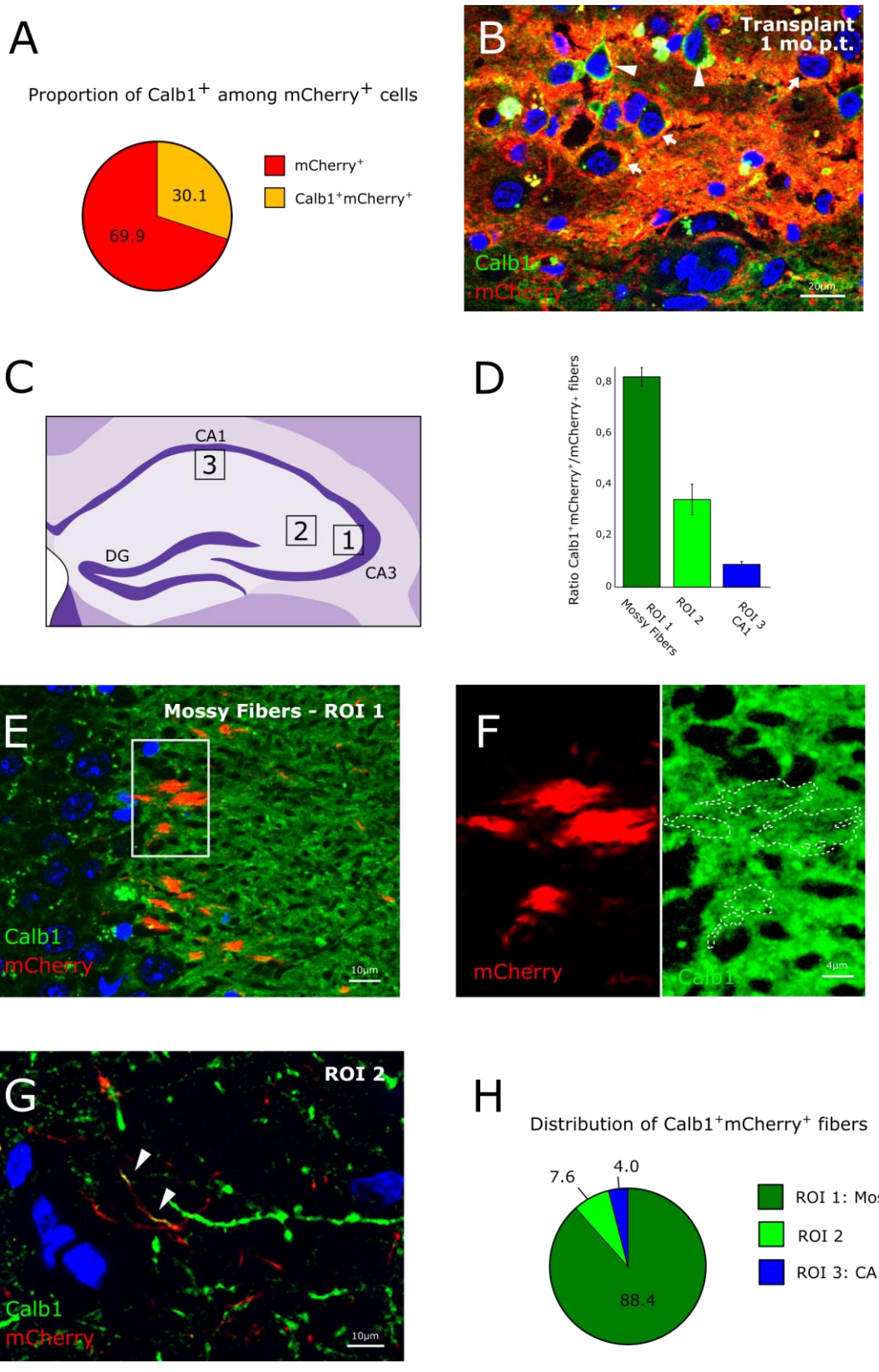
A
Proportion of Calb1+ among mCherry+ cells
30.1
69.9
mCherry+
Calb1+mCherry+
B
Transplant
1 mo p.t.
Calb1
mCherry
20µm
C
CA1
3
2
1
DG
CA3
D
Ratio Calb1+mCherry+/mCherry+ fibers
0,8
0,6
0,4
0,2
0
ROI 1
Mossy Fibers
ROI 2
ROI 3
CA1
E
Mossy Fibers - ROI 1
Calb1
mCherry
10µm
F
mCherry
Calb1
4µm
G
ROI 2
Calb1
mCherry
10µm
H
Distribution of Calb1+mCherry+ fibers
7.6
4.0
88.4
ROI 1: Mossy Fibers
ROI 2
ROI 3: CA1

Figure S3 Distribution of Calbindin 1 positive fibers from transplanted CHIR8 cells

A-B, Quantification of Calbindin 1 (Calb1)-positive cells. **A**, Percentage of Calb1-positive cells among the CHIR8 cells, one month p.t. **B**, ICD of Calb1- and mCherry-positive grafted cells in the hippocampus, one month p.t. Arrowheads indicate Calb1/mCherry double positive cells, while arrows point to cells containing only the mCherry label. C-H, Quantification of Calb1-positive fibers. **C**, Schematic representation of the regions of interest (ROIs) analysed. **D**, Ratio of Calb1/mCherry double-positive fibers on the total amount of mCherry-stained fibers in each ROI. **E**, ICD of Calb1 and mCherry in the Mossy Fibers, one month p.t. **F**, Zoom-in of the region indicated in E showing colocalization between Calb1 and mCherry signal. **G**, ICD of Calb1 and mCherry in ROI 2. **H**, Distribution of Calb1/mCherry double positive fibers among the three ROIs one month p.t.

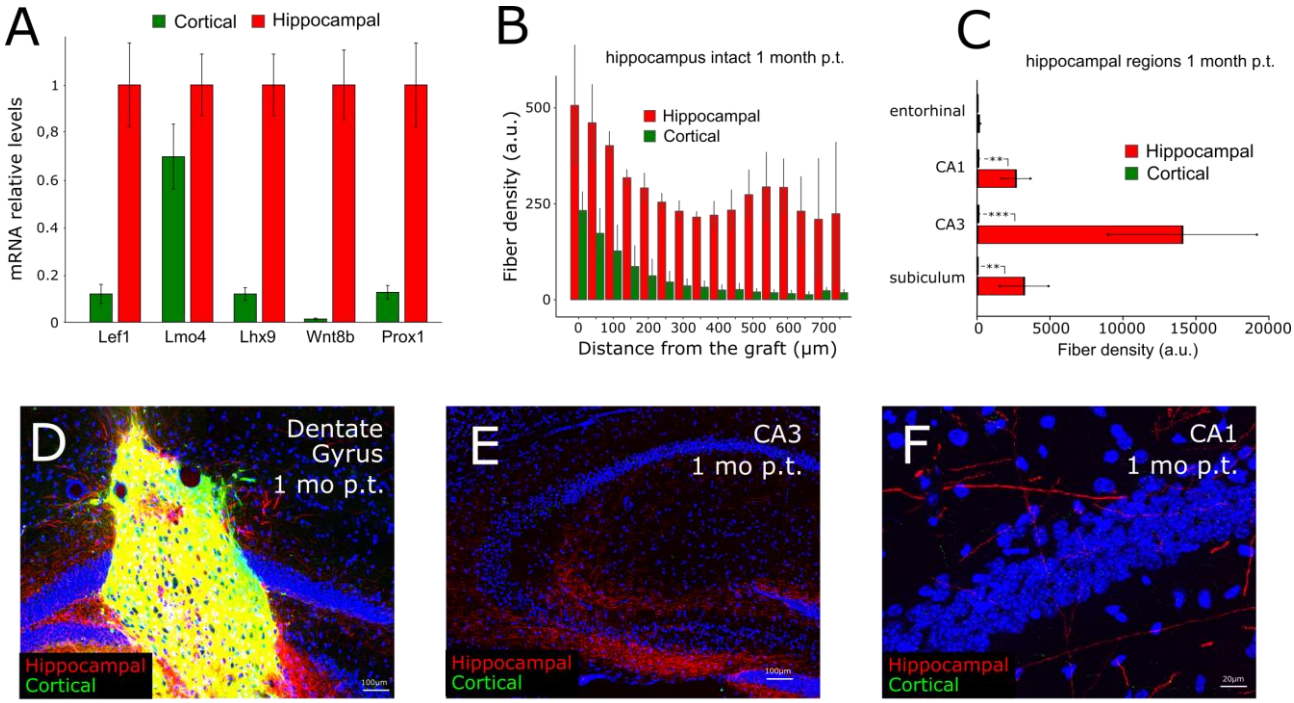

Figure S4 Fetal transplantation in intact hippocampus

A, Relative expression of hippocampal markers in cortical and hippocampal primary cultures (DIV 2) from E16 mice. **B,** Density of hippocampal and cortical projections at different distances from the graft, one month p.t. **C**, Quantification of hippocampal and cortical projections in different hippocampal regions, one month after the grafting. N≥ 3 transplanted animals were analyzed. **D-E-F**, ICD of hippocampal (red) and cortical (green) fibers one month p.t. in different regions, as indicated by labels.

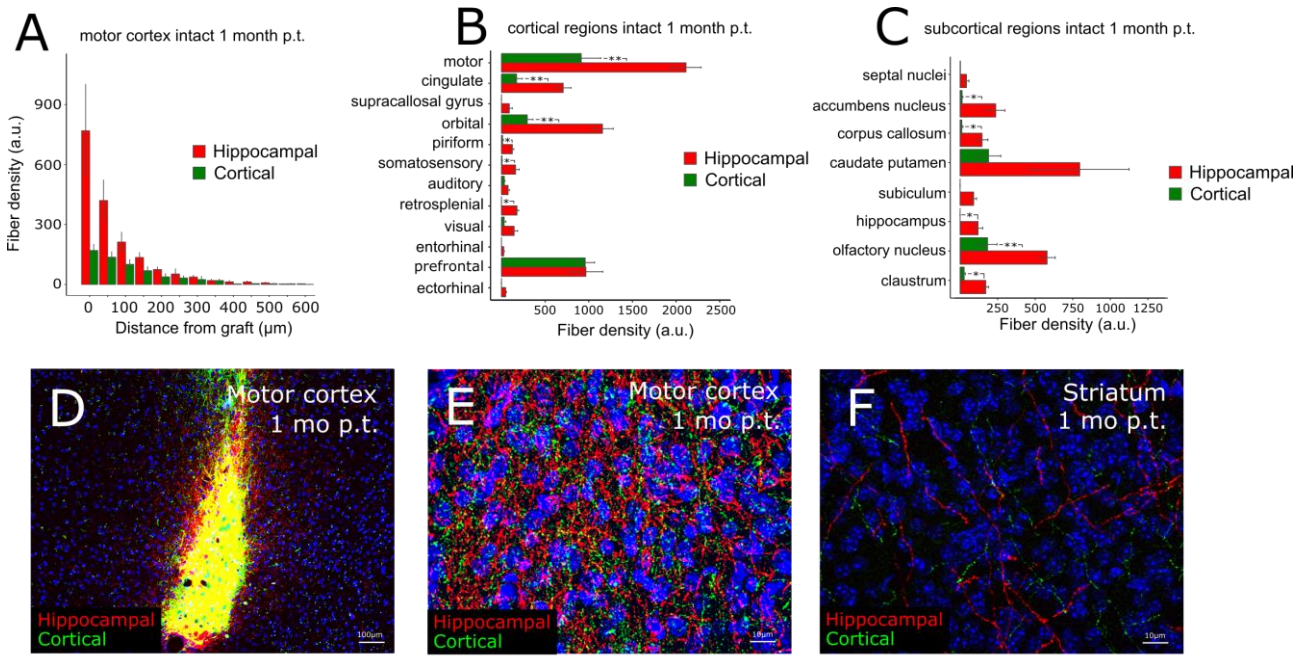

Figure S5 Fetal transplantation in intact motor cortex

A, Density of hippocampal and cortical projections at different distances from the graft, one month p.t. **B-C**, Quantification of hippocampal and cortical projections in different cortical (B) and subcortical (C) regions, one month after the grafting. N≥ 3 transplanted animals were analyzed. **D-E-F**, ICD of hippocampal and cortical fibers one month p.t. in different cortical and subcortical regions, as indicated by labels.

cortex vs hippo				
Annotation Cluster 1	Enrichment Score: 4.13			
Term	Count	Fold Enrichment	Benjamini	FDR
mmu04512:ECM-receptor interaction	12	6.46	1.17E-04	0.0024
mmu05146:Amoebiasis	12	4.86	9.40E-04	0.0388
mmu04974:Protein digestion and absorption	10	5.38	2.23E-03	0.1075
mmu04510:Focal adhesion	14	3.20	6.99E-03	0.4810
mmu04151:PI3K-Akt signaling pathway	18	2.43	0.0171	1.2991

Annotation Cluster 2	Enrichment Score: 3.80			
Term	Count	Fold Enrichment	Benjamini	FDR
mmu05217:Basal cell carcinoma	10	8.61	1.57E-04	2.16E-03
mmu04390:Hippo signaling pathway	14	4.39	6.91E-04	0.0190
mmu04550:Signaling pathways regulating pluripotency of stem cells	13	4.46	1.08E-03	0.0370
mmu04310:Wnt signaling pathway	12	4.03	3.87E-03	0.2129
mmu05200:Pathways in cancer	21	2.51	4.49E-03	0.2781
mmu04916:Melanogenesis	9	4.31	0.0159	1.3122
mmu05166:HTLV-I infection	11	1.87	0.3923	57.5199

wibi11 vs chir8				
Annotation Cluster 1	Enrichment Score: 2.74			
Term	Count	Fold Enrichment	Benjamini	FDR
mmu04512:ECM-receptor interaction	10	7.43	9.55E-04	7.37E-03
mmu04510:Focal adhesion	14	4.41	9.88E-04	0.0152
mmu04151:PI3K-Akt signaling pathway	17	3.26	2.33E-03	0.0539
mmu04974:Protein digestion and absorption	6	4.80	0.09568	8.8819
mmu04810:Regulation of actin cytoskeleton	8	2.47	0.33456	39.4830
mmu05146:Amoebiasis	5	2.76	0.52640	73.4147
mmu04611:Platelet activation	3	1.57	0.92679	99.9958
Annotation Cluster 2	Enrichment Score: 2.20			
Term	Count	Fold Enrichment	Benjamini	FDR
mmu05217:Basal cell carcinoma	7	8.09	7.46E-03	0.2305
mmu05200:Pathways in cancer	17	2.79	8.75E-03	0.3383
mmu04310:Wnt signaling pathway	9	4.16	0.0247	1.5323
mmu04916:Melanogenesis	6	3.90	0.1819	19.4796
mmu04550:Signaling pathways regulating pluripotency of stem cells	7	3.28	0.1782	20.2976
mmu04390:Hippo signaling pathway	6	2.60	0.4700	62.4205
mmu05166:HTLV-I infection	7	1.75	0.6686	93.4382

Table 1 Pathway enrichment analysis

Pathway enrichment analysis performed on the most differentially expressed genes (Fold change ≥3) between embryonic E15.5 isocortex and hippocampus, or Chir8 and WiBi11 cells, at DIV16.

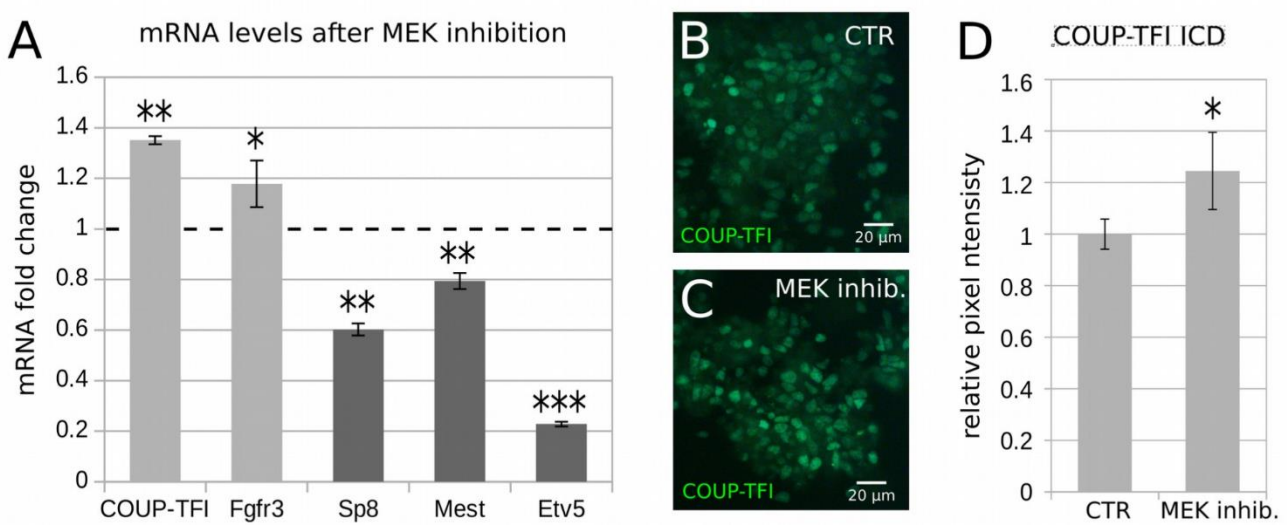

Figure S6 Effect of FGF signaling inhibition on A/P cortical markers and COUP-TFI protein

A, RT-PCR showing COUP-TFI, FGFR3, Sp8, Mest and Etv5 transcript levels at DIV 11, after 3 days of FGF signaling inhibition, performed by means of MEK inhibitor PD0325901 treatment. **B-C**, COUP-TFI immunodetection in control DIV 11 cells (B), and in DIV 11 cells after 3 days of MEK inhibition. D, relative pixel intensity of immunodetected COUP-TFI in control and MEK-inhibited cells as in B,C.

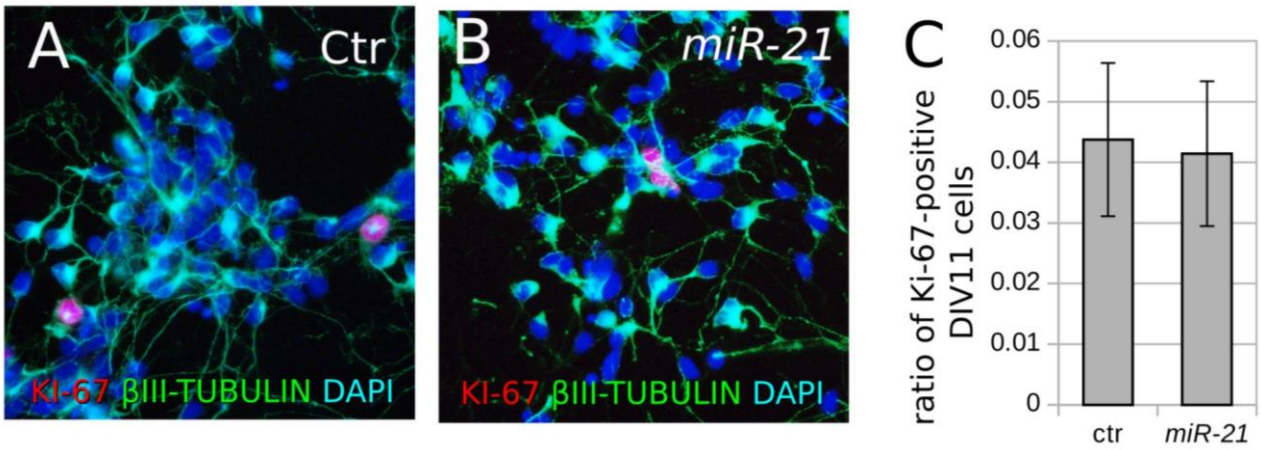

Figure S7 Effect of miR-21 upregulation on cell proliferation.

A-B, KI-67 (red) and βIII-TUBULIN (green) immunodetection in DIV 11 cortical cells lipofected with scrambled (A, Ctr) or miR-21 (B) mature miRNA at DIV 8. Nuclei counterstaining (blue) was obtained with DAPI. **C**, Quantification of KI-67- and βIII-TUBULIN-positive cell ratio. Error bars, SEM.

Figure S8 Mutagenesis of the predicted miR-21 and miR-132 binding sequences in COUP-TFI 3'UTR.

The dashed boxes indicates the seed sequence of miRNA/mRNA interaction predicted by miRANDA. Each seed sequence was mutated to generate distinct EGFP reporter mutants used in Fig. 12 F (see Methods).

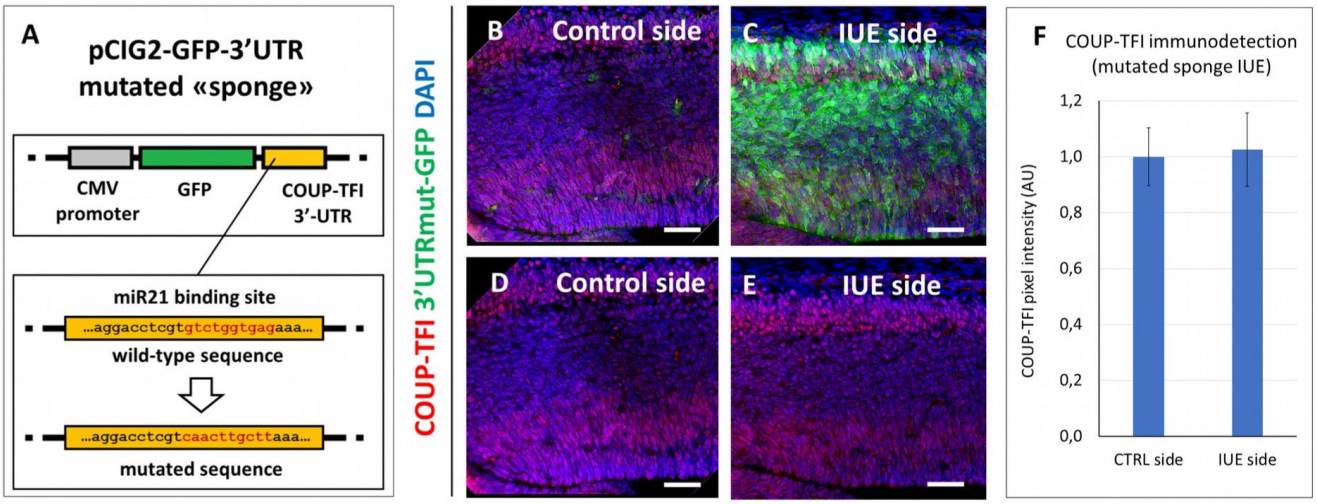

Figure S9 *In vivo* IUE of miR-21 seed-mutated sponge.

A, Schematics of the control in utero electroporation (IUE) experiment, using a mutated version of the COUP-TFI 3'UTR "sponge" plasmid. The seed sequence of the miR-21 binding site (GTCTGGTGAG) was replaced with a neutral mutated sequence (CAACTTGCTT; nucleotides highlighted in red). The mutated "sponge" plasmid was injected into the lateral/dorsal pallium of one telencephalic hemisphere and electroporated in neural progenitors, as for experiment in Figure 14. Brains were collected 48hrs later and processed for immunofluorescence. **B-E**, Immunofluorescence of COUP-TFI (red) and GFP (green) in brain sections electroporated with the mutated "sponge" plasmid at E12.5 and analyzed at E14.5. The lateral/dorsal pallium of the electroporated hemisphere (C,E) was compared to the contralateral control hemisphere (B,D). Nuclei counterstaining (blue) was

obtained with DAPI. Scale bars: 50 μm. **F**, Pixel intensity quantification (ImageJ) of COUP-TFI fluorescence in electroporated or control cortices. The staining was quantified only in the VZ and SVZ. Error bars, SEM.; there was not significant difference between the two conditions (t-test).

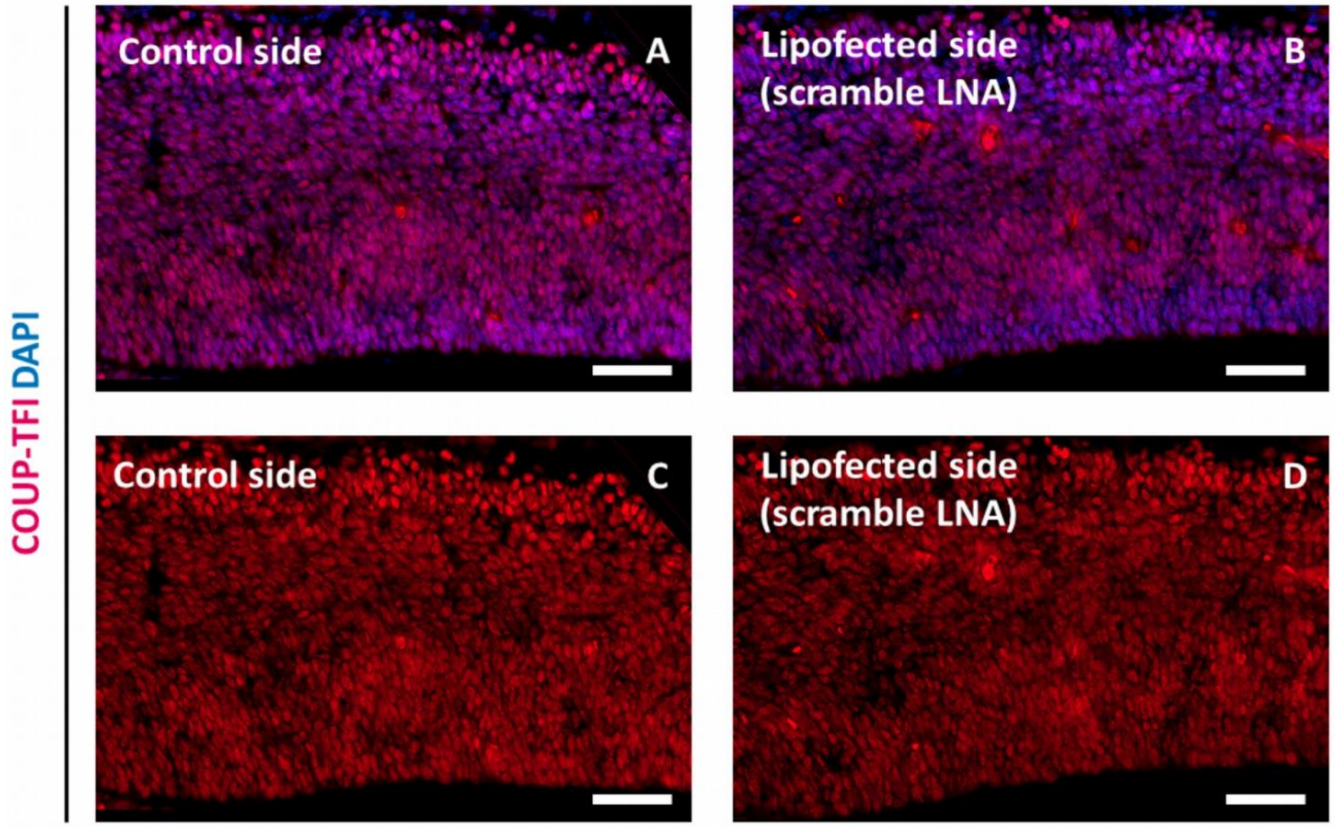

Figure S10 Control LNA lipofection *in vivo*

A-D, Immunodetection of COUP-TFI (red) in E14.5 brain sections, 2 days after in utero lipofection of a scramble (control) LNA. The fluorescence intensity of COUP-TFI protein in neural progenitor regions of the lipofected hemisphere (B,D) was compared to the contralateral control (non-lipofected) hemisphere (A,C). Nuclei counterstaining (blue) was obtained with DAPI. The graph showing pixel intensity quantification corresponding to these images is displayed in Fig 14 L. Scale bar: 50 μm

Table Primers

gene	forward sequence	reverse sequence
beta-actin	AATCGTGCGTGACATCAAAG	AAGGAAGGCTGGAAAAGAGC
couptfi	TGCTTGTGGCCTTGCGGATG	AGTTGCTCGATGACAGAGGAG
couptfii	TCAACTGCCACTCGTACCTG	CCATGATGTTGTTAGGCTGCAT
ctip2	GCCGACCCTGATCTACTCAC	CTCCTGCTTGGGACAGATGC
efr1	ACGCGACACTACATTCCCC	CTCTTCCGTGTTACGAAGGGC
emx1	GAAGAATCACTACGTGGTGGG	CCGTTTGTATTTTGTCCTCCGA
emx2	GGCTAGAGCACGCTTTTGAG	CACCGGTTAATGTGGTGTGT
en1	AGTGGCGGTGGTAGTGGA	CCTTCTCGTTCTTTTTCTTCTT
epha3	TTCTCCATCTCCGGTGAAAACA	ACCTCCCGACCAGAACATAGG
etv5	TCAGTCTGATAACTTGGTGCTTC	GGCTTCCTATCGTAGGCACAA
fgf15	ATGGCGAGAAAGTGGAACGG	CTGACACAGACTGGGATTGCT
fgf18	CCTGCACTTGCCTGTGTTTAC	TGCTTCCGACTCACATCATCT
fgf8	AGGGGAAGCTAATTGCCAAGA	CCTTGCGGGTAAAGGCCAT
fgfr3	GCCTGCGTGCTAGTGTTCT	TACCATCCTTAGCCCAGACCG
foxg1	CGACCCTGCCCTGTGAGT	TGGAAGAAGACCCCTGATTTTG
hey1	GCGCGGACGAGAATGGAAA	TCAGGTGATCCACAGTCATCTG
id3	CTGTCGGAACGTAGCCTGG	GTGGTTCATGTCGTCCAAGAG
irx3	AGTGCCTTGGAAGTGGAGAA	CGAGGAGAGAGCTGATAAGACC
klf3	GAAGCCCAACAAATATGGGGT	GGACGGGAACTTCAGAGAGG
krox20	GCCAAGGCCGTAGACAAAATC	CCACTCCGTTCATCTGGTCA
lef1	TCAAATAAAGTGCCCGTGGT	GGGGTAGAAGGTGGGGATT
lhx2	CTACCCCAGCAGCCAAAAGA	CCTGCCGTAAAAGGTTGC
lhx9	TCCAAAACGCACGAGCCAA	CAGGTCTGTTAAAGTGGTCGC
lmo3	ACACGAAGGCTAACCTTATCCT	AGTTTCCCGTTACACCAAACAG
lmo4	CGGACCGCTTTCTGCTCTATG	CATGCCGCTCTTGGTGTAACA
lmx1a	ACGGCCTGAAGATGGAGGA	CAGAAACCTGTCCGAGATGAC
mest	GTGGTGGGTCCAAGTAGGG	AAGCACAACTATCTCAGGGCT
otx2	CCACTTCGGGTATGGACTTG	GGTCTTGGCAAACAGAGCTT
pax6	CTTTGCTTGGGAAATCCGAG	AGCCAGGTTGCGAAGAACTC
prox1	AGAAGGGTTGACATTGGAGTGA	TGCGTGTTGCACCACAGAATA
ptn	ATGTCGTCCCAGCAATATCAGC	CCAAGATGAAAATCAATGCCAGG
satb2	CATGAGCCCTGGTCTTCTCT	AACTGCTCTGGGAATGGGTG
sfrp1	CAACGTGGGCTACAAGAAGAT	GGCCAGTAGAAGCCGAAGAAC
sp8	CTGGTAGAGGGTAAGGGCGG	AAGATTGGAAAGGGGGTAGTGA
spry2	TCCAATGACGATGAGGACAA	CACCCCTGGCACAATTTAAG
tbr1	CGCCCTCCTCCATCAAATCCATCG	GCAGTTCTTCTCGCAGTCCCGC

tbr2	GCGCATGTTTCCTTTCTTGAG	GGTCGGCCAGAACCACTTC
ttr	TTGCCTCGCTGGACTGGTA	TTACAGCCACGTCTACAGCAG
wnt8b	CGTGTGCGTTCTTCTAGTCACTT	CAACGGTCCCAAGCAAAC

ACKNOWLEDGEMENTS

I express my sincere gratitude to my advisor Prof. Federico Cremisi for the continuous support of my Ph.D study and related research, for his patience and motivation. His guidance helped me in all the time of research and writing of this thesis. Besides my advisor, I would like to thank Prof. Antonino Cattaneo, Prof. Alessandro Cellerino, Prof. Magdalena Götz, for allowing me to spend three wonderful months in her lab in Munich, for her time and feedbacks, Cristina di Primio, for her guidance and patience, Valentina Quercioli, Vania Liverani, Antonella Calvello, Alessandro Viegi, Prof. Michèle Studer, Sven Falk and my collaborators Roberto Ripa, Luca Dolfi, Manuella Mendes Martins, Keagan Dunville, Marta Pietrasanta, Claudia Alia, Irene Busti, Prof. Matteo Caleo, Valeria Arcucci, Michele Bertacchi, Marco Fantini, Michele Chirichella, Simonetta Lisi and Luca Pandolfini. Finally, I thank my fellow labmates for the stimulating discussions and for all the fun we have had in the last years. This long journey has come to an end, it is now time for me to start a new one on my own.

BIBLIOGRAPHY

Abbott, N. J., Rönnbäck, L., & Hansson, E. (2006). Astrocyte-endothelial interactions at the blood-brain barrier. Nature Reviews Neuroscience.

AbellÃ¡n, A., Desfilis, E., & Medina, L. (2014). Combinatorial expression of Lef1, Lhx2, Lhx5, Lhx9, Lmo3, Lmo4, and Prox1 helps to identify comparable subdivisions in the developing hippocampal formation of mouse and chicken. Frontiers in Neuroanatomy, 8(July), 1–22.

Acampora, D., Mazan, S., Lallemand, Y., Avantaggiato, V., Maury, M., Simeone, A., & Brûlet, P. (1995). Forebrain and midbrain regions are deleted in Otx2-/- mutants due to a defective anterior neuroectoderm specification during gastrulation. Development (Cambridge, England).

Aktas, O., Ullrich, O., Infante-Duarte, C., Nitsch, R., & Zipp, F. (2007). Neuronal damage in brain inflammation. Archives of Neurology.

Alexiades, M. R., & Cepko, C. (1996). Quantitative analysis of proliferation and cell cycle length during development of the rat retina. Developmental Dynamics.

Alia, C., Spalletti, C., Lai, S., Panarese, A., Micera, S., & Caleo, M. (2016). Reducing GABA A-mediated inhibition improves forelimb motor function after focal cortical stroke in mice. Scientific Reports, 6(November), 1–15.

Alper, J. (2009). Geron gets green light for human trial of ES cell–derived product. Nature Biotechnology.

Altaba, A. R., & Jessell, T. (1991). Retinoic acid modifies mesodermal patterning in early Xenopus embryos. Genes and Development.

Altaba, R. I., & Jessell, T. M. (1991). Retinoic acid modifies the pattern of cell differentiation in the central nervous system of neurula stage Xenopus embryos. Development.

Altman, J., & Bayer, S. A. (1990). Prolonged sojourn of developing pyramidal cells in the intermediate zone of the hippocampus and their settling in the stratum pyramidale. Journal of Comparative Neurology.

Alvarado-Mallart, R. -M. (1993). Fate and potentialities of the avian mesencephalic/metencephalic neuroepithelium. Journal of Neurobiology.

Alvarez-Garcia, I. (2005). MicroRNA functions in animal development and human disease. Development.

Anand, S., Majeti, B. K., Acevedo, L. M., Murphy, E. A., Mukthavaram, R., Scheppke, L., Huang, M., Shields, D. J., Lindquist, J. N., Lapinski, P. E., … Cheresh, D. A. (2010). MicroRNA-132-mediated loss of p120RasGAP activates the endothelium to facilitate pathological angiogenesis. Nature Medicine, 16(8), 909–914.

Anderegg, A., Lin, H. P., Chen, J. A., Caronia-Brown, G., Cherepanova, N., Yun, B., Joksimovic, M., Rock, J., Harfe, B. D., Johnson, R., & Awatramani, R. (2013). An Lmx1b-miR135a2 Regulatory Circuit Modulates Wnt1/Wnt Signaling and Determines the Size of the Midbrain Dopaminergic Progenitor Pool. PLoS Genetics.

Anderson, D. J. (1999). Lineages and transcription factors in the specification of vertebrate primary sensory neurons. Current Opinion in Neurobiology.

Andres, R. H., Horie, N., Slikker, W., Keren-Gill, H., Zhan, K., Sun, G., Manley, N. C., Pereira, M. P., Sheikh, L. A., McMillan, E. L., … Steinberg, G. K. (2011). Human neural stem cells enhance structural plasticity and axonal transport in the ischaemic brain. Brain.

Ang, E. S. B. C., Haydar, T. F., Gluncic, V., & Rakic, P. (2003). Four-dimensional migratory coordinates of GABAergic interneurons in the developing mouse cortex. Journal of Neuroscience.

Ang, S. L., Jin, O., Rhinn, M., Daigle, N., Stevenson, L., & Rossant, J. (1996). A targeted mouse Otx2 mutation leads to severe defects in gastrulation and formation of axial mesoderm and to deletion of rostral brain. Development (Cambridge, England).

Angevine. (1965). Time of neuron origin in the hippocampal region. An autoradiographic study in the mouse. Exp Neurol Suppl.

Aoto, K., Nishimura, T., Eto, K., & Motoyama, J. (2002). Mouse GLI3 regulates Fgf8 expression and apoptosis in the developing neural tube, face, and limb bud. Developmental Biology.

Arenillas, J. F., Sobrino, T., Castillo, J., & Dávalos, A. (2007). The role of angiogenesis in damage and recovery from ischemic stroke. Current Treatment Options in Cardiovascular Medicine.

Armentano, M., Chou, S. J., Srubek Tomassy, G., Leingärtner, A., O'Leary, D. D. M. M., & Studer, M. (2007). COUP-TFI regulates the balance of cortical patterning between frontal/motor and sensory areas. Nature Neuroscience, 10(10), 1277–1286.

Asano, H., Aonuma, M., Sanosaka, T., Kohyama, J., Namihira, M., & Nakashima, K. (2009). Astrocyte differentiation of neural precursor cells is enhanced by retinoic acid through a change in epigenetic modification. Stem Cells.

Assimacopoulos, S., Grove, E. A., & Ragsdale, C. W. (2003). Identification of a Pax6-dependent epidermal growth factor family signaling source at the lateral edge of the embryonic cerebral cortex. The Journal of Neuroscience : The Official Journal of the Society for Neuroscience.

Aubry, L., Bugi, A., Lefort, N., Rousseau, F., Peschanski, M., & Perrier, A. L. (2008). Striatal progenitors derived from human ES cells mature into DARPP32 neurons in vitro and in quinolinic acid-lesioned rats. Proceedings of the National Academy of Sciences.

Avilion, A. A., Nicolis, S. K., Pevny, L. H., Perez, L., Vivian, N., & Lovell-Badge, R. (2003). Multipotent cell lineages in early mouse development depend on SOX2 function. Genes and Development.

Bachler, M., & Neubüser, A. (2001). Expression of members of the Fgf family and their receptors during midfacial development. Mechanisms of Development.

Bacigaluppi, M., Pluchino, S., Jametti, L. P., Kilic, E., Kilic, Ü., Salani, G., Brambilla, E., West, M. J., Comi, G., Martino, G., & Hermann, D. M. (2009). Delayed post-ischaemic neuroprotection following systemic neural stem cell transplantation involves multiple mechanisms. Brain.

Backman, M., Machon, O., Mygland, L., Van Den Bout, C. J., Zhong, W., Taketo, M. M., & Krauss, S. (2005). Effects of canonical Wnt signaling on dorso-ventral specification of the mouse telencephalon. Developmental Biology.

Bailey, S. G., Sanchez-Elsner, T., Stephanou, A., Cragg, M. S., & Townsend, P. A. (2010). Regulating the genome surveillance system: MiRNAs and the p53 super family. Apoptosis.

Barberi, T., Klivenyi, P., Calingasan, N. Y., Lee, H., Kawamata, H., Loonam, K., Perrier, A. L., Bruses, J., Rubio, M. E., Topf, N., … Studer, L. (2003). Neural subtype specification of fertilization and nuclear transfer embryonic stem cells and application in parkinsonian mice. Nature Biotechnology.

Barca-Mayo, O., & De Pietri Tonelli, D. (2014). Convergent microRNA actions coordinate neocortical development. Cellular and Molecular Life Sciences.

Barry, G., Piper, M., Lindwall, C., Moldrich, R., Mason, S., Little, E., Sarkar, A., Tole, S., Gronostajski, R. M., & Richards, L. J. (2008). Specific Glial Populations Regulate Hippocampal Morphogenesis. Journal of Neuroscience.

Barth, K. A., Kishimoto, Y., Rohr, K. B., Seydler, C., Schulte-Merker, S., & Wilson, S. W. (1999). Bmp activity establishes a gradient of positional information throughout the entire neural plate. Development (Cambridge, England).

Basler, K., Edlund, T., Jessell, T. M., & Yamada, T. (1993). Control of cell pattern in the neural tube: Regulation of cell differentiation by dorsalin-1, a novel TGFβ family member. Cell.

Bayer, S. A. (1980). Development of the hippocampal region in the rat I. Neurogenesis examined with 3H-thymidine autoradiography. Journal of Comparative Neurology.

Becerra-Calixto, A., & Cardona-Gómez, G. P. (2017). The Role of Astrocytes in Neuroprotection after Brain Stroke: Potential in Cell Therapy. Frontiers in Molecular Neuroscience.

Begley, D. J., & Brightman, M. W. (2003). Structural and functional aspects of the blood-brain barrier. In Peptide Transport and Delivery into the Central Nervous System.

Bellairs, R. (1986). The primitive streak. Anatomy and Embryology.

Ben-David, U., & Benvenisty, N. (2011). The tumorigenicity of human embryonic and induced pluripotent stem cells. Nature Reviews Cancer.

Bertacchi, M., Pandolfini, L., D'Onofrio, M., Brandi, R., & Cremisi, F. (2015). The double inhibition of endogenously produced bmp and wnt factors synergistically triggers dorsal telencephalic differentiation of mouse es cells. Developmental Neurobiology, 75(1), 66–79.

Bertacchi, M., Pandolfini, L., Murenu, E., Viegi, A., Capsoni, S., Cellerino, A., Messina, A., Casarosa, S., & Cremisi, F. (2013). The positional identity of mouse ES cell-generated neurons is affected by BMP signaling. Cellular and Molecular Life Sciences, 70(6), 1095–1111.

Bertrand, V., Hudson, C., Caillol, D., Popovici, C., & Lemaire, P. (2003). Neural Tissue in Ascidian Embryos Is Induced by FGF9/16/20, Acting via a Combination of Maternal GATA and Ets Transcription Factors. Cell.

Betel, D., Wilson, M., Gabow, A., Marks, D. S., & Sander, C. (2008). The microRNA.org resource: Targets and expression. Nucleic Acids Research, 36(SUPPL. 1).

Bian, S., & Sun, T. (2011). Functions of noncoding RNAs in neural development and neurological diseases. Molecular Neurobiology.

Bishop, K. M., Goudreau, G., & O'Leary, D. D. M. (2000). Regulation of area identity in the mammalian neocortex by Emx2 and Pax6. Science.

Bishop, K. M., Rubenstein, J. L. R., & O'Leary, D. D. M. (2002). Distinct Actions of Emx1, Emx2, and Pax6 in Regulating the Specification of Areas in the Developing Neocortex. J. Neurosci.

Blackstad, T. W., Brink, K., Hem, J., & June, B. (1970). Distribution of hippocampal mossy fibers in the rat. An experimental study with silver impregnation methods. The Journal of Comparative Neurology, 138(4), 433–449.

Borello, U., Cobos, I., Long, J. E., McWhirter, J. R., Murre, C., & Rubenstein, J. L. (2008). Correction: FGF15 promotes neurnogenesis and opposes FGF8 function during neocortical development. Neural Development, 3(1), 31.

Borello, U., Madhavan, M., Vilinsky, I., Faedo, A., Pierani, A., Rubenstein, J., & Campbell, K. (2014). Sp8 and COUP-TF1 reciprocally regulate patterning and fgf signaling in cortical progenitors. Cerebral Cortex, 24(6), 1409–1421.

Borlongan, C. V, Tajima, Y., Trojanowski, J. Q., Lee, V. M., & Sanberg, P. R. (1998). Cerebral ischemia and CNS transplantation: differential effects of grafted fetal rat striatal cells and human neurons derived from a clonal cell line. Neuroreport, 9(16), 3703–3709.

Borlongan, C. V. (2016). Age of PISCES: stem-cell clinical trials in stroke. The Lancet.

Bouwmeester, T., Kim, S. H., Sasai, Y., Lu, B., & De Robertis, E. M. (1996). Cerberus is a head-inducing secreted factor expressed in the anterior endoderm of Spemann's organizer. Nature.

Branney, P. A., Faas, L., Steane, S. E., Pownall, M. E., & Isaacs, H. V. (2009). Characterisation of the fibroblast growth factor dependent transcriptome in early development. PLoS ONE.

Brons, I. G. M., Smithers, L. E., Trotter, M. W. B., Rugg-Gunn, P., Sun, B., Chuva De Sousa Lopes, S. M., Howlett, S. K., Clarkson, A., Ahrlund-Richter, L., Pedersen, R. A., & Vallier, L. (2007). Derivation of pluripotent epiblast stem cells from mammalian embryos. Nature.

Broughton, J. P., Lovci, M. T., Huang, J. L., Yeo, G. W., & Pasquinelli, A. E. (2016). Pairing beyond the Seed Supports MicroRNA Targeting Specificity. Molecular Cell.

Bryson, J. B., Machado, C. B., Crossley, M., Stevenson, D., Bros-Facer, V., Burrone, J., Greensmith, L., & Lieberam, I. (2014). Optical control of muscle function by transplantation of stem cell-derived motor neurons in mice. Science.

Bulchand, S., Grove, E. A., Porter, F. D., & Tole, S. (2001). LIM-homeodomain gene Lhx2 regulates the formation of the cortical hem. Mechanisms of Development.

Bulfone, A., Smiga, S. M., Shimamura, K., Peterson, A., Puelles, L., & Rubenstein, J. L. R. (2016). T-Brain-1: A homolog of Brachyury whose expression defines molecularly distinct domains within the cerebral cortex. Neuron, 15(1), 63–78.

Camicioli, R., Moore, M. M., Kinney, A., Corbridge, E., Glassberg, K., & Kaye, J. a. (2003). Parkinson's disease is associated with hippocampal atrophy. Movement Disorders : Official Journal of the Movement Disorder Society, 18(7), 784–790.

Camp, J. G., Badsha, F., Florio, M., Kanton, S., Gerber, T., Wilsch-Bräuninger, M., Lewitus, E., Sykes, A., Hevers, W., Lancaster, M., … Treutlein, B. (2015). Human cerebral organoids recapitulate gene expression programs of fetal neocortex development. Proceedings of the National Academy of Sciences, 112(51), 201520760.

Carpenter, E. M., Manley, N. R., Goddard, J. M., Chisaka, O., & Capecchi, M. R. (1993). Loss of Hox-A1 (Hox-1.6) function results in the reorganization of the murine hindbrain. Development (Cambridge, England).

Chambers, S. M., Fasano, C. A., Papapetrou, E. P., Tomishima, M., Sadelain, M., & Studer, L. (2009). Highly efficient neural conversion of human ES and iPS cells by dual inhibition of SMAD signaling. Nature Biotechnology, 27(3), 275–280.

Chang, D. J., Lee, N., Park, I. H., Choi, C., Jeon, I., Kwon, J., Oh, S. H., Shin, D. A., Do, J. T., Lee, D. R., … Song, J. (2013). Therapeutic potential of human induced pluripotent stem cells in experimental stroke. Cell Transplantation, 22(8), 1427–1440.

Chau, M. J., Deveau, T. C., Song, M., Gu, X., Chen, D., & Wei, L. (2014). IPSC transplantation increases regeneration and functional recovery after ischemic stroke in neonatal rats. Stem Cells.

Chen, J., Li, Y., Katakowski, M., Chen, X., Wang, L., Lu, D., Lu, M., Gautam, S. C., & Chopp, M. (2003). Intravenous bone marrow stromal cell therapy reduces apoptosis and promotes endogenous cell proliferation after stroke in female rat. Journal of Neuroscience Research, 73(6), 778–786.

Chiang, C., Litingtung, Y., Lee, E., Young, K. E., Corden, J. L., Westphal, H., & Beachy, P. A. (1996). Cyclopia and defective axial patterning in mice lacking Sonic hedgehog gene function. Nature.

Chiba, S., Ikeda, R., Kurokawa, M. S., Yoshikawa, H., Takeno, M., Nagafuchi, H., Tadokoro, M., Sekino, H., Hashimoto, T., & Suzuki, N. (2004). Anatomical and functional recovery by embryonic stem cell-derived neural tissue of a mouse model of brain damage. Journal of the Neurological Sciences.

Chiba, S., Kurokawa, M. S., Yoshikawa, H., Ikeda, R., Takeno, M., Tadokoro, M., Sekino, H., Hashimoto, T., & Suzuki, N. (2005). Noggin and basic FGF were implicated in forebrain fate and caudal fate, respectively, of the neural tube-like structures emerging in mouse ES cell culture. Experimental Brain Research, 163(1), 86–99.

Chizhikov, V. V., & Millen, K. J. (2005). Roof plate-dependent patterning of the vertebrate dorsal central nervous system. Developmental Biology.

Cho, T., Bae, J. H., Choi, H. B., Kim, S. S., McLarnon, J. G., Suh-Kim, H., Kim, S. U., & Min, C. K. (2002). Human neural stem cells: Electrophysiological properties of voltage-gated ion channels. NeuroReport.

Cholfin, J. A., & Rubenstein, J. L. (2007). Patterning of frontal cortex subdivisions by Fgf17. Proceedings of the National Academy of Sciences of the United States of America.

Cholfin, J. A., & Rubenstein, J. L. R. (2008). Frontal cortex subdivision patterning is coordinately regulated by Fgf8, Fgf17, and Emx2. Journal of Comparative Neurology, 509(2), 144–155.

Chu, K., Kim, M., Jeong, S. W., Kim, S. U., & Yoon, B. W. (2003). Human neural stem cells can migrate, differentiate, and integrate after intravenous transplantation in adult rats with transient forebrain ischemia. Neuroscience Letters.

Chuang, J.-H., Tung, L.-C., & Lin, Y. (2015). Neural differentiation from embryonic stem cells in vitro: An overview of the signaling pathways. World Journal of Stem Cells, 7(2), 437–47.

Claiborne, B. J., Amaral, D. G., & Cowan, W. M. (1986). A light and electron microscopic analysis of the mossy fibers of the rat dentate gyrus. The Journal of Comparative Neurology, 246(4), 435–458.

Coolen, M., & Bally-Cuif, L. (2009). MicroRNAs in brain development and physiology. Current Opinion in Neurobiology.

Corbin, J. G., Gaiano, N., Machold, R. P., Langston, A., & Fishell, G. (2000). The Gsh2 homeodomain gene controls multiple aspects of telencephalic development. Development (Cambridge, England).

Corbin, Joshua G and Rutlin, Michael and Gaiano, Nicholas and Fishell, G. (2003). Combinatorial function of the homeodomain proteins Nkx2.1 and Gsh2 in ventral telencephalic patterning. Development.

Cox, W. G., & Hemmati-Brivanlou, A. (1995). Caudalization of neural fate by tissue recombination and bFGF. Development.

Crossley, P. H., Martinez, S., & Martin, G. R. (1996). Midbrain development induced by FGF8 in the chick embryo. Nature.

Crossley, P. H., & Martin, G. R. (1995). The mouse Fgf8 gene encodes a family of polypeptides and is expressed in regions that direct outgrowth and patterning in the developing embryo. Development (Cambridge, England).

Danesin, C., Peres, J. N., Johansson, M., Snowden, V., Cording, A., Papalopulu, N., & Houart, C. (2009). Integration of Telencephalic Wnt and Hedgehog Signaling Center Activities by Foxg1. Developmental Cell.

Danglot, L., Triller, A., & Marty, S. (2006). The development of hippocampal interneurons in rodents. Hippocampus.

D'Autilia, S., Decembrini, S., Casarosa, S., He, R. Q., Barsacchi, G., Cremisi, F., & Andreazzoli, M. (2006). Cloning and developmental expression of the Xenopus homeobox gene Xvsx1. Development Genes and Evolution.

Davis, B. N., Hilyard, A. C., Lagna, G., & Hata, A. (2008). SMAD proteins control DROSHA-mediated microRNA maturation. Nature.

Davis, T. H., Cuellar, T. L., Koch, S. M., Barker, A. J., Harfe, B. D., McManus, M. T., & Ullian, E. M. (2008). Conditional Loss of Dicer Disrupts Cellular and Tissue Morphogenesis in the Cortex and Hippocampus. Journal of Neuroscience.

De Chevigny, A., Coré, N., Follert, P., Gaudin, M., Barbry, P., Béclin, C., & Cremer, H. (2012). MiR-7a regulation of Pax6 controls spatial origin of forebrain dopaminergic neurons. Nature Neuroscience.

De Feo, D., Merlini, A., Laterza, C., & Martino, G. (2012). Neural stem cell transplantation in central nervous system disorders: From cell replacement to neuroprotection. Current Opinion in Neurology.

De La Calle-Mustienes, E., Feijóo, C. G., Manzanares, M., Tena, J. J., Rodríguez-Seguel, E., Letizia, A., Allende, M. L., & Gómez-Skarmeta, J. L. (2005). A functional survey of the enhancer activity of conserved non-coding sequences from vertebrate Iroquois cluster gene deserts. Genome Research.

De Pietri Tonelli, D., Pulvers, J. N., Haffner, C., Murchison, E. P., Hannon, G. J., & Huttner, W. B. (2008). miRNAs are essential for survival and differentiation of newborn neurons

but not for expansion of neural progenitors during early neurogenesis in the mouse embryonic neocortex. Development.

Decembrini, S., Andreazzoli, M., Vignali, R., Barsacchi, G., & Cremisi, F. (2006). Timing the generation of distinct retinal cells by homeobox proteins. PLoS Biology.

Decembrini, S., Bressan, D., Vignali, R., Pitto, L., Mariotti, S., Rainaldi, G., Wang, X., Evangelista, M., Barsacchi, G., & Cremisi, F. (2009). MicroRNAs couple cell fate and developmental timing in retina. Proceedings of the National Academy of Sciences.

Deguchi, Y., Donato, F., Galimberti, I., Cabuy, E., & Caroni, P. (2011). Temporally matched subpopulations of selectively interconnected principal neurons in the hippocampus. Nature Neuroscience.

Del Río, J. A., Heimrich, B., Borrell, V., Förster, E., Drakew, A., Alcántara, S., Nakajima, K., Miyata, T., Ogawa, M., Mikoshiba, K., … Soriano, E. (1997). A role for Cajal-retzius cells and reelin in the development of hippocampal connections. Nature.

Del Río, J. A., Martinez, A., Fonseca, M., Auladell, C., & Soriano, E. (1995). Glutamate-like immunoreactivity and fate of cajal-retzius cells in the murine cortex as identified with calretinin antibody. Cerebral Cortex.

Delaune, E. (2005). Neural induction in Xenopus requires early FGF signalling in addition to BMP inhibition. Development.

Dell'Anno, M. T., Caiazzo, M., Leo, D., Dvoretskova, E., Medrihan, L., Colasante, G., Giannelli, S., Theka, I., Russo, G., Mus, L., … Broccoli, V. (2014). Remote control of induced dopaminergic neurons in parkinsonian rats. Journal of Clinical Investigation.

Dickinson, M. E., Selleck, M. a, McMahon, a P., & Bronner-Fraser, M. (1995). Dorsalization of the neural tube by the non-neural ectoderm. Development (Cambridge, England).

Doniach, T. (1995). Basic FGF as an inducer of anteroposterior neural pattern. Cell.

Dou, C. L., Li, S., & Lai, E. (1999). Dual role of brain factor-1 in regulating growth and patterning of the cerebral hemispheres. Cerebral Cortex.

Durston, A. J., Timmermans, J. P. M., Hage, W. J., Hendriks, H. F. J., De Vries, N. J., Heideveld, M., & Nieuwkoop, P. D. (1989). Retinoic acid causes an anteroposterior transformation in the developing central nervous system. Nature.

Echelard, Y., Epstein, D. J., St-Jacques, B., Shen, L., Mohler, J., McMahon, J. A., & McMahon, A. P. (1993). Sonic hedgehog, a member of a family of putative signaling molecules, is implicated in the regulation of CNS polarity. Cell.

Eckert, A., Huang, L., Gonzalez, R., Kim, H.-S., Hamblin, M. H., & Lee, J.-P. (2015). Bystander Effect Fuels Human Induced Pluripotent Stem Cell-Derived Neural Stem Cells to Quickly Attenuate Early Stage Neurological Deficits After Stroke. STEM CELLS Translational Medicine.

Edri, R., Yaffe, Y., Ziller, M. J., Mutukula, N., Volkman, R., David, E., Jacob-Hirsch, J., Malcov, H., Levy, C., Rechavi, G., … Elkabetz, Y. (2015). Analysing human neural stem cell ontogeny by consecutive isolation of Notch active neural progenitors. Nature Communications, 6, 6500.

Eiraku, M., Watanabe, K., Matsuo-Takasaki, M., Kawada, M., Yonemura, S., Matsumura, M., Wataya, T., Nishiyama, A., Muguruma, K., & Sasai, Y. (2008). Self-Organized Formation of Polarized Cortical Tissues from ESCs and Its Active Manipulation by Extrinsic Signals. Cell Stem Cell.

Elkouby, Y. M., Elias, S., Casey, E. S., Blythe, S. A., Tsabar, N., Klein, P. S., Root, H., Liu, K. J., & Frank, D. (2010). Mesodermal Wnt signaling organizes the neural plate via Meis3. Development.

Emanueli, C., Schratzberger, P., Kirchmair, R., & Madeddu, P. (2003). Paracrine control of vascularization and neurogenesis by neurotrophins. In British Journal of Pharmacology.

Enright, A. J., John, B., Gaul, U., Tuschl, T., Sander, C., & Marks, D. S. (2003). MicroRNA targets in Drosophila. Genome Biology, 5(1), R1.

Ericson, J., Muhr, J., Placzek, M., Lints, T., Jessel, T. M., & Edlund, T. (1995). Sonic hedgehog induces the differentiation of ventral forebrain neurons: A common signal for ventral patterning within the neural tube. Cell.

Eriksson, P. S., Perfilieva, E., Bjork-Eriksson, T., Alborn, A. M., Nordborg, C., Peterson, D. A., & Gage, F. H. (1998). Neurogenesis in the adult human hippocampus. Nat Med, 4(11), 1313–1317.

Espuny-Camacho, I., Michelsen, K. a, Gall, D., Linaro, D., Hasche, A., Bonnefont, J., Bali, C., Orduz, D., Bilheu, A., Herpoel, A., … Vanderhaeghen, P. (2013). Pyramidal neurons derived from human pluripotent stem cells integrate efficiently into mouse brain circuits in vivo. Neuron, 77(3), 440–56.

Evans, M. J., & Kaufman, M. H. (1981). Establishment in culture of pluripotential cells from mouse embryos. Nature.

Faedo, A., Tomassy, G. S., Ruan, Y., Teichmann, H., Krauss, S., Pleasure, S. J., Tsai, S. Y., Tsai, M. J., Studer, M., & Rubenstein, J. L. R. (2008). COUP-TFI coordinates cortical patterning, neurogenesis, and laminar fate and modulates MAPK/ERK, AKT, and β-catenin signaling. Cerebral Cortex, 18(9), 2117–2131.

Falkner, S., Grade, S., Dimou, L., Conzelmann, K.-K., Bonhoeffer, T., Götz, M., & Hübener, M. (2016). Transplanted embryonic neurons integrate into adult neocortical circuits. Nature, 539(7628), 248–253.

Fernandes, M., Gutin, G., Alcorn, H., McConnell, S. K., & Hebert, J. M. (2007). Mutations in the BMP pathway in mice support the existence of two molecular classes of holoprosencephaly. Development.

Fineberg, S. K., Kosik, K. S., & Davidson, B. L. (2009). MicroRNAs Potentiate Neural Development. Neuron.

Fletcher, R. B., & Harland, R. M. (2008). The role of FGF signaling in the establishment and maintenance of mesodermal gene expression in Xenopus. Developmental Dynamics.

François, V., & Bier, E. (1995). Xenopus chordin and Drosophila short gastrulation genes encode homologous proteins functioning in dorsal-ventral axis formation. Cell.

Fricker-Gates, R. a, Shin, J. J., Tai, C. C., Catapano, L. a, & Macklis, J. D. (2002). Late-stage immature neocortical neurons reconstruct interhemispheric connections and form synaptic contacts with increased efficiency in adult mouse cortex undergoing targeted neurodegeneration. The Journal of Neuroscience : The Official Journal of the Society for Neuroscience, 22(10), 4045–56.

Friling, S., Andersson, E., Thompson, L. H., Jonsson, M. E., Hebsgaard, J. B., Nanou, E., Alekseenko, Z., Marklund, U., Kjellander, S., Volakakis, N., … Ericson, J. (2009). Efficient production of mesencephalic dopamine neurons by Lmx1a expression in embryonic stem cells. Proceedings of the National Academy of Sciences.

Fu, G., Brkić, J., Hayder, H., & Peng, C. (2013). MicroRNAs in human placental development and pregnancy complications. International Journal of Molecular Sciences.

Fuccillo, M., Joyner, A. L., & Fishell, G. (2006). Morphogen to mitogen: The multiple roles of hedgehog signalling in vertebrate neural development. Nature Reviews Neuroscience.

Fukuchi-Shimogori, T. (2001). Neocortex Patterning by the Secreted Signaling Molecule FGF8. Science, 294(5544), 1071–1074.

Fukuchi-Shimogori, T., & Grove, E. A. (2001). Neocortex patterning by the secreted signaling molecute FGF8. Science.

Fukuchi-Shimogori, T., & Grove, E. A. (2003). Emx2 patterns the neocortex by regulating FGF positional signaling. Nature Neuroscience, 6(8), 825–831.

Furuta, Y., Piston, D. W., & Hogan, B. L. M. (1997). Bone morphogenetic proteins (BMPs) as regulators of dorsal forebrain development. Development (Cambridge, England).

Gaarskjaer, F. B. (1978). Organization of the mossy fiber system of the rat studied in extneded hippocampi. J Comp Neurol, 178, 73–88.

Gage, F. H., Coates, P. W., Palmer, T. D., Kuhn, H. G., Fisher, L. J., Suhonen, J. O., Peterson, D. a, Suhr, S. T., & Ray, J. (1995). Survival and differentiation of adult neuronal progenitor cells transplanted to the adult brain. Proceedings of the National Academy of Sciences of the United States of America, 92(25), 11879–11883.

Gaillard, A., Prestoz, L., Dumartin, B., Cantereau, A., Morel, F., Roger, M., & Jaber, M. (2007). Reestablishment of damaged adult motor pathways by grafted embryonic cortical neurons. Nature Neuroscience, 10(10), 1294–1299.

Galceran, J., Miyashita-Lin, E. M., Devaney, E., Rubenstein, J. L., & Grosschedl, R. (2000). Hippocampus development and generation of dentate gyrus granule cells is regulated by LEF1. Development (Cambridge, England).

Garcia-Castro, M., & Bronner-Fraser, M. (1999). Induction and differentiation of the neural crest. Current Opinion in Cell Biology, 11(6), 695–698.

Garcia-Lopez, R., & Martinez, S. (2010). Oligodendrocyte precursors originate in the parabasal band of the basal plate in prosomere 1 and migrate into the alar prosencephalon during chick development. GLIA.

Garel, S. (2003). Molecular regionalization of the neocortex is disrupted in Fgf8 hypomorphic mutants. Development, 130(9), 1903–1914.

Gaspard, N., Bouschet, T., Herpoel, A., Naeije, G., van den Ameele, J., & Vanderhaeghen, P. (2009). Generation of cortical neurons from mouse embryonic stem cells. Nature Protocols, 4(10), 1454–63.

Gaspard, N., Bouschet, T., Hourez, R., Dimidschstein, J., Naeije, G., van den Ameele, J., Espuny-Camacho, I., Herpoel, A., Passante, L., Schiffmann, S. N., … Vanderhaeghen, P. (2008). An intrinsic mechanism of corticogenesis from embryonic stem cells. Nature, 455(7211), 351–7.

Gaulden, J., & Reiter, J. F. (2008). Neur-ons and neur-offs: Regulators of neural induction in vertebrate embryos and embryonic stem cells. Human Molecular Genetics.

Gendron, A., Teitelbaum, J., Cossette, C., Nuara, S., Dumont, M., Geadah, D., Du Souich, P., & Kouassi, E. (2002). Temporal effects of left versus right middle cerebral artery occlusion on spleen lymphocyte subsets and mitogenic response in Wistar rats. Brain Research.

George, P. M., & Steinberg, G. K. (2015). Novel Stroke Therapeutics: Unraveling Stroke Pathophysiology and Its Impact on Clinical Treatments. Neuron, 87(2), 297–309.

Gerber, H. P., McMurtrey, A., Kowalski, J., Yan, M., Keyt, B. A., Dixit, V., & Ferrara, N. (1998). Vascular endothelial growth factor regulates endothelial cell survival through the phosphatidylinositol 3'-kinase/Akt signal transduction pathway: Requirement for Flk-1/KDR activation. Journal of Biological Chemistry.

Ghosh, T., Aprea, J., Nardelli, J., Engel, H., Selinger, C., Mombereau, C., Lemonnier, T., Moutkine, I., Schwendimann, L., Dori, M., … Groszer, M. (2014). MicroRNAs Establish Robustness and Adaptability of a Critical Gene Network to Regulate Progenitor Fate Decisions during Cortical Neurogenesis. Cell Reports.

Giralt, A., Saavedra, A., Alberch, J., & Pérez-Navarro, E. (2012). Cognitive dysfunction in Huntington's disease: Humans, mouse models and molecular mechanisms. Journal of Huntington's Disease, 1(2), 155–173.

Glavic, A., Gómez-Skarmeta, J. L., & Mayor, R. (2002). {T}he homeoprotein {X}iro1 is required for midbrain-hindbrain boundary formation. Development.

Glinka, A., Wu, W., Delius, H., Monaghan, A. P., Blumenstock, C., & Niehrs, C. (1998). Dickkopf-1 is a member of a new family of secreted proteins and functions in head induction. Nature.

Gorski, J. A., Talley, T., Qiu, M., Puelles, L., Rubenstein, J. L. R., & Jones, K. R. (2002). Cortical excitatory neurons and glia, but not GABAergic neurons, are produced in the Emx1-expressing lineage. The Journal of Neuroscience : The Official Journal of the Society for Neuroscience.

Goss, J. R., O'Malley, M. E., Zou, L., Styren, S. D., Kochanek, P. M., & Dekosky, S. T. (1998). Astrocytes are the major source of nerve growth factor upregulation following traumatic brain injury in the rat. Experimental Neurology.

Greig, L. C., Woodworth, M. B., Galazo, M. J., Padmanabhan, H., & Macklis, J. D. (2013). Molecular logic of neocortical projection neuron specification, development and diversity. Nature Reviews Neuroscience.

Grove, E. A., Tole, S., Limon, J., Yip, L., & Ragsdale, C. W. (1998). The hem of the embryonic cerebral cortex is defined by the expression of multiple Wnt genes and is compromised in Gli3-deficient mice. Development (Cambridge, England).

Grove, E. A., & Tole, S. (1999). Patterning events and specification signals in the developing hippocampus. Cerebral Cortex.

Guitet, J., Garnier, C., Ebrahimi-Gaillard, A., & Roger, M. (1994). Efferents of frontal or occipital cortex grafted into adult rat's motor cortex. Neuroscience Letters, 180(2), 265–268.

Gunhaga, L., Marklund, M., Sjödal, M., Hsieh, J. C., Jessell, T. M., & Edlund, T. (2003). Specification of dorsal telencephalic character by sequential Wnt and FGF signaling. Nature Neuroscience.

Gutin, G. (2006). FGF signalling generates ventral telencephalic cells independently of SHH. Development.

Gyorgy, A. B., Szemes, M., De Juan Romero, C., Tarabykin, V., & Agoston, D. V. (2008). SATB2 interacts with chromatin-remodeling molecules in differentiating cortical neurons. European Journal of Neuroscience, 27(4), 865–873.

Ha, M., & Kim, V. N. (2014). Regulation of microRNA biogenesis. Nature Reviews. Molecular Cell Biology.

Hamasaki, T., Leingärtner, A., Ringstedt, T., & O'Leary, D. D. M. (2004). EMX2 regulates sizes and positioning of the primary sensory and motor areas in neocortex by direct specification of cortical progenitors. Neuron.

Hamburger, V. (1969). Hans Spemann and the organizer concept. Experientia.

Hanashima, C., Fernandes, M., Hebert, J. M., & Fishell, G. (2007). The Role of Foxg1 and Dorsal Midline Signaling in the Generation of Cajal-Retzius Subtypes. Journal of Neuroscience.

Hansen, D. V. D., Rubenstein, J. J. L. R., & Kriegstein, A. R. (2011). Deriving excitatory neurons of the neocortex from pluripotent stem cells. Neuron, 70(4), 645–660.

Hargus, G., Cooper, O., Deleidi, M., Levy, A., Lee, K., Marlow, E., Yow, A., Soldner, F., Hockemeyer, D., Hallett, P. J., … Isacson, O. (2010). Differentiated Parkinson patient-derived induced pluripotent stem cells grow in the adult rodent brain and reduce motor asymmetry in Parkinsonian rats. Proceedings of the National Academy of Sciences.

Hashimoto, K., & Nakatsuji, N. (1989). Formation of the Primitive Streak and Mesoderm Cells in Mouse Embryos -Detailed Scanning Electron Microscopical Study, 31(3), 209–218.

Hassani, Z., O'Reilly, J., Pearse, Y., Stroemer, P., Tang, E., Sinden, J., Price, J., & Thuret, S. (2012). Human Neural Progenitor Cell Engraftment Increases Neurogenesis and Microglial Recruitment in the Brain of Rats with Stroke. PLoS ONE.

Hattori, N. (2014). Cerebral organoids model human brain development and microcephaly. Movement Disorders, 29(2), 185–185.

Hauptmann, G., & Gerster, T. (1996). Complex expression of the zp-50 pou gene in the embryonic zebrafish brain is altered by overexpression of sonic hedgehog. Development (Cambridge, England).

Hayashi, T., Abe, K., & Itoyama, Y. (1998). Reduction of ischemic damage by application of vascular endothelial growth factor in rat brain after transient ischemia. Journal of Cerebral Blood Flow and Metabolism.

Hébert, J. M., Hayhurst, M., Marks, M. E., Kulessa, H., Hogan, B. L. M., & McConnell, S. K. (2003). BMP ligands act redundantly to pattern the dorsal telencephalic midline. Genesis.

Hébert, J. M., & McConnell, S. K. (2000). Targeting of cre to the Foxg1 (BF-1) Locus Mediates loxP Recombination in the Telencephalon and Other Developing Head Structures. Developmental Biology, 222(2), 296–306.

Heisenberg, C. P., Houart, C., Take-Uchi, M., Rauch, G. J., Young, N., Coutinho, P., Masai, I., Caneparo, L., Concha, M. L., Geisler, R., … Stemple, D. L. (2001). A mutation in the Gsk3-binding domain of zebrafish masterblind/Axin1 leads to a fate transformation of telencephalon and eyes to diencephalon. Genes and Development.

HemmatiBrivanlou, A., & Melton, D. (1997). Vertebrate neural induction. ANNUAL REVIEW OF NEUROSCIENCE.

Hemmati-Brivanlou, A., Kelly, O. G., & Melton, D. A. (1994). Follistatin, an antagonist of activin, is expressed in the Spemann organizer and displays direct neuralizing activity. Cell.

Hendrickx, M., Van, X. H., & Leyns, L. (2009). Anterior-posterior patterning of neural differentiated embryonic stem cells by canonical Wnts, Fgfs, Bmp4 and their respective antagonists. Development Growth and Differentiation, 51(8), 687–698.

Hidalgo-Sánchez, M., Millet, S., Bloch-Gallego, E., & Alvarado-Mallart, R. M. (2005). Specification of the meso-isthmo-cerebellar region: The Otx2/Gbx2 boundary. Brain Research Reviews.

Hooiveld, M. H. W., Morgan, R., In Der Rieden, P., Houtzager, E., Pannese, M., Damen, K., Boncinelli, E., & Durston, A. J. (1999). Novel interactions between vertebrate Hox genes. International Journal of Developmental Biology.

Houart, C., Westerfield, M., & Wilson, S. W. (1998). A small population of anterior cells patterns the forebrain during zebrafish gastrulation. Nature.

Houart, C., Caneparo, L., Heisenberg, C. P., Barth, K. A., Take-Uchi, M., & Wilson, S. W. (2002). Establishment of the telencephalon during gastrulation by local antagonism of Wnt signaling. Neuron.

Huang, E. J., & Reichardt, L. F. (2001). Neurotrophins: roles in neuronal development and function. Annual Review of Neuroscience.

Huang, L., Wong, S., Snyder, E. Y., Hamblin, M. H., & Lee, J. P. (2014). Human neural stem cells rapidly ameliorate symptomatic inflammation in early-stage ischemic-reperfusion cerebral injury. Stem Cell Research and Therapy.

Huang, L., Wu, Z. B., ZhuGe, Q., Zheng, W., Shao, B., Wang, B., Sun, F., & Jin, K. (2014). Glial scar formation occurs in the human brain after ischemic stroke. International Journal of Medical Sciences.

Huang, Y., Osorno, R., Tsakiridis, A., & Wilson, V. (2012). In Vivo Differentiation Potential of Epiblast Stem Cells Revealed by Chimeric Embryo Formation. Cell Reports.

Hynes, M., Poulsen, K., Tessier-Lavigne, M., & Rosenthal, A. (1995). Control of neuronal diversity by the floor plate: Contact-mediated induction of midbrain dopaminergic neurons. Cell.

Ideguchi, M., Palmer, T. D., Recht, L. D., & Weimann, J. M. (2010). Murine embryonic stem cell-derived pyramidal neurons integrate into the cerebral cortex and appropriately project axons to subcortical targets. The Journal of Neuroscience : The Official Journal of the Society for Neuroscience, 30(3), 894–904.

Imayoshi, I., Shimogori, T., Ohtsuka, T., & Kageyama, R. (2008). Hes genes and neurogenin regulate non-neural versus neural fate specification in the dorsal telencephalic midline. Development, 135(15), 2531–2541.

Imayoshi, I., Sakamoto, M., Ohtsuka, T., Takao, K., Miyakawa, T., Yamaguchi, M., Mori, K., Ikeda, T., Itohara, S., & Kageyama, R. (2008). Roles of continuous neurogenesis in the structural and functional integrity of the adult forebrain. Nature Neuroscience.

Inoue, T., Nakamura, S., & Osumi, N. (2000). Fate mapping of the mouse prosencephalic neural plate. Developmental Biology.

Iqbal, K., Liu, F., & Gong, C.-X. (2015). Tau and neurodegenerative disease: the story so far. Nature Reviews Neurology, 12(1), 15–27.

Jiao, H., Wang, Z., Liu, Y., Wang, P., & Xue, Y. (2011). Specific role of tight junction proteins claudin-5, occludin, and ZO-1 of the blood-brain barrier in a focal cerebral ischemic insult. Journal of Molecular Neuroscience.

Jin, K., Wang, X., Xie, L., Mao, X. O., Zhu, W., Wang, Y., Shen, J., Mao, Y., Banwait, S., & Greenberg, D. A. (2006). Evidence for stroke-induced neurogenesis in the human brain. Proceedings of the National Academy of Sciences.

Jin, K., Xie, L., Mao, X., Greenberg, M. B., Moore, A., Peng, B., Greenberg, R. B., & Greenberg, D. A. (2011). Effect of human neural precursor cell transplantation on endogenous neurogenesis after focal cerebral ischemia in the rat. Brain Research.

Johnson, W., Onuma, O., Owolabi, M., & Sachdev, S. (2016). Stroke: A global response is needed. Bulletin of the World Health Organization.

Joyner, A. L., Liu, A., & Millet, S. (2000). Otx2, Gbx2 and Fgf8 interact to position and maintain a mid-hindbrain organizer. Current Opinion in Cell Biology.

Kalladka, D., Sinden, J., Pollock, K., Haig, C., McLean, J., Smith, W., McConnachie, A., Santosh, C., Bath, P. M., Dunn, L., & Muir, K. W. (2016). Human neural stem cells in patients with chronic ischaemic stroke (PISCES): a phase 1, first-in-man study. The Lancet.

Karow, M., Camp, J. G., Falk, S., Gerber, T., Pataskar, A., Gac-Santel, M., Kageyama, J., Brazovskaja, A., Garding, A., Fan, W., … Berninger, B. (2018). Direct pericyte-to-neuron reprogramming via unfolding of a neural stem cell-like program. Nature Neuroscience.

Kawai, H., Yamashita, T., Ohta, Y., Deguchi, K., Nagotani, S., Zhang, X., Ikeda, Y., Matsuura, T., & Abe, K. (2010). Tridermal tumorigenesis of induced pluripotent stem cells transplanted in ischemic brain. Journal of Cerebral Blood Flow and Metabolism.

Kawano, Y. (2003). Secreted antagonists of the Wnt signalling pathway. Journal of Cell Science.

Kawase-Koga, Y., Otaegi, G., & Sun, T. (2009). Different timings of dicer deletion affect neurogenesis and gliogenesis in the developing mouse central nervous system. Developmental Dynamics.

Kaya, D., Gürsoy-Özdemir, Y., Yemisci, M., Tuncer, N., Aktan, S., & Dalkara, T. (2005). VEGF protects brain against focal ischemia without increasing blood-brain permeability when administered intracerebroventricularly. Journal of Cerebral Blood Flow and Metabolism.

Keirstead, H. S. (2005). Human Embryonic Stem Cell-Derived Oligodendrocyte Progenitor Cell Transplants Remyelinate and Restore Locomotion after Spinal Cord Injury. Journal of Neuroscience.

Kelly, O. G., & Melton, D. A. (1995). Induction and patterning of the vertebrate nervous system. Trends in Genetics.

Kengaku, M., & Okamoto, H. (1995). bFGF as a possible morphogen for the anteroposterior axis of the central nervous system in Xenopus. Development (Cambridge, England).

Kernie, S. G., & Parent, J. M. (2010). Forebrain neurogenesis after focal Ischemic and traumatic brain injury. Neurobiology of Disease.

Kiecker, C., & Niehrs, C. (2001). A morphogen gradient of Wnt/{beta}-catenin signalling regulates anteroposterior neural patterning in Xenopus. Development.

Kim, A. S., Anderson, S. A., Rubenstein, J. L. R., Lowenstein, D. H., & Pleasure, S. J. (2001). Pax-6 regulates expression of SFRP-2 and Wnt-7b in the developing CNS. The Journal of Neuroscience.

Kim, A. S., Lowenstein, D. H., & Pleasure, S. J. (2001). Wnt receptors and Wnt inhibitors are expressed in gradients in the developing telencephalon. Mechanisms of Development.

Kim, J. H., Auerbach, J. M., Rodríguez-Gómez, J. A., Velasco, I., Gavin, D., Lumelsky, N., Lee, S. H., Nguyen, J., Sánchez-Pernaute, R., Bankiewicz, K., & McKay, R. (2002). Dopamine neurons derived from embryonic stem cells function in an animal model of Parkinson's disease. Nature.

Kimura, J. (2005). Emx2 and Pax6 Function in Cooperation with Otx2 and Otx1 to Develop Caudal Forebrain Primordium That Includes Future Archipallium. Journal of Neuroscience.

Knoepfler, P. S. (2009). Deconstructing stem cell tumorigenicity: A roadmap to safe regenerative medicine. Stem Cells.

Kohtz, J. D., Baker, D. P., Corte, G., & Fishell, G. (1998). Regionalization within the mammalian telencephalon is mediated by changes in responsiveness to Sonic Hedgehog. Development.

Kojima, Y., Kaufman-Francis, K., Studdert, J. B., Steiner, K. A., Power, M. D., Loebel, D. A. F., Jones, V., Hor, A., De Alencastro, G., Logan, G. J., … Tam, P. P. L. (2014). The transcriptional and functional properties of mouse epiblast stem cells resemble the anterior primitive streak. Cell Stem Cell.

König, N., & Marty, R. (1981). Early neurogenesis and synaptogenesis in cerebral cortex. Bibl.Anat.

König, N., Valat, J., Fulcrand, J., & Marty, R. (1977). The time of origin of Cajal-Retzius cells in the rat temporal cortex. An autoradiographic study. Neuroscience Letters.

Kono, H., & Rock, K. L. (2008). How dying cells alert the immune system to danger. Nature Reviews Immunology.

Kornblum, H. I., Hussain, R. J., Bronstein, J. M., Gall, C. M., Lee, D. C., & Seroogy, K. B. (1997). Prenatal ontogeny of the epidermal growth factor receptor and its ligand, transforming growth factor alpha, in the rat brain. Journal of Comparative Neurology.

Kriegstein, A. R., & Noctor, S. C. (2004). Patterns of neuronal migration in the embryonic cortex. Trends in Neurosciences.

Kriks, S., Shim, J.-W., Piao, J., Ganat, Y. M., Wakeman, D. R., Xie, Z., Carrillo-Reid, L., Auyeung, G., Antonacci, C., Buch, A., … Studer, L. (2011). Dopamine neurons derived from human ES cells efficiently engraft in animal models of Parkinson's disease. Nature.

Krol, J., Loedige, I., & Filipowicz, W. (2010). The widespread regulation of microRNA biogenesis, function and decay. Nature Reviews Genetics.

Krueger, M., Bechmann, I., Immig, K., Reichenbach, A., Härtig, W., & Michalski, D. (2015). Blood-brain barrier breakdown involves four distinct stages of vascular damage in various models of experimental focal cerebral ischemia. Journal of Cerebral Blood Flow and Metabolism.

Krupinski, J., Kaluza, J., Kumar, P., Kumar, S., & Wang, J. M. (1994). Role of angiogenesis in patients with cerebral ischemic stroke. Stroke.

Kunath, T., Saba-El-Leil, M. K., Almousailleakh, M., Wray, J., Meloche, S., & Smith, A. (2007). FGF stimulation of the Erk1/2 signalling cascade triggers transition of pluripotent embryonic stem cells from self-renewal to lineage commitment. Development.

Kuschel, S., Rüther, U., & Theil, T. (2003). A disrupted balance between Bmp/Wnt and Fgf signaling underlies the ventralization of the Gli3 mutant telencephalon. Developmental Biology.

Kuwamura, M., Muraguchi, T., Matsui, T., Ueno, M., Takenaka, S., Yamate, J., Kotani, T., Kuramoto, T., Guénet, J. L., Kitada, K., & Serikawa, T. (2005). Mutation at the Lmx1a locus provokes aberrant brain development in the rat. Developmental Brain Research, 155(2), 99–106.

Kwan, K. M., Fujimoto, E., Grabher, C., Mangum, B. D., Hardy, M. E., Campbell, D. S., Parant, J. M., Yost, H. J., Kanki, J. P., & Chien, C. Bin. (2007). The Tol2kit: A multisite gateway-based construction Kit for Tol2 transposon transgenesis constructs. Developmental Dynamics, 236(11), 3088–3099.

Lacar, B., Herman, P., Platel, J.-C., Kubera, C., Hyder, F., & Bordey, A. (2012). Neural Progenitor Cells Regulate Capillary Blood Flow in the Postnatal Subventricular Zone. Journal of Neuroscience.

Ladher, R. K., Church, V. L., Allen, S., Robson, L., Abdelfattah, A., Brown, N. A., Hattersley, G., Rosen, V., Luyten, F. P., Dale, L., & Francis-West, P. H. (2000). Cloning and expression of the Wnt antagonists Sfrp-2 and Frzb during chick development. Developmental Biology.

Laeng, P., Pitts, R. L., Lemire, A. L., Drabik, C. E., Weiner, A., Tang, H., Thyagarajan, R., Mallon, B. S., & Altar, C. A. (2004). The mood stabilizer valproic acid stimulates GABA neurogenesis from rat forebrain stem cells. Journal of Neurochemistry.

Lagos, D., Pollara, G., Henderson, S., Gratrix, F., Fabani, M., Milne, R. S. B., Gotch, F., & Boshoff, C. (2010). MiR-132 regulates antiviral innate immunity through suppression of the p300 transcriptional co-activator. Nature Cell Biology, 12(5), 513–519.

Lai, S., Panarese, A., Spalletti, C., Alia, C., Ghionzoli, A., Caleo, M., & Micera, S. (2014). Quantitative Kinematic Characterization of Reaching Impairments in Mice After a Stroke. Neurorehabilitation and Neural Repair, 29(4), 382–392.

Lamb, T. M., Knecht, A. K., Smith, W. C., Stachel, S. E., Economides, A. N., Stahl, N., Yancopolous, G. D., & Harland, R. M. (1993). Neural induction by the secreted polypeptide noggin. Science.

Lamb, T. M., & Harland, R. M. (1995). Fibroblast growth factor is a direct neural inducer, which combined with noggin generates anterior-posterior neural pattern. Development.

Lamba, D. A., Gust, J., & Reh, T. A. (2009). Transplantation of Human Embryonic Stem Cell-Derived Photoreceptors Restores Some Visual Function in Crx-Deficient Mice. Cell Stem Cell.

Le Douarin, N. M., & Kalcheim, C. (1999). The neural crest. Developmental and Cell Biology.

Lee, H. J., Lim, I. J., Lee, M. C., & Kim, S. U. (2010). Human neural stem cells genetically modified to overexpress brain-derived neurotrophic factor promote functional recovery and neuroprotection in a mouse stroke model. Journal of Neuroscience Research.

Lee, H. J., Lim, I. J., Lee, M. C., & Kim, S. U. (2010). Human neural stem cells genetically modified to overexpress brain-derived neurotrophic factor promote functional recovery and neuroprotection in a mouse stroke model. Journal of Neuroscience Research.

Lee, K. J., & Jessell, T. M. (1999). THE SPECIFICATION OF DORSAL CELL FATES IN THE VERTEBRATE CENTRAL NERVOUS SYSTEM. Annual Review of Neuroscience.

Lee, S. M., Tole, S., Grove, E., McMahon, a P., & Scott M. K. Lee1,*, Shubha Tole2,‡, E. G. and A. P. M. (2000). A local Wnt-3a signal is required for development of the mammalian hippocampus. Development (Cambridge, England), 127(3), 457–67.

Lee, S. T., Chu, K., Jung, K. H., Kim, S. J., Kim, D. H., Kang, K. M., Hong, N. H., Kim, J. H., Ban, J. J., Park, H. K., … Roh, J. K. (2008). Anti-inflammatory mechanism of intravascular neural stem cell transplantation in haemorrhagic stroke. Brain, 131(3), 616–629.

Leemput, J. Van De, Boles, N. C., Kiehl, T. R., Corneo, B., Lederman, P., Menon, V., Lee, C., Martinez, R. A., Levi, B. P., Thompson, C. L., … Fasano, C. A. (2014). NeuroResource CORTECON : A Temporal Transcriptome Analysis of In Vitro Human Cerebral Cortex Development from Human Embryonic Stem Cells. Neuron, 83(1), 51–68.

Leid, M., Ishmael, J., & Avram, D. (2004). CTIP1 and CTIP2 are differentially expressed during mouse embryogenesis. Gene Expression, 4(6), 1–12.

Letinic, K., Zoncu, R., & Rakic, P. (2002). Origin of GABAergic neurons in the human neocortex. Nature.

Leung, D. W., Cachianes, G., Kuang, W. J., Goeddel, D. V., & Ferrara, N. (1989). Vascular endothelial growth factor is a secreted angiogenic mitogen. Science.

Liem, K. F., Tremml, G., & Jessell, T. M. (1997). A role for the roof plate and its resident TGFβ-related proteins in neuronal patterning in the dorsal spinal cord. Cell.

Liem, K. F., Tremml, G., Roelink, H., & Jessell, T. M. (1995). Dorsal differentiation of neural plate cells induced by BMP-mediated signals from epidermal ectoderm. Cell.

Liguori, G. L., Echevarría, D., Improta, R., Signore, M., Adamson, E., Martínez, S., & Persico, M. G. (2003). Anterior neural plate regionalization in cripto null mutant mouse embryos in the absence of node and primitive streak. Developmental Biology.

Lim, J. Y., Park, S. I., Oh, J. H., Kim, S. M., Jeong, C. H., Jun, J. A., Lee, K., Oh, W., Lee, J., & Jeun, S. (2008). Brain-derived neurotrophic factor stimulates the neural differentiation of human umbilical cord blood-derived mesenchymal stem cells and survival of differentiated cells through MAPK/ERK and PI3K/Akt-dependent signaling pathways. Journal of Neuroscience Research, 86(10), 2168–2178.

Lipton, P. (1999). Ischemic Cell Death in Brain Neurons. Physiological Reviews.

Litingtung, Y., & Chiang, C. (2000). Specification of ventral neuron types is mediated by an antagonistic interaction between Shh and Gli3. Nature Neuroscience.

Liu, J. P., Laufer, E., & Jessell, T. M. (2001). Assigning the positional identity of spinal motor neurons: Rostrocaudal patterning of Hox-c expression by FGFs, Gdf11, and retinoids. Neuron.

Liu, Q., Dwyer, N. D., & O'Leary, D. D. (2010). Differential expression of COUP-TFI, CHL1, and two novel genes in developing neocortex identified by differential display PCR. The Journal of Neuroscience : The Official Journal of the Society for Neuroscience.

Luikart, B. W., Perederiy, J. V., & Westbrook, G. L. (2012). Dentate gyrus neurogenesis, integration and microRNAs. Behavioural Brain Research.

Lumsden, A., & Keynes, R. (1989). Segmental patterns of neuronal development in the chick hindbrain. Nature.

Lupo, G., Bertacchi, M., Carucci, N., Augusti-Tocco, G., Biagioni, S., & Cremisi, F. (2014). From pluripotency to forebrain patterning: An in vitro journey astride embryonic stem cells. Cellular and Molecular Life Sciences, 71(15), 2917–2930.

Lv, X., Jiang, H., Liu, Y., Lei, X., & Jiao, J. (2014). MicroRNA-15b promotes neurogenesis and inhibits neural progenitor proliferation by directly repressing TET3 during early neocortical development. EMBO Reports.

Ma, L., Hu, B., Liu, Y., Vermilyea, S. C., Liu, H., Gao, L., Sun, Y., Zhang, X., & Zhang, S. C. (2012). Human embryonic stem cell-derived GABA neurons correct locomotion deficits in quinolinic acid-lesioned mice. Cell Stem Cell.

Macdonald, R., Barth, K. A., Xu, Q., Holder, N., Mikkola, I., & Wilson, S. W. (1995). Midline signalling is required for Pax gene regulation and patterning of the eyes. Development (Cambridge, England).

Machon, O., Backman, M., Machonova, O., Kozmik, Z., Vacik, T., Andersen, L., & Krauss, S. (2007). A dynamic gradient of Wnt signaling controls initiation of neurogenesis in the mammalian cortex and cellular specification in the hippocampus. Developmental Biology, 311(1), 223–237.

Maden, M. (2007). An essential role for retinoid signaling in anteroposterior neural patterning. Nature Reviews. Neuroscience.

Magavi, S. S., Leavitt, B. R., & Macklis, J. D. (2000). Induction of neurogenesis in the neocortex of adult mice. Nature, 405(6789), 951–955.

Mallamaci, A., Mercurio, S., Muzio, L., Cecchi, C., Pardini, C. L., Gruss, P., & Boncinelli, E. (2000). The Lack of Emx2 Causes Impairment of Reelin Signaling and Defects of Neuronal Migration in the Developing Cerebral Cortex. J. Neurosci.

Mallamaci, A., Muzio, L., Chan, C. H., Parnavelas, J., & Boncinelli, E. (2000). Area identity shifts in the early cerebral cortex of Emx2(-/-) mutant mice. Nature Neuroscience.

Mampalam, T. J., Gonzalez, M. F., Weinstein, P., & Sharp, F. R. (1988). Neuronal changes in fetal cortex transplanted to ischemic adult rat cortex. Journal of Neurosurgery, 69(6), 904–12.

Manent, J.-B. (2006). Glutamate Acting on AMPA But Not NMDA Receptors Modulates the Migration of Hippocampal Interneurons. Journal of Neuroscience.

Mangale, V. S., Hirokawa, K. E., Satyaki, P. R. V., Gokulchandran, N., Chikbire, S., Subramanian, L., Shetty, A. S., Martynoga, B., Paul, J., Mai, M. V., … Monuki, E. S. (2008). Lhx2 selector activity specifies cortical identity and suppresses hippocampal organizer fate. Science.

Manley, N. C., Priest, C. A., Denham, J., Wirth, E. D., & Lebkowski, J. S. (2017). Human Embryonic Stem Cell-Derived Oligodendrocyte Progenitor Cells: Preclinical Efficacy and Safety in Cervical Spinal Cord Injury. Stem Cells Translational Medicine.

Manley, N. C., Priest, C. A., Denham, J., Wirth, E. D., & Lebkowski, J. S. (2017). Human Embryonic Stem Cell-Derived Oligodendrocyte Progenitor Cells: Preclinical Efficacy and Safety in Cervical Spinal Cord Injury. Stem Cells Translational Medicine.

Mariani, J., Vittoria, M., Palejev, D., & Tomasini, Livia; Coppola, G.; Szekely, A.M.; Horvath, T.L.; Vaccarino, M. V. (2012). Modeling human cortical development in vitro using induced pluripotent stem cells. Proceedings of the National Academy of Sciences, 109(31), 12770–12775.

Marín, F., Aroca, P., & Puelles, L. (2008). Hox gene colinear expression in the avian medulla oblongata is correlated with pseudorhombomeric domains. Developmental Biology.

Marin, O., Rubenstein, J. L. R., & Marín, O. (2003). Cell migration in the forebrain. Annu Rev Neurosci.

Marks, H., Kalkan, T., Menafra, R., Denissov, S., Jones, K., Hofemeister, H., Nichols, J., Kranz, A., Francis Stewart, A., Smith, A., & Stunnenberg, H. G. (2012). The transcriptional and epigenomic foundations of ground state pluripotency. Cell.

Martello, G., Bertone, P., & Smith, A. (2013). Identification of the missing pluripotency mediator downstream of leukaemia inhibitory factor. EMBO Journal.

Martin, G. R. (1981). Isolation of a pluripotent cell line from early mouse embryos cultured in medium conditioned by teratocarcinoma stem cells. Proceedings of the National Academy of Sciences.

Martynoga, B., Morrison, H., Price, D. J., & Mason, J. O. (2005). Foxg1 is required for specification of ventral telencephalon and region-specific regulation of dorsal telencephalic precursor proliferation and apoptosis. Developmental Biology.

Maruoka, Y., Ohbayashi, N., Hoshikawa, M., Itoh, N., Hogan, B. L. m., & Furuta, Y. (1998). Comparison of the expression of three highly related genes, Fgf8, Fgf17 and Fgf18, in the mouse embryo. Mechanisms of Development.

Masai, I., Heisenberg, C. P., Barth, K. A., Macdonald, R., Adamek, S., & Wilson, S. W. (1997). Floating head and masterblind regulate neuronal patterning in the roof of the forebrain. Neuron.

Masui, S., Nakatake, Y., Toyooka, Y., Shimosato, D., Yagi, R., Takahashi, K., Okochi, H., Okuda, A., Matoba, R., Sharov, A. A., … Niwa, H. (2007). Pluripotency governed by Sox2 via regulation of Oct3/4 expression in mouse embryonic stem cells. Nature Cell Biology.

Matsui, Y., Zsebo, K., & Hogan, B. L. M. (1992). Derivation of pluripotential embryonic stem cells from murine primordial germ cells in culture. Cell.

Matsuo, I., Kuratani, S., Kimura, C., Takeda, N., & Aizawa, S. (1995). Mouse Otx2 functions in the formation and patterning of rostral head. Genes and Development.

McMahon, A. P., & Bradley, A. (1990). The Wnt-1 (int-1) proto-oncogene is required for development of a large region of the mouse brain. Cell.

McWhirter JR Weiner JA, Chun J, Murre C, G. M. (1997). A novel fibroblast growth factor gene expressed in the developing nervous system is a downstream target of the chimeric homeodomain oncoprotein E2A-Pbx1. Development.

Meyers, E. N., Lewandoski, M., & Martin, G. R. (1998). An Fgf8 mutant allelic series generated by Cre-and Flp-mediated recombination. Nature Genetics.

Michelsen, K. A., Acosta-Verdugo, S., Benoit-Marand, M., Espuny-Camacho, I., Gaspard, N., Saha, B., Gaillard, A., & Vanderhaeghen, P. (2015). Area-Specific Reestablishment of Damaged Circuits in the Adult Cerebral Cortex by Cortical Neurons Derived from Mouse Embryonic Stem Cells. Neuron, 85(5), 982–997.

Millonig, J. H., Millen, K. J., & Hatten, M. E. (2000). The mouse Dreher gene Lmx1a controls formation of the roof plate in the vertebrate CNS. Nature, 403(6771), 764–769.

Mine, Y., Tatarishvili, J., Oki, K., Monni, E., Kokaia, Z., & Lindvall, O. (2013). Grafted human neural stem cells enhance several steps of endogenous neurogenesis and improve behavioral recovery after middle cerebral artery occlusion in rats. Neurobiology of Disease.

Mione, M. C., Danevic, C., Boardman, P., Harris, B., & Parnavelas, J. G. (1994). Lineage analysis reveals neurotransmitter (GABA or glutamate) but not calcium-binding protein homogeneity in clonally related cortical neurons. The Journal of Neuroscience : The Official Journal of the Society for Neuroscience.

Miska, E., Alvarez-Saavedra, E., Townsend, M., Yoshii, A., Sestan, N., Rakic, P., Constantine-Paton, M., & Horvitz, H. R. (2004). Microarray analysis of microRNA expression in the developing mammalian brain. Genome Biology.

Mizuseki, K., Sakamoto, T., Watanabe, K., Muguruma, K., Ikeya, M., Nishiyama, A., Arakawa, A., Suemori, H., Nakatsuji, N., Kawasaki, H., … Sasai, Y. (2003). Generation of neural crest-derived peripheral neurons and floor plate cells from mouse and primate embryonic stem cells. Proceedings of the National Academy of Sciences.

Mizuseki, K., Kishi, M., Matsui, M., Nakanishi, S., & Sasai, Y. (1998). Xenopus Zic-related-1 and Sox-2, two factors induced by chordin, have distinct activities in the initiation of neural induction. Development (Cambridge, England).

Modo, M., Stroemer, R. P., Tang, E., Patel, S., & Hodges, H. (2002). Effects of implantation site of stem cell grafts on behavioral recovery from stroke damage. Stroke, 33(9), 2270–2278.

Moldrich, R. X., Gobius, I., Pollak, T., Zhang, J., Ren, T., Brown, L., Mori, S., De Juan Romero, C., Britanova, O., Tarabykin, V., & Richards, L. J. (2010). Molecular regulation of the developing commissural plate. Journal of Comparative Neurology.

Molyneaux, B. J., Arlotta, P., Menezes, J. R. L., & Macklis, J. D. (2007). Neuronal subtype specification in the cerebral cortex. Nature Reviews Neuroscience.

Monuki, E. S., Porter, F. D., & Walsh, C. A. (2001). Patterning of the dorsal telencephalon and cerebral cortex by a roof plate-lhx2 pathway. Neuron, 32(4), 591–604.

Moriyama, Y., Takagi, N., Hashimura, K., Itokawa, C., & Tanonaka, K. (2013). Intravenous injection of neural progenitor cells facilitates angiogenesis after cerebral ischemia. Brain and Behavior.

Moury, J. D., & Schoenwolf, G. C. (1995). Cooperative model of epithelial shaping and bending during avian neurulation: Autonomous movements of the neural plate, autonomous movements of the epidermis, and interactions in the neural plate/epidermis transition zone. Developmental Dynamics.

Mukhopadhyay, M., Shtrom, S., Rodriguez-Esteban, C., Chen, L., Tsukui, T., Gomer, L., Dorward, D. W., Glinka, A., Grinberg, A., Huang, S.-P., … Westphal, H. (2001).

Dickkopf1 Is Required for Embryonic Head Induction and Limb Morphogenesis in the Mouse. Developmental Cell.

Muñoz-Sanjuán, I., & Brivanlou, A. H. (2002). Neural induction, the default model and embryonic stem cells. Nature Reviews Neuroscience.

Muzio, L. (2005). Foxg1 Confines Cajal-Retzius Neuronogenesis and Hippocampal Morphogenesis to the Dorsomedial Pallium. Journal of Neuroscience.

Muzio, L., Soria, J. M., Pannese, M., Piccolo, S., & Mallamaci, A. (2005). A mutually stimulating loop involving emx2 and canonical wnt signalling specifically promotes expansion of occipital cortex and hippocampus. Cerebral Cortex (New York, N.Y. : 1991).

Muzio, L., DiBenedetto, B., Stoykova, A., Boncinelli, E., Gruss, P., & Mallamaci, A. (2002). Emx2 and Pax6 control regionalization of the pre-neuronogenic cortical primordium. Cerebral Cortex (New York, N.Y. : 1991), 12(2), 129–139.

Muzio, L., & Mallamaci, A. (2005). Foxg1 Confines Cajal-Retzius Neuronogenesis and Hippocampal Morphogenesis to the Dorsomedial Pallium 10.1523/JNEUROSCI.4804-04.2005. J. Neurosci.

Nadarajah, B., Brunstrom, J. E., Grutzendler, J., Wong, R. O. L., & Pearlman, A. L. (2001). Two modes of radial migration in early development of the cerebral cortex. Nature Neuroscience.

Nakagomi, T., Molnár, Z., Nakano-Doi, A., Taguchi, A., Saino, O., Kubo, S., Clausen, M., Yoshikawa, H., Nakagomi, N., & Matsuyama, T. (2011). Ischemia-Induced Neural Stem/Progenitor Cells in the Pia Mater Following Cortical Infarction. Stem Cells and Development.

Nathan, C., & Ding, A. (2010). Nonresolving Inflammation. Cell.

Nery, S., Fishell, G., & Corbin, J. G. (2002). The caudal ganglionic eminence is a source of distinct cortical and subcortical cell populations. Nature Neuroscience.

Ng, H. H., & Surani, M. A. (2011). The transcriptional and signalling networks of pluripotency. Nature Cell Biology.

Nichols, J., Zevnik, B., Anastassiadis, K., Niwa, H., Klewe-Nebenius, D., Chambers, I., Schöler, H., & Smith, A. (1998). Formation of pluripotent stem cells in the mammalian embryo depends on the POU transcription factor Oct4. Cell.

Nielsen, J. V., Blom, J. B., Noraberg, J., & Jensen, N. A. (2010). Zbtb20-Induced CA1 pyramidal neuron development and area enlargement in the cerebral midline cortex of mice. Cerebral Cortex, 20(8), 1904–1914.

Nielsen, J. A., Lau, P., Maric, D., Barker, J. L., & Hudson, L. D. (2009). Integrating microRNA and mRNA expression profiles of neuronal progenitors to identify regulatory networks underlying the onset of cortical neurogenesis. BMC Neuroscience.

Nieuwkoop, P., & Nigtevecht, G. (1954). Neural activation and transformation in explants of competent ectoderm under the influence of fragments of anterior notochord in urodeles. Journal of Embryology and ….

Niwa, H., Ogawa, K., Shimosato, D., & Adachi, K. (2009). A parallel circuit of LIF signalling pathways maintains pluripotency of mouse ES cells. Nature.

Nordgård, O., Kvaløy, J. T., Farmen, R. K., & Heikkilä, R. (2006). Error propagation in relative real-time reverse transcription polymerase chain reaction quantification models: The balance between accuracy and precision. Analytical Biochemistry, 356(2), 182–193.

Nori, S., Okada, Y., Nishimura, S., Sasaki, T., Itakura, G., Kobayashi, Y., Renault-Mihara, F., Shimizu, A., Koya, I., Yoshida, R., … Okano, H. (2015). Long-term safety issues of iPSC-based cell therapy in a spinal cord injury model: Oncogenic transformation with epithelial-mesenchymal transition. Stem Cell Reports.

Nowakowski, T. J., Fotaki, V., Pollock, A., Sun, T., Pratt, T., & Price, D. J. (2013). MicroRNA-92b regulates the development of intermediate cortical progenitors in embryonic mouse brain. Proceedings of the National Academy of Sciences.

Nowakowski, T. J., Mysiak, K. S., Pratt, T., & Price, D. J. (2011). Functional dicer is necessary for appropriate specification of radial glia during early development of mouse telencephalon. PLoS ONE.

Obermeier, B., Daneman, R., & Ransohoff, R. M. (2013). Development, maintenance and disruption of the blood-brain barrier. Nature Medicine.

Ohkubo, Y., Chiang, C., & Rubenstein, J. L. R. (2002). Coordinate regulation and synergistic actions of BMP4, SHH and FGF8 in the rostral prosencephalon regulate morphogenesis of the telencephalic and optic vesicles. Neuroscience.

Okada, Y., Shimazaki, T., Sobue, G., & Okano, H. (2004). Retinoic-acid-concentration-dependent acquisition of neural cell identity during in vitro differentiation of mouse embryonic stem cells. Developmental Biology.

O'Leary, D. D. M., Chou, S. J., & Sahara, S. (2007). Area patterning of the mammalian cortex. Neuron.

O'Leary, D. D. M., & Nakagawa, Y. (2002). Patterning centers, regulatory genes and extrinsic mechanisms controlling arealization of the neocortex. Current Opinion in Neurobiology.

O'Leary, D. D., & Sahara, S. (2008). Genetic regulation of arealization of the neocortex. Current Opinion in Neurobiology.

Paek, H., Gutin, G., & Hebert, J. M. (2009). FGF signaling is strictly required to maintain early telencephalic precursor cell survival. Development.

Papalopulu, N., Clarke, J. D., Bradley, L., Wilkinson, D., Krumlauf, R., & Holder, N. (1991). Retinoic acid causes abnormal development and segmental patterning of the anterior hindbrain in Xenopus embryos. Development.

Paridaen, J. T., & Huttner, W. B. (2014). Neurogenesis during development of the vertebrate central nervous system. EMBO Reports.

Paul, P., Chakraborty, A., Sarkar, D., Langthasa, M., Rahman, M., Bari, M., Singha, R. K. S., Malakar, A. K., & Chakraborty, S. (2018). Interplay between miRNAs and human diseases. Journal of Cellular Physiology.

Pearson, J. C., Lemons, D., & McGinnis, W. (2005). Modulating Hox gene functions during animal body patterning. Nature Reviews Genetics.

Pera, E. M., Ikeda, A., Eivers, E., & De Robertis, E. M. (2003). Integration of IGF, FGF, and anti-BMP signals via Smad1 phosphorylation in neural induction. Genes and Development.

Pera, M. F. (2004). Regulation of human embryonic stem cell differentiation by BMP-2 and its antagonist noggin. Journal of Cell Science.

Perez Villegas, E. M., Olivier, C., Spassky, N., Poncet, C., Cochard, P., Zalc, B., Thomas, J. L., & Martínez, S. (1999). Early specification of oligodendrocytes in the chick embryonic brain. Developmental Biology.

Perrier, A. L., Tabar, V., Barberi, T., Rubio, M. E., Bruses, J., Topf, N., Harrison, N. L., & Studer, L. (2004). Derivation of midbrain dopamine neurons from human embryonic stem cells. Proceedings of the National Academy of Sciences.

Petrovic-Djergovic, D., Goonewardena, S. N., & Pinsky, D. J. (2016). Inflammatory disequilibrium in stroke. Circulation Research.

Piccolo, S., Sasai, Y., Lu, B., & De Robertis, E. M. (1996). Dorsoventral patterning in Xenopus: Inhibition of ventral signals by direct binding of chordin to BMP-4. Cell.

Pitto, L., & Cremisi, F. (2010). Timing neurogenesis by cell cycle? Cell Cycle.

Plate, K. H., Beck, H., Danner, S., Allegrini, P. R., & Wiessner, C. (1999). Cell type specific upregulation of vascular endothelial growth factor in an MCA-occlusion model of cerebral infarct. Journal of Neuropathology and Experimental Neurology.

Pleasure, S. J., Anderson, S., Hevner, R., Bagri, A., Marin, O., Lowenstein, D. H., & Rubenstein, J. L. R. (2000). Cell migration from the ganglionic eminences is required for the development of hippocampal GABAergic interneurons. Neuron.

Poewe, W., Seppi, K., Tanner, C. M., Halliday, G. M., Brundin, P., Volkmann, J., Schrag, A.-E., & Lang, A. E. (2017). Parkinson disease. Nature Reviews Disease Primers, 3, 17013.

Pop, V., & Badaut, J. (2011). A Neurovascular Perspective for Long-Term Changes After Brain Trauma. Translational Stroke Research.

Priest, C. A., Manley, N. C., Denham, J., Wirth, E. D., & Lebkowski, J. S. (2015). Preclinical safety of human embryonic stem cell-derived oligodendrocyte progenitors supporting clinical trials in spinal cord injury. Regenerative Medicine.

Qiu, D., Ye, S., Ruiz, B., Zhou, X., Liu, D., Zhang, Q., & Ying, Q. L. (2015). Klf2 and Tfcp2l1, Two Wnt/β-Catenin Targets, Act Synergistically to Induce and Maintain Naive Pluripotency. Stem Cell Reports.

Rajman, M., & Schratt, G. (2017). MicroRNAs in neural development: from master regulators to fine-tuners. Development.

Rallu M, Machold R, Gaiano N, Corbin JG, & Fishell G. (2002). Dorsoventral patterning is established in the telencephalon of mutants lacking both Gli3 and Hedgehog signaling . Development.

Ransohoff, R. M., & Engelhardt, B. (2012). The anatomical and cellular basis of immune surveillance in the central nervous system. Nature Reviews Immunology.

Rash, B. G., & Grove, E. A. (2007). Patterning the Dorsal Telencephalon: A Role for Sonic Hedgehog? Journal of Neuroscience.

Rash, B. G., & Grove, E. A. (2006). Area and layer patterning in the developing cerebral cortex. Current Opinion in Neurobiology.

Rattner, A., Hsieh, J.-C., Smallwood, P. M., Gilbert, D. J., Copeland, N. G., Jenkins, N. A., & Nathans, J. (1997). A family of secreted proteins contains homology to the cysteine-rich ligand-binding domain of frizzled receptors. Proceedings of the National Academy of Sciences.

Rhinn, M., & Brand, M. (2001). The midbrain-hindbrain boundary organizer. Current Opinion in Neurobiology.

Rodríguez-Seguel, E., Alarcón, P., & Gómez-Skarmeta, J. L. (2009). The Xenopus Irx genes are essential for neural patterning and define the border between prethalamus and thalamus through mutual antagonism with the anterior repressors Fezf and Arx. Developmental Biology.

Roelink, H., Augsburger, A., Heemskerk, J., Korzh, V., Norlin, S., Ruiz i Altaba, A., Tanabe, Y., Placzek, M., Edlund, T., Jessell, T. M., & Dodd, J. (1994). Floor plate and motor neuron induction by vhh-1, a vertebrate homolog of hedgehog expressed by the notochord. Cell.

Roelink, H., Porter, J. A., Chiang, C., Tanabe, Y., Chang, D. T., Beachy, P. A., & Jessell, T. M. (1995). Floor plate and motor neuron induction by different concentrations of the amino-terminal cleavage product of sonic hedgehog autoproteolysis. Cell.

Roitbak, T., & Syková, E. (1999). Diffusion barriers evoked in the rat cortex by reactive astrogliosis. GLIA.

Rowitch, D. H., S-Jacques, B., Lee, S. M., Flax, J. D., Snyder, E. Y., & McMahon, A. P. (1999). Sonic hedgehog regulates proliferation and inhibits differentiation of CNS precursor cells. The Journal of Neuroscience : The Official Journal of the Society for Neuroscience.

Roy, N. S., Cleren, C., Singh, S. K., Yang, L., Beal, M. F., & Goldman, S. A. (2006). Functional engraftment of human ES cell-derived dopaminergic neurons enriched by coculture with telomerase-immortalized midbrain astrocytes. Nature Medicine.

Rubenstein, J. L., & Beachy, P. A. (1998). Patterning of the embryonic forebrain. Current Opinion in Neurobiology.

Ryu, S., Lee, S. H., Kim, S. U., & Yoon, B. W. (2016). Human neural stem cells promote proliferation of endogenous neural stem cells and enhance angiogenesis in ischemic rat brain. Neural Regeneration Research.

Sahara, S., Kawakami, Y., Izpisua Belmonte, J., O'Leary, D. D. D. M., Belmonte, J. C. I., & O'Leary, D. D. D. M. (2007). Sp8 exhibits reciprocal induction with Fgf8 but has an opposing effect on anterior-posterior cortical area patterning. Neural Development, 2(1), 10.

Sahara, S., & O'Leary, D. D. M. (2009). Fgf10 Regulates Transition Period of Cortical Stem Cell Differentiation to Radial Glia Controlling Generation of Neurons and Basal Progenitors. Neuron.

Sakata, H., Narasimhan, P., Niizuma, K., Maier, C. M., Wakai, T., & Chan, P. H. (2012). Interleukin 6-preconditioned neural stem cells reduce ischaemic injury in stroke mice. Brain.

Salero, E., & Hatten, M. E. (2007). Differentiation of ES cells into cerebellar neurons. Proceedings of the National Academy of Sciences.

Sansom, S. N., & Livesey, F. J. (2009). Gradients in the brain: the control of the development of form and function in the cerebral cortex. Cold Spring Harbor Perspectives in Biology.

Sarkar, A., Mei, A., Paquola, A. C. M., Stern, S., Bardy, C., Klug, J. R., Kim, S., Neshat, N., Kim, H. J., Ku, M., … Gage, F. H. (2018). Efficient Generation of CA3 Neurons from Human Pluripotent Stem Cells Enables Modeling of Hippocampal Connectivity In Vitro. Cell Stem Cell.

Schoenwolf, G. C. (1988). Microsurgical analyses of avian neurulation: Separation of medial and lateral tissues. Journal of Comparative Neurology.

Schoknecht, K., David, Y., & Heinemann, U. (2015). The blood-brain barrier-Gatekeeper to neuronal homeostasis: Clinical implications in the setting of stroke. Seminars in Cell and Developmental Biology.

Schouten, M., Renate Buijink, M., Lucassen, P. J., & Fitzsimons, C. P. (2012). New neurons in aging brains: Molecular control by small non-coding RNAs. Frontiers in Neuroscience.

Sciences, C., Neurobiology, R., & Foundation, H. (2014). P LURIPOTENT S TEM C ELLS Optogenetics Reveal Delayed Afferent Synaptogenesis on Grafted Human-Induced Pluripotent Stem Cell-Derived Neural Progenitors, 3088–3098.

Shanmugalingam, S., Houart, C., Picker, a, Reifers, F., Macdonald, R., Barth, a, Griffin, K., Brand, M., & Wilson, S. W. (2000). Ace/Fgf8 is required for forebrain commissure formation and patterning of the telencephalon. Development (Cambridge, England), 127(12), 2549–2561.

Sharp, J., Frame, J., Siegenthaler, M., Nistor, G., & Keirstead, H. S. (2010). Human embryonic stem cell-derived oligodendrocyte progenitor cell transplants improve recovery after cervical spinal cord injury. Stem Cells.

Shawlot, W., & Behringer, R. R. (1995). Requirement for liml in head-organizer function. Nature.

Sheen, V. L., Arnold, M. W., Wang, Y., & Macklis, J. D. (1999). Neural precursor differentiation following transplantation into neocortex is dependent on intrinsic developmental state and receptor competence. Experimental Neurology, 158(1), 47–62.

Shen, Q., Wang, Y., Dimos, J. T., Fasano, C. a, Phoenix, T. N., Lemischka, I. R., Ivanova, N. B., Stifani, S., Morrisey, E. E., & Temple, S. (2006). The timing of cortical neurogenesis is encoded within lineages of individual progenitor cells. Nature Neuroscience, 9(6), 743–51.

Shetty, A. K., & Turner, D. A. (1996). Development of fetal hippocampal grafts in intact and lesioned hippocampus. Progress in Neurobiology, 50(5–6), 597–653.

Shi, Y., Kirwan, P., Smith, J., Robinson, H. P. C., & Livesey, F. J. (2012). Human cerebral cortex development from pluripotent stem cells to functional excitatory synapses. Nature Neuroscience, 15(3), 477–486.

Shimamura, K., & Rubenstein, J. L. (1997). Inductive interactions direct early regionalization of the mouse forebrain. Development (Cambridge, England).

Shimogori, T. (2004). Embryonic signaling centers expressing BMP, WNT and FGF proteins interact to pattern the cerebral cortex. Development.

Shin, J. J., Fricker-Gates, R. a, Perez, F. a, Leavitt, B. R., Zurakowski, D., & Macklis, J. D. (2000). Transplanted neuroblasts differentiate appropriately into projection neurons with correct neurotransmitter and receptor phenotype in neocortex undergoing targeted projection neuron degeneration. The Journal of Neuroscience : The Official Journal of the Society for Neuroscience, 20(19), 7404–16.

Shinozaki, K., Yoshida, M., Nakamura, M., Aizawa, S., & Suda, Y. (2004). Emx1 and Emx2 cooperate in initial phase of archipallium development. Mech Dev.

Shinya, M., Koshida, S., Sawada, A., Kuroiwa, A., & Takeda, H. (2001). Fgf signalling through MAPK cascade is required for development of the subpallial telencephalon in zebrafish embryos. Development (Cambridge, England).

Shiraishi, A., Muguruma, K., & Sasai, Y. (2017). Generation of thalamic neurons from mouse embryonic stem cells. Development, 144(7), 1211–1220.

Silva, J., Nichols, J., Theunissen, T. W., Guo, G., van Oosten, A. L., Barrandon, O., Wray, J., Yamanaka, S., Chambers, I., & Smith, A. (2009). Nanog Is the Gateway to the Pluripotent Ground State. Cell.

Simeone, A., Acampora, D., Gulisano, M., Stornaiuolo, A., & Boncinelli, E. (1992). Nested expression domains of four homeobox genes in developing rostral brain. Nature.

Simon, H., Hornbruch, A., & Lumsden, A. (1995). Independent assignment of antero-posterior and dorso-ventral positional values in the developing chick hindbrain. Current Biology.

Sloviter, R. S. (1989). Calcium-binding protein (calbindin-D28k) and parvalbumin immunocytochemistry: Localization in the rat hippocampus with specific reference to the selective vulnerability of hippocampal neurons to seizure activity. Journal of Comparative Neurology, 280(2), 183–196.

Smith, H. K., & Gavins, F. N. E. (2012). The potential of stem cell therapy for stroke: is PISCES the sign? The FASEB Journal.

Smith, W. C., Knecht, A. K., Wu, M., & Harland, R. M. (1993). Secreted noggin protein mimics the Spemann organizer in dorsalizing Xenopus mesoderm. Nature.

Snow, M. H. L. (1976). Embryo growth during the immediate postimplantation period. Embryogenesis in Mammals, 53–70.

Snyder, E. Y., Yoon, C., Flax, J. D., & Macklis, J. D. (1997). Multipotent neural precursors can differentiate toward replacement of neurons undergoing targeted apoptotic degeneration in adult mouse neocortex. Proceedings of the National Academy of Sciences of the United States of America, 94(21), 11663–11668.

Solnica-Krezel, L., & Sepich, D. S. (2012). Gastrulation: Making and Shaping Germ Layers. Annual Review of Cell and Developmental Biology.

Song, M., Kim, Y. J., Kim, Y. H., Roh, J., Kim, E. C., Lee, H. J., Kim, S. U., & Yoon, B. W. (2015). Long-term effects of magnetically targeted ferumoxide-labeled human neural stem cells in focal cerebral ischemia. Cell Transplantation.

Stanfield, B. B., & Cowan, W. M. (1979). The development of the hippocampus and dentate gyrus in normal and reeler mice. Journal of Comparative Neurology.

Stappert, L., Borghese, L., Roese-Koerner, B., Weinhold, S., Koch, P., Terstegge, S., Uhrberg, M., Wernet, P., & Brüstle, O. (2013). MicroRNA-Based Promotion of Human Neuronal Differentiation and Subtype Specification. PLoS ONE.

Stefani, G., & Slack, F. J. (2008). Small non-coding RNAs in animal development. Nature Reviews Molecular Cell Biology.

Stenvang, J., Petri, A., Lindow, M., Obad, S., & Kauppinen, S. (2012). Inhibition of microRNA function by antimiR oligonucleotides. Silence, 3(1), 1.

Stephen N. Sansom, Jean M. Hébert, Uruporn Thammongkol, James Smith, Grace Nisbet, M. Azim Surani, Susan K. McConnell, F. J. L. (2005). Genomic characterisation of a Fgf-regulated gradient-based neocortical protomap. Development, 132(17), 3947–3961.

Stern, C. D. (2006). Neural induction: 10 years on since the “default model.” Current Opinion in Cell Biology.

Storm, E. E. (2006). Dose-dependent functions of Fgf8 in regulating telencephalic patterning centers. Development, 133(9), 1831–1844.

Storm, E. E., Rubenstein, J. L. R., & Martin, G. R. (2003). Dosage of Fgf8 determines whether cell survival is positively or negatively regulated in the developing forebrain. Proceedings of the National Academy of Sciences.

Stoykova, A., Götz, M., Gruss, P., Price, J., & Gotz, M. (1997). Pax6-dependent regulation of adhesive patterning, R-cadherin expression and boundary formation in developing forebrain. Development (Cambridge, England).

Stoykova, A., Fritsch, R., Walther, C., & Gruss, P. (1996). Forebrain patterning defects in Small eye mutant mice. Development (Cambridge, England).

Stoykova, A., Treichel, D., Hallonet, M., & Gruss, P. (2000). Pax6 Modulates the Dorsoventral Patterning of the Mammalian Telencephalon. The Journal of Neuroscience.

Streit, A., Berliner, A. J., Papanayotou, C., Slrulnik, A., & Stern, C. D. (2000). Initiation of neural induction by FGF signalling before gastrulation. Nature.

Stroemer, P., Patel, S., Hope, A., Oliveira, C., Pollock, K., & Sinden, J. (2009). The neural stem cell line CTX0E03 promotes behavioral recovery and endogenous neurogenesis after experimental stroke in a dose-dependent fashion. Neurorehabilitation and Neural Repair.

Subramanian, L., Remedios, R., Shetty, A., & Tole, S. (2009). Signals from the edges: The cortical hem and antihem in telencephalic development. Seminars in Cell and Developmental Biology, 20(6), 712–718.

Sun, Y., Jin, K., Xie, L., Childs, J., Mao, X. O., Logvinova, A., & Greenberg, D. A. (2003). VEGF-induced neuroprotection, neurogenesis, and angiogenesis after focal cerebral ischemia. Journal of Clinical Investigation.

Sur, M., & Rubenstein, J. L. R. (2005). Patterning and plasticity of the cerebral cortex. Science.

Suzuki, A., Raya, A., Kawakami, Y., Morita, M., Matsui, T., Nakashima, K., Gage, F. H., Rodriguez-Esteban, C., & Izpisua Belmonte, J. C. (2006). Nanog binds to Smad1 and blocks bone morphogenetic protein-induced differentiation of embryonic stem cells. Proceedings of the National Academy of Sciences.

Swanson, L. W., Wyss, J. M., & Cowan, W. M. (1978). An autoradiographic study of the organization of intrahippocampal association pathways in the rat. Journal of Comparative Neurology, 181(4), 681–715.

Tabar, V., Panagiotakos, G., Greenberg, E. D., Chan, B. K., Sadelain, M., Gutin, P. H., & Studer, L. (2005). Migration and differentiation of neural precursors derived from human embryonic stem cells in the rat brain. Nature Biotechnology.

Tabata, H., & Nakajima, K. (2003). Multipolar Migration: The Third Mode of Radial Neuronal Migration in the Developing Cerebral Cortex. The Journal of Neuroscience.

Takahashi, K., & Yamanaka, S. (2006). Induction of Pluripotent Stem Cells from Mouse Embryonic and Adult Fibroblast Cultures by Defined Factors. Cell.

Tam, P. P. L., & Behringer, R. R. (1997). Mouse gastrulation: The formation of a mammalian body plan. Mechanisms of Development.

Tanabe, Y., & Jessell, T. M. (1996). Diversity and pattern in the developing spinal cord. Science.

Tanabe, Y., Roelink, H., & Jessell, T. M. (1995). Induction of motor neurons by Sonic hedgehog is independent of floor plate differentiation. Current Biology.

Tang, Y., Wang, J., Lin, X., Wang, L., Shao, B., Jin, K., Wang, Y., & Yang, G. Y. (2014). Neural stem cell protects aged rat brain from ischemia-reperfusion injury through neurogenesis and angiogenesis. Journal of Cerebral Blood Flow and Metabolism.

Tao, W., & Lai, E. (1992). Telencephalon-restricted expression of BF-1, a new member of the HNF-3/fork head gene family, in the developing rat brain. Neuron.

Taylor, R. A., & Sansing, L. H. (2013). Microglial responses after ischemic stroke and intracerebral hemorrhage. Clinical and Developmental Immunology.

Teng, H., Zhang, Z. G., Wang, L., Zhang, R. L., Zhang, L., Morris, D., Gregg, S. R., Wu, Z., Jiang, A., Lu, M., … Chopp, M. (2008). Coupling of angiogenesis and neurogenesis in cultured endothelial cells and neural progenitor cells after stroke. Journal of Cerebral Blood Flow and Metabolism.

Tennant, K. A., Adkins, D. L., Donlan, N. A., Asay, A. L., Thomas, N., Kleim, J. A., & Jones, T. A. (2011). The organization of the forelimb representation of the C57BL/6 mouse motor cortex as defined by intracortical microstimulation and cytoarchitecture. Cerebral Cortex, 21(4), 865–876.

Terrigno, M., Bertacchi, M., Pandolfini, L., Baumgart, M., Calvello, M., Cellerino, A., Studer, M., & Cremisi, F. (2018). The microRNA miR-21 Is a Mediator of FGF8 Action on Cortical COUP-TFI Translation. Stem Cell Reports.

Terrigno, M., Busti, I., Alia, C., Pietrasanta, M., Arisi, I., D'Onofrio, M., Caleo, M., & Cremisi, F. (2018). Neurons Generated by Mouse ESCs with Hippocampal or Cortical Identity Display Distinct Projection Patterns When Co-transplanted in the Adult Brain. Stem Cell Reports.

Tesar, P. J., Chenoweth, J. G., Brook, F. A., Davies, T. J., Evans, E. P., Mack, D. L., Gardner, R. L., & McKay, R. D. G. (2007). New cell lines from mouse epiblast share defining features with human embryonic stem cells. Nature.

Theil, T., Alvarez-Bolado, G., Walter, A., Rüther, U., Acampora, D., Avantaggiato, V., Tuorto, F., Simeone, A., Belloni, E., Muenke, M., … Aizawa, S. (1999). Gli3 is required for Emx gene expression during dorsal telencephalon development. Development (Cambridge, England).

Theil, T., Aydin, S., Koch, S., Grotewold, L., & Rüther, U. (2002). Wnt and Bmp signalling cooperatively regulate graded Emx2 expression in the dorsal telencephalon. Development (Cambridge, England), 129(13), 3045–54.

Theil, T., Dominguez-Frutos, E., & Schimmang, T. (2008). Differential requirements for Fgf3 and Fgf8 during mouse forebrain development. Developmental Dynamics.

Thom, M. (2009). Hippocampal sclerosis: Progress since sommer. Brain Pathology, 19(4), 565–572.

Thomsen, G. H. (1997). Antagonism within and around the organizer: BMP inhibitors in vertebrate body patterning. Trends in Genetics : TIG.

Thomson, M., Liu, S. J., Zou, L. N., Smith, Z., Meissner, A., & Ramanathan, S. (2011). Pluripotency factors in embryonic stem cells regulate differentiation into germ layers. Cell.

Thored, P., Wood, J., Arvidsson, A., Cammenga, J., Kokaia, Z., & Lindvall, O. (2007). Long-term neuroblast migration along blood vessels in an area with transient angiogenesis and increased vascularization after stroke. Stroke.

Tole, S., Ragsdale, C. W., & Grove, E. A. (2000). Dorsoventral patterning of the telencephalon is disrupted in the mouse mutant extra-toes. Developmental Biology.

Tomassy, G. S., De Leonibus, E., Jabaudon, D., Lodato, S., Alfano, C., Mele, A., Macklis, J. D., & Studer, M. (2010). Area-specific temporal control of corticospinal motor neuron differentiation by COUP-TFI. Proceedings of the National Academy of Sciences, 107(8), 3576–3581.

Toresson, H., Potter, S. S., & Campbell, K. (2000). Genetic control of dorsal-ventral identity in the telencephalon: opposing roles for Pax6 and Gsh2. Development.

Tornero, D., Wattananit, S., Madsen, M. G., Koch, P., Wood, J., Tatarishvili, J., Mine, Y., Ge, R., Monni, E., Devaraju, K., … Kokaia, Z. (2013). Human induced pluripotent stem cell-derived cortical neurons integrate in stroke-injured cortex and improve functional recovery. Brain, 136(12), 3561–3577.

Tornero, D., Wattananit, S., Madsen, M. G., Koch, P., Wood, J., Tatarishvili, J., Mine, Y., Ge, R., Monni, E., Devaraju, K., … Bru, O. (2013). cortical neurons integrate in stroke-injured cortex and improve functional recovery.

Toyoda, R., Assimacopoulos, S., Wilcoxon, J., Taylor, A., Feldman, P., Suzuki-Hirano, A., Shimogori, T., & Grove, E. A. (2010). FGF8 acts as a classic diffusible morphogen to pattern the neocortex. Development, 137(20), 3439–3448.

Tricoire, L., Pelkey, K. A., Erkkila, B. E., Jeffries, B. W., Yuan, X., & McBain, C. J. (2011). A Blueprint for the Spatiotemporal Origins of Mouse Hippocampal Interneuron Diversity. Journal of Neuroscience.

Tropepe, V., Hitoshi, S., Sirard, C., Mak, T. W., Rossant, J., & van der Kooy, D. (2001). Direct neural fate specification from embryonic stem cells: a primitive mammalian neural stem cell stage acquired through a default mechanism. Neuron, 30(1), 65–78.

Tüfekci, K. U., Öner, M. G., Meuwissen, R. L. J., & Genç, Ş. (2014). The role of microRNAs in human diseases. Methods in Molecular Biology.

Vallone, F., Lai, S., Spalletti, C., Panarese, A., Alia, C., Micera, S., Caleo, M., & Di Garbo, A. (2016). Post-stroke longitudinal alterations of inter-hemispheric correlation and hemispheric dominance in mouse pre-motor cortex. PLoS ONE, 11(1), 1–26.

Van den Ameele, J., Tiberi, L., Vanderhaeghen, P., & Espuny-Camacho, I. (2014). Thinking out of the dish: What to learn about cortical development using pluripotent stem cells. Trends in Neurosciences.

van Praag, H., Schinder, A. F., Christie, B. R., Toni, N., Palmer, T. D., & Gage, F. H. (2002). Functional neurogenesis in the adult hippocampus. Nature, 415(6875), 1030–1034.

Vasudevan, S. (2012). Posttranscriptional Upregulation by MicroRNAs. Wiley Interdisciplinary Reviews: RNA.

Viczian, A. S. (2003). XOtx5b and XOtx2 regulate photoreceptor and bipolar fates in the Xenopus retina. Development.

W.-R., S., T., S., C.M., C.-K., S., S., C., S., A., S., & H.G., K. (2007). Intravenous brain-derived neurotrophic factor enhances poststroke sensorimotor recovery and stimulates neurogenesis. Stroke.

Walshe, J. (2003). Unique and combinatorial functions of Fgf3 and Fgf8 during zebrafish forebrain development. Development.

Walshe, J., & Mason, I. (2003). Fgf signalling is required for formation of cartilage in the head. Developmental Biology.

Wang, W.-C., Lin, F.-M., Chang, W.-C., Lin, K.-Y., Huang, H.-D., & Lin, N.-S. (2009). miRExpress: Analyzing high-throughput sequencing data for profiling microRNA expression. BMC Bioinformatics, 10(1), 328.

Wang, Y. Q., Cui, H. R., Yang, S. Z., Sun, H. P., Qiu, M. H., Feng, X. Y., & Sun, F. Y. (2009). VEGF enhance cortical newborn neurons and their neurite development in adult rat brain after cerebral ischemia. Neurochemistry International.

Waskiewicz, A. J., Rikhof, H. A., & Moens, C. B. (2002). Eliminating zebrafish Pbx proteins reveals a hindbrain ground state. Developmental Cell.

Wassarman, K. M., Lewandoski, M., Campbell, K., Joyner, A. L., Rubenstein, J. L., Martinez, S., & Martin, G. R. (1997). Specification of the anterior hindbrain and establishment of a normal mid/hindbrain organizer is dependent on Gbx2 gene function. Development (Cambridge, England).

Watanabe, K., Kamiya, D., Nishiyama, A., Katayama, T., Nozaki, S., Kawasaki, H., Watanabe, Y., Mizuseki, K., & Sasai, Y. (2005). Directed differentiation of telencephalic precursors from embryonic stem cells. Nature Neuroscience.

Water, S. Van De, & Wetering, M. Van De. (2001). Ectopic Wnt signal determines the eyeless phenotype of zebrafish masterblind mutant. Development (Cambridge, England).

Wattananit, S., Tornero, D., Graubardt, N., Memanishvili, T., Monni, E., Tatarishvili, J., Miskinyte, G., Ge, R., Ahlenius, H., Lindvall, O., … Kokaia, Z. (2016). Monocyte-Derived Macrophages Contribute to Spontaneous Long-Term Functional Recovery after Stroke in Mice. Journal of Neuroscience.

Wei, L., Fraser, J. L., Lu, Z. Y., Hu, X., & Yu, S. P. (2012). Transplantation of hypoxia preconditioned bone marrow mesenchymal stem cells enhances angiogenesis and neurogenesis after cerebral ischemia in rats. Neurobiology of Disease.

Weick, J. P., Liu, Y., & Zhang, S.-C. (2011). Human embryonic stem cell-derived neurons adopt and regulate the activity of an established neural network. Proceedings of the National Academy of Sciences.

Weick, J. P., Johnson, M. A., Skroch, S. P., Williams, J. C., Deisseroth, K., & Zhang, S. C. (2010). Functional control of transplantable human ESC-derived neurons via optogenetic targeting. Stem Cells.

Weidemann, A., Krohne, T. U., Aguilar, E., Kurihara, T., Takeda, N., Dorrell, M. I., Simon, M. C., Haase, V. H., Friedlander, M., & Johnson, R. S. (2010). Astrocyte hypoxic response is essential for pathological but not developmental angiogenesis of the retina. GLIA.

Weinstein, D. C., & Hemmati-Brivanlou, A. (1997). Neural induction in Xenopus laevis: Evidence for the default model. Current Opinion in Neurobiology.

Wernig, M., Zhao, J.-P., Pruszak, J., Hedlund, E., Fu, D., Soldner, F., Broccoli, V., Constantine-Paton, M., Isacson, O., & Jaenisch, R. (2008). Neurons derived from reprogrammed fibroblasts functionally integrate into the fetal brain and improve symptoms of rats with Parkinson's disease. Proceedings of the National Academy of Sciences.

Wichterle, H., Lieberam, I., Porter, J. A., & Jessell, T. M. (2002). Directed differentiation of embryonic stem cells into motor neurons. Cell.

Wichterle, H., Turnbull, D. H., Nery, S., Fishell, G., & Alvarez-Buylla, A. (2001). In utero fate mapping reveals distinct migratory pathways and fates of neurons born in the mammalian basal forebrain. Development (Cambridge, England).

Wilton, L. J., & Trounson, a O. (1989). Biopsy of preimplantation mouse embryos: development of micromanipulated embryos and proliferation of single blastomeres in vitro. Biology of Reproduction.

Winkel, G. K., & Pedersen, R. A. (1988). Fate of the inner cell mass in mouse embryos as studied by microinjection of lineage tracers. Developmental Biology, 127(1), 143–156.

Wu, J., Okamura, D., Li, M., Suzuki, K., Luo, C., Ma, L., He, Y., Li, Z., Benner, C., Tamura, I., … Belmonte, J. C. I. (2015). An alternative pluripotent state confers interspecies chimaeric competency. Nature.

Wu, J., Yamauchi, T., & Izpisua Belmonte, J. C. (2016). An overview of mammalian pluripotency. Development.

Wurst, W., Auerbach, A. B., Joyner, A. L., Alvarado-Mallart, R.-M., Martinez, S., Lance-Jones, C. C., Bally-Cuif, L., Alvarado-Mallart, R.-M., Darnell, D. K., Wassef, M., … McMahon, A. P. (1994). Multiple developmental defects in Engrailed-1 mutant mice: an early mid-hindbrain deletion and patterning defects in forelimbs and sternum. Development (Cambridge, England).

Xuan, S., Baptista, C. A., Balas, G., Tao, W., Soares, V. C., & Lai, E. (1995). Winged helix transcription factor BF-1 is essential for the development of the cerebral hemispheres. Neuron.

Yamashita, T., & Abe, K. (2011). Therapeutic approaches to vascular protection in ischemic stroke. Acta Medica Okayama.

Yamashita, T., Deguchi, K., Nagotani, S., & Abe, K. (2011). Vascular protection and restorative therapy in ischemic stroke. Cell Transplantation.

Yang, D., Li, T., Wang, Y., Tang, Y., Cui, H., Tang, Y., Zhang, X., Chen, D., Shen, N., & Le, W. (2012). miR-132 regulates the differentiation of dopamine neurons by directly targeting Nurr1 expression. Journal of Cell Science.

Yang, D., Zhang, Z.-J., Oldenburg, M., Ayala, M., & Zhang, S.-C. (2008). Human Embryonic Stem Cell-Derived Dopaminergic Neurons Reverse Functional Deficit in Parkinsonian Rats. Stem Cells.

Yao, M.-J., Chen, G., Zhao, P.-P., Lu, M.-H., Jian, J., Liu, M.-F., & Yuan, X.-B. (2012). Transcriptome analysis of microRNAs in developing cerebral cortex of rat. BMC Genomics, 13(1), 232.

Yao, Z., Mich, J. K., Ku, S., Menon, V., Krostag, A. R., Martinez, R. A., Furchtgott, L., Mulholland, H., Bort, S., Fuqua, M. A., … Ramanathan, S. (2017). A Single-Cell Roadmap of Lineage Bifurcation in Human ESC Models of Embryonic Brain Development. Cell Stem Cell, 20(1), 120–134.

Ying, Q. L., Nichols, J., Chambers, I., & Smith, A. (2003). BMP induction of Id proteins suppresses differentiation and sustains embryonic stem cell self-renewal in collaboration with STAT3. Cell.

Ying, Q. L., Wray, J., Nichols, J., Batlle-Morera, L., Doble, B., Woodgett, J., Cohen, P., & Smith, A. (2008). The ground state of embryonic stem cell self-renewal. Nature.

Yoshida, M. (2006). Massive loss of Cajal-Retzius cells does not disrupt neocortical layer order. Development.

Yoshida, M., Suda, Y., Matsuo, I., Miyamoto, N., Takeda, N., Kuratani, S., & Aizawa, S. (1997). Emx1 and Emx2 functions in development of dorsal telencephalon. Development, 124, 101–111.

Young, R. A. (2011). Control of the embryonic stem cell state. Cell.

Yu, D. X., Di Giorgio, F. P., Yao, J., Marchetto, M. C., Brennand, K., Wright, R., Mei, A., McHenry, L., Lisuk, D., Grasmick, J. M., … Gage, F. H. (2014). Modeling hippocampal neurogenesis using human pluripotent stem cells. Stem Cell Reports, 2(3), 295–310.

Yu, S. W., Friedman, B., Cheng, Q., & Lyden, P. D. (2007). Stroke-evoked angiogenesis results in a transient population of microvessels. Journal of Cerebral Blood Flow and Metabolism.

Yu, T. S., Washington, P. M., & Kernie, S. G. (2016). Injury-Induced Neurogenesis: Mechanisms and Relevance. Neuroscientist.

Yuan, H., Corbi, N., Basilico, C., & Dailey, L. (1995). Developmental-specific activity of the FGF-4 enhancer requires the synergistic action of Sox2 and Oct-3. Genes and Development.

Yuan, M., Wen, S. J., Yang, C. X., Pang, Y. G., Gao, X. Q., Liu, X. Q., Huang, L., & Yuan, Q. L. (2013). Transplantation of neural stem cells overexpressing glial cell line-derived neurotrophic factor enhances Akt and Erk1/2 signaling and neurogenesis in rats after stroke. Chinese Medical Journal.

Yun, K., Potter, S., & Rubenstein, J. L. R. (2001). Gsh2 and Pax6 play complementary roles in dorsoventral patterning of the mammalian telencephalon. Development.

Zaman, V., & Shetty, a K. (2001). Fetal hippocampal CA3 cell grafts transplanted to lesioned CA3 region of the adult hippocampus exhibit long-term survival in a rat model of temporal lobe epilepsy. Neurobiology of Disease, 8(6), 942–52.

Zembrzycki, A., Griesel, G., Stoykova, A., & Mansouri, A. (2007). Genetic interplay between the transcription factors Sp8 and Emx2 in the patterning of the forebrain. Neural Development.

Zhang, J.-J., Zhu, J.-J., Hu, Y.-B., Xiang, G.-H., Deng, L.-C., Wu, F.-Z., Wei, X.-J., Wang, Y.-H., Sun, L.-Y., Lou, X.-Q., … Xiao, J. (2017). Transplantation of bFGF-expressing neural stem cells promotes cell migration and functional recovery in rat brain after transient ischemic stroke. Oncotarget, 8(60), 102067–102077.

Zhang, R., Zhang, Z., Wang, L., Wang, Y., Gousev, A., Zhang, L., Ho, K. L., Morshead, C., & Chopp, M. (2004). Activated Neural Stem Cells Contribute to Stroke-Induced Neurogenesis and Neuroblast Migration Toward the Infarct Boundary in Adult Rats. Journal of Cerebral Blood Flow and Metabolism.

Zhang, S. C., Wernig, M., Duncan, I. D., Brüstle, O., & Thomson, J. A. (2001). In vitro differentiation of transplantable neural precursors from human embryonic stem cells. Nature Biotechnology.

Zhang, T., Yang, X., Liu, T., Shao, J., Fu, N., Yan, A., Geng, K., & Xia, W. (2017). Adjudin-preconditioned neural stem cells enhance neuroprotection after ischemia reperfusion in mice. Stem Cell Research and Therapy.

Zhao, L., Wu, T. W., & Brinton, R. D. (2004). Estrogen receptor subtypes alpha and beta contribute to neuroprotection and increased Bcl-2 expression in primary hippocampal neurons. Brain Research.

Zhou, C.-J. (2004). Wnt Signaling Mutants Have Decreased Dentate Granule Cell Production and Radial Glial Scaffolding Abnormalities. Journal of Neuroscience.

Zufferey, R., Nagy, D., Mandel, R. J., Naldini, L., & Trono, D. (1997). Multiply attenuated lentiviral vector achieves efficient gene delivery in vivo. Nature Biotechnology, 15(9), 871–875.